BRNO UNIVERSITY OF TECHNOLOGY
VYSOKÉ UČENÍ TECHNICKÉ V BRNĚ

FACULTY OF INFORMATION TECHNOLOGY
FAKULTA INFORMAČNÍCH TECHNOLOGIÍ

DEPARTMENT OF COMPUTER SYSTEMS
ÚSTAV POČÍTAČOVÝCH SYSTÉMŮ

DEVELOPING BRAIN COMPUTER INTERFACE FOR IMAGINED MOVEMENTS
VÝVOJ ROZHRANÍ BRAIN COMPUTER PRO PŘEDSTAVOVANÉ POHYBY

MASTER'S THESIS
DIPLOMOVÁ PRÁCE

AUTHOR **Bc. BARBORA BLAŠKOVÁ**
AUTOR PRÁCE

SUPERVISOR **doc. AAMIR SAEED MALIK, Ph.D.**
VEDOUCÍ PRÁCE

BRNO 2023

Master's Thesis Assignment

144825

Institut: Department of Computer Systems (UPSY)

Student: **Blašková Barbora, Bc.**

Programme: Information Technology and Artificial Intelligence

Specialization: Cyberphysical Systems

Title: **Developing Brain Computer Interface for Imagined Movements**

Category: Biocomputing

Academic year: 2022/23

Assignment:

1. Study and learn about the Brain-Computer Interface (BCI) and how the imagined movements play a role in BCI.
2. Get acquainted with signal & image processing methods as well as machine learning techniques and their application to the brain EEG signals and images.
3. Find out the challenges in detection of imagined movements from brain signals and images as well as the limitations of the existing methods.
4. Design an algorithm for detection of imagined movements from brain EEG signals and images.
5. Implement the designed algorithm.
6. Create a set of benchmark tasks to evaluate the quality of Brain-Computer Interface as well as the corresponding computational performance and memory usage.
7. Conduct critical analysis and discuss the achieved results and their contribution.

Literature:

- According to supervisor's advice.

Requirements for the semestral defence:

- Items 1 to 4 of the assignment.

Detailed formal requirements can be found at https://www.fit.vut.cz/study/theses/

Supervisor: **Malik Aamir Saeed, doc., Ph.D.**

Head of Department: Sekanina Lukáš, prof. Ing., Ph.D.

Beginning of work: 1.11.2022

Submission deadline: 31.7.2023

Approval date: 31.10.2022

Abstract

Brain disorders and diseases affect 1 in 6 people worldwide and in many cases result in a condition that profusely impacts the life of patient. Mental health topics surge as 1 in 10 people is diagnosed with a mental health disorder. It is therefore crucial to study the organ that is still in a big part a mystery to the researchers - brain.

The focus of this thesis is on Brain Computer Interface (BCI) which can act as a intermediary between the brain and a device by acquiring the brain signals and translating them into a set of actions or commands. One of the methods to control a device by thoughts is motor imagery, which is based on the fact that imagining moving a part of the body elicits the same brain response as actual movement. This thesis proposes to utilize a recent field of the EEG for the BCI applications - microstate analysis. Classifier for distinguishing between the motor imagery tasks is proposed as a combination of microstate features extracted from different regions of the brain with the already established features such as from frequency or time-domain.

The subject-specific classifiers was trained for 30 participants. Two distinct classifiers were implemented - one for the classification of the rest versus activity and second for the classification of the left versus right motor imagery. The mean accuracy across participants for the rest versus activity classification was 0.85. The mean accuracy across participants for the left versus right motor imagery classification was 0.74.

The microstates proved to be helpful in distinguishing between different conditions in a task settings, but need some improvements in terms of the further research.

Abstrakt

Rôzne poruchy a choroby mozgu postihujú približne každého šiesteho človeka a veľa z nich necháva na pacientoch trvalé následky. Téma mentálneho zdravia je čoraz viac dôležitá, keďže každý desiaty človek má diagnostikovanú mentálnu poruchu. Je preto dôležité študovať orgán, ktorý je stále z veľkej čati záhadou - mozog.

Diplomová práca sa zameriava na Brain Computer Interface (BCI) - rozhranie, ktoré ponúka priame komunikačné spojenie medzi mozgom a vonkajším svetom. Základná myšlienka BCI je veľmi jednoduchá - najprv získať signál z mozgu, dekódovať ho a vykonať akciu vychádzajúcu zo zámeru užívateľa. Jedna z metód ako pomocou mozgu priamo komunikovať sú predstavované pohyby, čo je metóda založená na fakte, že predstava pohybu vyvoláva v mozgu rovnakú odozvu ako skutočný pohyb. V diplomovej práci je navrhnuté použiť EEG a jeho relatívne novú metódu analýzy - mikrostavy. Klasifikátor na rozlišovanie medzi úlohami predstavovaných pohybov je navrhnutý ako kombinácia vlastností mikrostavov extrahovaných z rôznych oblastí mozgu s už známymi vlastnosťami, ako napríklad frekvenčné alebo časové vlastnosti signálu.

Klasifikátory boli natrénované na 30 účastníkoch, pre každého zvlášť. Boli implementované dva odlišné klasifikátory - jeden na klasifikáciu nečinnosti oproti aktivite a druhý na klasifikáciu predstavy pohybu ľavej ruky verzus pravej ruky. Priemerná presnosť klasifikácie nečinnosti a aktivity bola 0.85. Priemerná presnosť klasifikácie predstavy pohybu ľavej a pravej ruky bola 0.74.

Ukázalo sa, že mikrostavy sú užitočné pri rozlišovaní medzi rôznymi stavmi v kontexte predstavovaných pohybov a BCI, ale potrebujú určité vylepšenia z hľadiska ďalšieho výskumu.

Keywords

brain computer interface, electroencephalography, motor imagery, biocomputing, microstate analysis

Klíčová slova

rozhranie mozog-počítač, elektroencefalografia, predstavované pohyby, analýza mikrostavov EEG

Reference

BLAŠKOVÁ, Barbora. *Developing Brain Computer Interface for Imagined Movements*. Brno, 2023. Master's thesis. Brno University of Technology, Faculty of Information Technology. Supervisor doc. Aamir Saeed Malik, Ph.D.

Rozšířený abstrakt

Hlavným cieľom diplomovej práce je navrhnúť Brain Computer Interface pre predstavované pohyby za využitia analýzy mikrostavov zo signálu elektroencefalografie.

Mozog, najkomplikovanejší orgán ľudského tela, je pre nás stále záhadou. Rôzne poruchy a choroby mozgu postihujú približne každého šiesteho človeka a veľa z nich necháva na pacientoch trvalé následky. 15 miliónov ľudí každoročne postihne mŕtvica a z nich 5 miliónov ostáva zdravotne postihnutých - od straty schopnosti hýbať určitou časťou tela až po celkovú paralýzu. Rehabilitácia pre takýchto pacientov je nevyhnutnosť a často jediná možnosť, ako získať späť stratené schopnosti. Avšak prináša so sebou mnoho problémov - je finančne a časovo náročná pre pacienta aj personál, nakoľko je vysoko individuálna. Pacient musí dochádzať na miesto rehabilitácie, a napriek úsiliu a dlhodobej liečbe nemusí byť nakoniec účinná. Moderný svet však trápia aj mentálne poruchy, ktoré sú často na prvý pohľad neviditeľné a veľmi ťažko diagnostikovateľné. Je preto potrebné prísť na spôsoby, ako diagnostikovať a liečit práve mozog.

V posledných rokoch záujem o štúdium mozgu a hlavne o to, ako dekódovať ľudské myšlienky, výrazne vzrástol. Brain Computer Interface (BCI) sa stal odetvím technológie, ktorá fascinuje nielen vedcov ale aj širokú verejnosť. BCI je rozhranie, ktoré ponúka priame komunikačné spojenie medzi mozgom a vonkajším svetom. Základná myšlienka BCI je veľmi jednoduchá - najprv získať signál z mozgu, dekódovať ho a vykonať akciu vychádzajúcu zo zámeru užívateľa. Potenciál využitia BCI je obrovský - od medicíny, cez priemysel až po zábavu. V medicíne to je práve napríklad využitie pri rehabilitácii, kedy pacient môže ovládať robotickú ruku len za pomoci myšlienok a trénovať tak mozog, aby rozhýbal nakoniec aj ruku skutočnú. Takáto rehabilitácia už bola v minulosti odskúšaná a ukázala sa ako účinná. Ďalší prípad kde BCI funguje už pomerne dlho a ukázalo sa ako nenahraditeľné je komunikácia s pacientmi, ktorí sú úplne paralyzovaní. Pre nich je BCI kde komunikujú len cez myšlienky nevyhnutná vec, keďže nemôžu hýbať telom ani sa prejavovať verbálne. Okrem medicíny je ale ľahké predstaviť si využitie BCI aj v priemyselnej sfére - kontrolovať zariadenia myšlienkami, monitorovať užívateľovu náladu alebo mentálnu únavu pomocou mozgových signálov a prispôsobiť takýmto postupom pracovné procesy. Tieto možnosti môžu v budúcnosti zefektívniť pracovné úlohy.

Existuje veľa možností ako zachytiť mozgový signál pre BCI využitie, či už ide o funkčnú magnetickú rezonanciu, kde je možné dostať signál aj z oblastí vo vnútri mozgu, alebo elektroencefalografiu (EEG), kde je signál dostupný len z vrchných oblastí mozgu. V tejto diplomovej práci bolo využité EEG vďaka jeho výbornému časovému rozlíšeniu, a pretože je to najpopulárnejšia metóda zachytenia mozgových signálov pre BCI. Predstavované pohyby sú taktiež jednou z populárnych možností ako pomocou myšlienok niečo ovládať. Predstava pohybu vyvoláva v mozgu rovnakú odozvu ako skutočný pohyb, ktorý vyvoláva reakciu v primárnej motorickej kôrovej oblasti mozgu.

Pre analýzu predstavovaných pohybov je použitá analýza mikrostavov, čo je relatívne nový prístup k analýze EEG, ktorý v kontexte BCI ešte nebol použitý. Mikrostavy sú prechodné, vzorované, kvázi stabilné stavy alebo vzory EEG, ktoré sa držia po dobu niekoľko milisekúnd (20 - 250 ms) a následne sa rapídne vymenia. Z EEG signálu sa extrahujú pomocou metód zhlukovania.

V diplomovej práci je navrhnutý postup spracovania EEG signálu pre extrakciu mikrostavov. V práci je taktiež navrhnuté použiť lokalizované mikrostavy, ktoré sú extrahované z centrálnej, frontocentrálnej a celej oblasti hlavy a počet použitých mikrostavov je navrhnuté vyvodiť z presnosti klasifikácie pohybov. Okrem mikrostvov boli na klasifikáciu predstavovaných pohybov použité taktiež ostatné bežné analýzy EEG, ako napríklad frekvenčná

analýza a analýza signálu v časovej doméne. V práci bol použitý verejne dostupný dataset EEG signálov nahraných pri vykonávaní predstavovaných a skutočných pohybov pravej a ľavej ruky.

V práci sú navrhnuté dva rôzne druhy klasifikátorov - jeden na rozlíšenie medzi pohybom a nečinnosťou a jeden na rozlíšenie medzi pohybom pravej a ľavej ruky. Dva rôzne klasifikátori boli vybrané aby sa ukázalo, či má zmysel lokalizovať mikrostavy - hypoteticky, mikrostavy z frontocentrálnj oblasti by mali byť informatívne pri rozlišovaní medzi pohybom a nečinnosťou a mikrostavy z centrálnej oblasti medzi ľavým a pravým pohybom ruky.

Výsledky ukázali, že natrénovaný klasifikátor na pohyb verzus nečinnosť dosahoval priližne 85% presnosť za použitia vlastností mikrostavov, frekvenčných vlastností a časových vlasností EEG signálu. Klasifikátor na pohyb ľavej verzus pravej ruky dosahoval presnosti približne 74%. Klasifikátor pre rozlíšenie pohybu verzus nečinnosti bol porovnaný s klasifikátorom natrénovaným na dátach s reálnym pohybom a taktiež na klasifikátore natrénovaným na dátach len s frenvenčnými vlastnosťami. Klasifikácia na reálnom pohybe bola úspešnejšia a klasifikácia len z frekvenčných vlastností bola menej úspešná, podľa očakávania. Mikrostavy v celej topografii boli úspešnejšie ako mikrostavy z lokalizovaných topografií.

Záverom práce je, že vlastnosti mikrostavov pomohli v klasifikácii predstavovaných pohybov ako je zrejmé z porovnania voči iným modelom. Je však stále veľa priestoru na zlepšenie, a to hlavne v procese extrahovania mikrostavov.

Developing Brain Computer Interface for Imagined Movements

Declaration

I hereby declare that this Master's thesis was prepared as an original work by the author under the supervision of doc. Aamir Saeed Malik, Ph.D. I have listed all the literary sources, publications and other sources, which were used during the preparation of this thesis.

. . . .
Barbora Blašková
July 30, 2023

Acknowledgements

Contents

List of Figures

4

List of Tables

List of abbreviations

Chapter 1

Introduction

Brain, the most intricate and complex organ in a human body, is still a mystery for us. Brain disorders and diseases affect 1 in 6 people worldwide and in many cases result in a condition that profusely impacts the life of patient. 15 million people worldwide each year suffer a stroke and 5 million of them are left with permanent brain damage and get disabled in some way. In developed countries, which are currently dealing with a trend of an aging population, the Alzheimer's disease is also on the rise, as 1 in 9 people aged 65 or more have it. The mental health topics are also getting more important as 1 in 10 people is diagnosed with a mental health disorder and it is estimated that 50 % of the population at some point in their life suffer from it [1].

However, there is little to no cure for the ones affected by the brain disorders. In case of a stroke patients, the rehabilitation takes a lot of time, is tedious and in some cases does not even bring any improvement. The development of the brain imagining technologies made it possible to learn about a ways a brain is processing information in the real time and allowed us a glimpse into the complex organ a brain is. Brain Computer Interface (BCI) is the recent result of an ongoing technological developments in this area, which has shown an immense potential in helping those whose suffer from the brain disorders.

BCIs record the signals from a brain, decode it and based on the intention of a user, perform an action. It was already proven to be invaluable to completely locked-in patients who are unable to communicate with the outside world, as the BCI provides a way for them to relay their thoughts without moving a muscle. BCI has found usage in multiple medical fields, helping with rehabilitation, diagnosis or treatment of many different brain conditions. It is not hard to see that BCI will also play an important role in the industrial settings, from control of the machines in a dangerous environments, to playing an actual mind games with friends on a Friday night. The possibilities ranging from entertainment to a industry devices acting on our thoughts are seemingly endless.

It's a no-brainer to strive for a way to directly „observe" and translate human thoughts into actions by getting as close as possible to the brain, the absolute source of our thinking. However our limited understanding of its function as well as limitations of the technology and methodology make the industrial BCI still a song of a future. From a technical standpoint, the current brain recording devices fall into two categories. Some are highly efficient in decoding deep brain signals but come with a hefty price tag and require a room-sized machine. On the other hand, there are more affordable and wearable options that strap onto your head, but they provide only limited insights into the brain's inner workings. Cur-

---

[1]https://www.cdc.gov/mentalhealth/learn/index.htm

rently, the most optimal middle ground is represented by Electroencephalography (EEG), which is fast, compact, relatively inexpensive and its disadvantages can be outweighted by the current state-of-the-art algorithms and techniques to get as much information out of it as possible.

On the functional side of the things, over the centuries the researchers have figured out which areas of a human brain are approximately responsible to perform what function. But only recently (at around 1990) have we started to also look into how the areas are communicating between each other. From the communication between the brain regions, there is seemingly only a small step to forming the whole paths the information might take and indeed, major paths such as how is visual information processed inside the brain are already documented. But the small and complex information hidden deep inside brain structures, including our emotions, dreams, complex decision making and many other are still a mystery. It is therefore crucial to find new ways of looking into the information that we can observe and find even the smallest of bread crumbs in the vast space of billions of neurons to one day put together a comprehensive picture that would allow us to understand ourselves better. And maybe learn to read minds in the process.

Limitations mentioned above are the reason why researchers are always coming up with new ways how to interpret the signal that we can record directly from our brain. The main objective of the thesis is to therefore contribute to the research of the BCI and include, along with the established features, the newest EEG paradigm - microstate analysis. Microstate analysis is a study of the brain patterns, which has previously demonstrated a success in distinguishing between a healthy and mentally ill patients (mostly in schizophrenia). It is based on the fact, that at any given point in time, the so-called activated and deactivated brain areas form some topography which hold for several milliseconds. The topographies are usually repeating, forming a set of a few maps that can represent majority of the topographies during the recording. In the context of the BCI, it has not yet been studied extensively and only a handful of studies were published where the microstate analysis was used in the context of motor imagery. Motor imagery is one of the most prevalent BCI paradigms, where the device is controlled by the thought of moving left or right limb, which is very useful in the machine control in paralysed patients and also have ample potential in the industry. The goal of the thesis is to in incorporate microstate analysis into the BCI for the imagined movements.

The thesis is structured as follows - the Chapter 2 gives the introduction to the brain and the BCI for an overview about the brain structure, goal of the BCI, its paradigms, usage and current applications and limitations. Chapter 3 gives an overview on the EEG, its signal acquisition, preprocessing and general overview on the most usual types of analysis. Chapter 4 gives a proposed solution to the thesis - the selection of the dataset for the appropriate for the thesis objective, data preprocessing steps, detailed description about the extraction of the microstate maps and classification. Chapter 5 deals with the implementation details of the proposed solution and Chapter 6 will give an evaluation and benchmark result of the solution. Finally, the thesis is concluded in the Chapter 7.

Chapter 2

Brain Computer Interface

Brain Computer Interface (BCI) provides a direct communication path between the brain and the external world. The basic idea is very simple one - to observe the user's mental state we read the various signals coming from the brain, decode those signals and make actions accordingly to the user's intent. The overall components comprising the BCI can be summarized as the following:

1. way to measure brain signals
2. methods to process these signals and predict the user's intentions
3. interface to communicate with the external application or device

They are pictured in Figure 2.1.
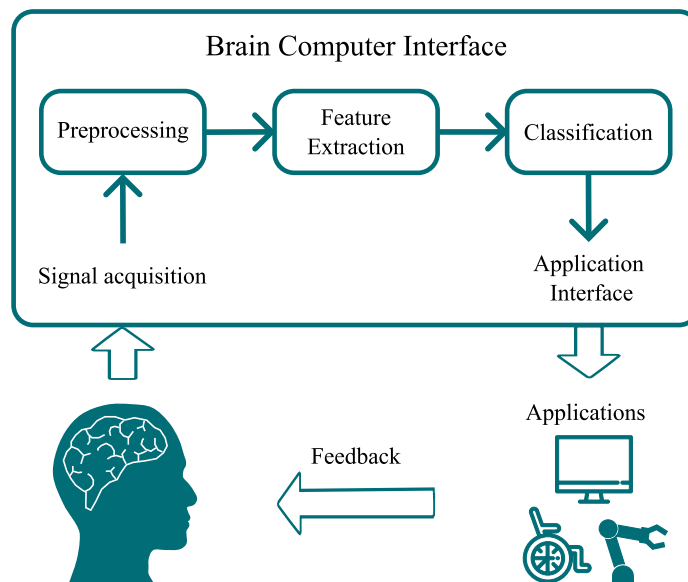
Figure 2.1: BCI scheme.

The inputs therefore, are raw brain signals measured by different modalities, depending on the use of the BCI. One could measure electrical impulses generated in the brain, or blood flow in certain brain areas. The signal processing part of the BCI transforms these raw signals into information from which we can make conclusions about the user's

state or intent, based on classification output and the use of the various machine learning techniques. Finally, these classification or recognition results are translated into the actions and communicated through the application interface to a device that performs them. While these components form a complete BCI structure, one can argue about adding the feedback loop, which is undoubtedly the most important part in neurofeedback applications, where users learn to regulate and modulate their brain activity [39].

The history of the BCI started in 1924 with the Hans Berger's discovery of brain's electrical activity and subsequent invention of the electroencephalography, which measures electrical potentials of the brain. At first, it was used to study brain pathology and diseases. In 1973, Jacques J. Vidal published the first BCI paper utilizing the electroencephalography and coined the term brain computer interface [168]. The first experiments were carried out on monkeys and first human experiments were carried out in the 90s [80].

Over the years, the popularity of the BCI slowly rose, and while between 1979 and 2011 there were only around 2000 publications regarding the BCI, in the last decade alone this number tripled [147]. The rapid development can be attributed not only to the fast development in the technology, robotics, artificial intelligence, but also the growing popularity of cognitive sciences, cognitive psychology or neuroscience [80].

BCIs are used in researching the brain as we know, in augmenting or repairing the human cognitive or motor functions, in assisting the impaired people in their daily tasks, enhancing the user's experience in gaming and many more. It is safe to say that the BCI will only gain more popularity as science and technology advancements are finally making it possible to study the most complex organ in the human body - brain.

This chapter will cover the basics of the brain anatomy and function to have the necessary knowledge for constructing any BCI. It will give the definitions of the different types of the BCI, their advantages and disadvantages and what purpose they serve. It will give a review about the current utilization of the BCI in various fields including medical and industrial. Last section will cover the current challenges the BCI faces and the views for the future.

2.1 Brain

It is crucial for the reliable construction of a BCI system to have a basic understanding of the anatomy and structure of a brain. Brain is a complicated organ and to this day we do not have a complete image of how it might function. With the understanding of responsibilities of each part of our brain, BCI researchers can conveniently pinpoint the exact location that needs to be recorded or stimulated in order to achieve the defined results of the BCI task.

Our nervous system is divided into two distinct systems - the Central Nervous System (CNS) which acts as the body's processing centre and the Peripheral Nervous System (PNS) which relays information from the CNS to the organs and limbs. Brain, along with a spinal cord, is part of a CNS.

The CNS consists of two basic cell types: neurons and glia. Neurons are the information messengers, conveying information through electrical impulses and chemical signals between different regions of the brain and also between the brain an the rest of the body. The major parts of a neuron are the cell body, dendrites, and the axon as can be seen in Figure 2.2a.

Neurons are connected with each other through synaptic connection, which is when the tip of axon of one neuron connects to another neuron through its dendrites or cell body. The neurons communicate through the exchange of the neurotransmitters, which are chemical messengers of the body. This transmission is a very quick process, taking no more than

a few milliseconds to happen [162]. When neurotransmitters reach the neuron, they are converted into the action potential, electrical signal, which travels through the neuron to the axon, to pass the information to the next neuron. As depicted in Figure 2.2b, there is an area between the axon of one neuron and the receiving neuron and they are not directly connected.

(a) Basic neuron structure.

(b) Synaptic connection.
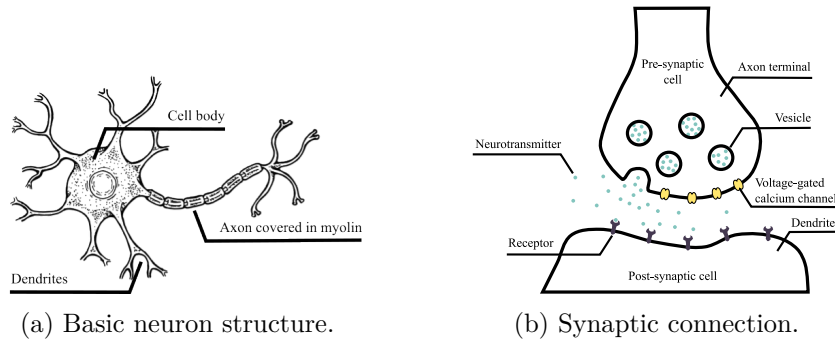
Figure 2.2: Neuron structure and connection between two neurons.

When dissecting a brain, there is a distinguishable layer of grayish matter followed by the white matter (Figure 2.3b). In 19th century it was discovered that gray matter consisted of aggregations of neuron cell bodies called nuclei and that white matter was comprised of axons [126].

At the highest level, the brain can be divided into cerebrum, brain stem and cerebellum as depicted in Figure 2.3a.

(a) Different brain regions.

(b) Gray and white matter.
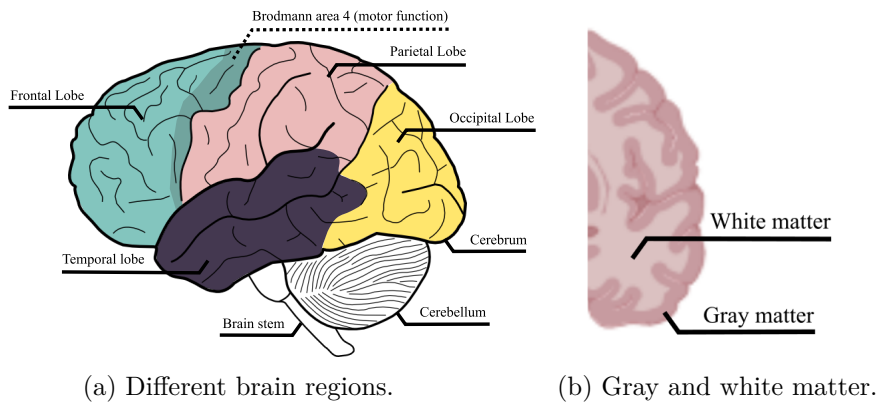
Figure 2.3: Structure of the brain.

For the purposes of the BCI, the cerebrum with its cerebral cortex (gray matter covering the cerebrum) is of the biggest importance, because it is the closest to the skull and therefore it is easiest to record the signal from it. Moreover, the cerebral cortex (cortex) is involved in high-level functions, such as reasoning, emotion, personality, memory and language, among many others.

The cortex can be anatomically divided into four lobes by the major fissures (deep grooves on the surface of the brain) - frontal, parietal, occipital and temporal lobe. These lobes are shown in Figure 2.3a.

Each of the lobes is associated with multiple functions:

1. Frontal lobe - high-level functions, such as decision making or planning. Area dedicated to the movement is also located on a frontal lobe.
2. Parietal lobe - sensory information such as smell, touch or pain.
3. Occipital lobe - primary vision processing area.
4. Temporal lobe - memory, hearing and speech functions.

The cortex does not have a uniform structure. Its thickness as well as layering of different neuron cell varies. The older cortex areas (in terms of evolution), for example, only consist of three cell layers, while the newer ones, called neocortex consist of six cell layers [126]. Based on the different layering of the cells and lobes, Korbinian Brodmann in 1909 [22] divided the cerebral cortex into 52 areas, with some of them also having a specific function. For instance the Brodmann area 4 (Figure 2.3a), which is located in the frontal lobe is the primary motor area of the brain, or Brodmann areas 17 and 18 located in the occipital lobe are the primary visual areas. Since Brodmann, several areas have been further subdivided, but his division is still widely used [126].

2.2 Classification of the brain-computer interfaces

Over the years, several types of the BCIs have emerged and are used in today's applications. The division is vast and at the highest level, the BCI systems can be divided by the means of their recording method, dependability and mode of operation [143].

Dependability refers to the need of an active participation in the task. Dependent BCIs require user to do some activity, for example imagine a movement or move their eyes in order to produce an action. Independent or spontaneous BCI is based on the spontaneous activity in the human brain, elicited by external stimuli, such as visual or auditory.

Mode of operation can be synchronous or asynchronous. Synchronous BCI require the brain signals to be time-locked, so the participant usually sees some cue on the screen and performs the task at that time. Asynchronous BCI try to predict the intention of an user without any information about when are they performing an action. Understandably, the synchronous BCI is easier to implement, as it is possible to precisely time the actions of the user. However, it is also much less user-friendly - ideally, the BCI should be able to recognize the intents of the user without any cues.

The following subsections will talk about the measurement techniques most commonly used in the BCI and their advantages or disadvantages.

2.2.1 Recording Methods

The recording method refers to the placement of the measuring device inside or outside of the skull to record brain activity and also the type of the recording device used.

Invasive BCI

Invasive BCI applications are single unit BCIs that place the micro electrodes directly into the cortex to measure electrical activity of a single area of brain cells. The placement of the electrodes is shown in Figure 2.4. The invasive BCI require subject to undergo a

neurosurgery, which might be expensive and risky operation, although with right procedures the actual number of recorded problems seem to be minimal [172].

Still, invasive BCIs are used only when the patient's condition is so severe, that the advantages outweigh the risks, for example in paralyzed or blind patients. The potential dangers of placing the electrodes directly into the cortex besides the risk of the operation itself include body rejecting the foreign object or scar tissue forming around the electrode, which might render the signal unusable after some time.

The quality of the signal is very high due to the proximity to the source with little to no noise. The spatial resolution of invasive BCI is within the 0.1 mm and temporal resolution is around 0.003 s [123].

Semi-invasive BCI

Semi-invasive BCIs are mostly built upon the Electrocorticography (ECoG) which places electrodes not directly in the cortex, but rather in the area called dura mater, which is outer membrane layer located directly under the skull as depicted in Figure 2.4. The operation to implant small number of electrodes therefore require only small burr hole and do not penetrate the brain tissue itself [183].

Most of the research regarding the semi-invasive BCIs comes from the patients diagnosed with epilepsy [67]. These patients are implanted with the electrode array for limited duration (~1 week) to monitor their brain activity for precise localization of epileptogenic area [85]. During this time, they are often asked whether they would be willing to participate in the BCI research, utilizing already implanted array of electrodes.

Signal-to-noise ratio of a data recorded from ECoG is superior to that of a non-invasive method and the implants themselves are less dangerous than invasive ones. The spatial resolution is approximately 1 mm and spatial resolution is around 0.003 s [123]. Still, there is some surgical intervention necessary.

The quality of the data might be the reason that companies are starting to develop ways to implant the electrodes more efficiently and commercially, for example the company Neuralink[1], which also came with the way to implant these electrodes by the use of the robotic electrode inserter [118].
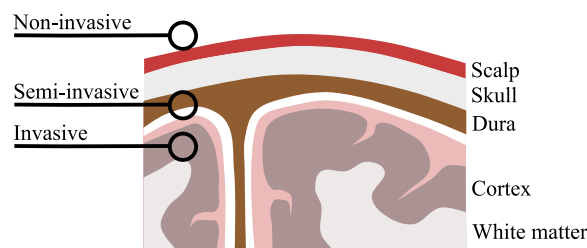
Figure 2.4: Brain layers and corresponding electrode placement in them.

Non-invasive BCI

Non-invasive BCIs measure brain activity from the surface of the scalp and eliminate the need for any neurosurgical intervention. This in itself brings a notable advantage over the invasive ones, as it eliminates not only any risk associated with the operation, but also

---

[1]https://neuralink.com/

the need for medical staff and need for any operational recovery. There are multiple types of non-invasive recording devices that can measure different processes inside of the brain. These modalities are explained in more detail in the next section.

2.2.2 Measurement Modalities for non-invasive BCI

The decision on the measurement modality used in the BCI usually comes down to four different factors and what role do they play in the intended use of the BCI. These factors are the temporal and spatial resolution of the modality, its portability and cost [143]. The decision might also come down to the type of the processes recorded, as some modalities measure metabolic activities and some electrical properties of the brain.

Functional Magnetic Resonance Imaging

Functional Magnetic Resonance Imaging (FMRI) measures brain activity by detecting changes associated with blood flow [72]. When there is a neuronal activity in an area of the brain, blood flow to that region increases to deliver the energy in the form of glucose to the neurons. This process is called hemodynamic response. It utilizes MRI machine that can capture the brain structure using magnetism and radio waves. The fMRI, on the other hand, captures the functional activity of the brain, but with the same machine.

The fMRI has an excellent spatial resolution, being able to pinpoint the precise location inside the brain of around $3mm^3$ [58]. Due to the hemodynamic response being a slow process, the neuronal actions following the stimuli peak between 2-5 seconds, which makes fMRI having a very poor temporal resolution. In addition to that, it is not portable and MRI machines are very expensive, being used mostly in the clinical settings. This makes fMRI being used primarily in the neurofeedback settings, where patients learn to volitionally control the activation of certain brain regions [72]. This method has been utilized to treat patients with addictions [79] [82], psychiatric patients with problems controlling their emotions [97] or in epilepsy detection [38]. All of these applications require a precise location of the activity in the structures deep inside of the brain, but are not so dependent on the precise time information and rapid actions, making fMRI a preferred choice.

Functional Near-Infrared Spectroscopy

Functional Near-Infrared Spectroscopy (FNIRS) is based on the same concept as the fMRI. The oxygenated and deoxygenated hemoglobin scatter near-infrared (NIR) light differently. It is possible to measure the absorption of NIR light by placing light emitters and photodetectors on a scalp and capture the ratio of the oxygented and deoxynated blood present in the area. Compared to fMRI, the fNIRS is fully portable and does not require expensive MRI machine, but in return offers only a fraction of the fMRI's spatial resolution.

Because the hemodynamic response is a slow process, the time resolution of fNIRS is only between 0.1-1 seconds. A depth sensitivity is approximately 1.5 cm, and a spatial resolution up to 1 cm [141]. Its less susceptible to electrical and movement noise (as opposed to to fMRI and EEG), however, due to it not yet being used widely, it is still more expensive than EEG [122]. The fNIRS is fully portable, making it very suitable for any commercially used BCI. It is expected that this field will grow and there is much undiscovered potential in it [122].

Magnetoencephalography

Magnetoencephalography (MEG) measures magnetic field generated by the electrical activity of neurons firing. Usually, it is combined with MRI to give better structural overview of the patient's brain [158].

MEG based BCIs are usually used for motor movement and motor imagery tasks [109][146] and have improved spatial resolution over EEG. However, they are not portable as MEG requires large immovable hardware. The research towards more portable MEG devices is currently ongoing [129].

Electroencephalography

Electroencephalography (EEG) captures the postsynaptic potentials of the neurons that are located in the cortex. The electrodes placed on the scalp measure the voltage fluctuations, which are then sent to the amplifier to obtain the electrogram.

Since the EEG captures the electrical activity of the neurons in the cortex, it has an excellent temporal resolution, measuring the events in the milliseconds. However, it suffers from the poor spatial resolution of only around 1 cm, limited to the cortex area. It is fully portable and the most popular BCI modality among the researchers [89]. This popularity drove the price of the EEG down and made it considerably cheaper when compared to the others. The number of electrodes used to record the signal will determine the price, but for some applications where there is no need to have more than 8 electrodes, the price could be even lower.

2.2.3 Comparison Summary

The comparison in terms of spatial and temporal resolution between the different modalities can be seen in Figure 2.5. In these domains, the invasive methods without a doubt outperform the non-invasive ones, as they are able to pinpoint the exact signal location within milliseconds. As was mentioned before, the risk of body rejecting the electrodes and the risk and costs of neurosurgery itself are the reasons that invasive BCIs are only used in medical settings - usually for patients with serious impairments.
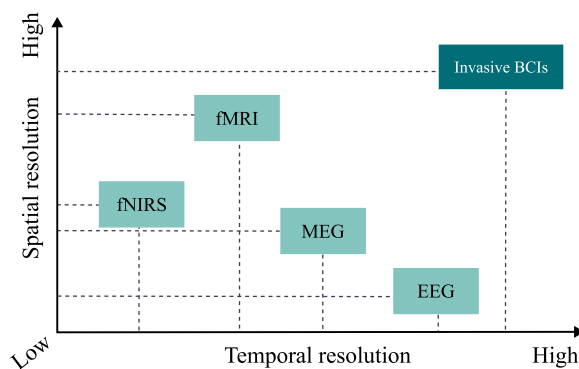
Figure 2.5: Comparison of different BCI modalities in terms of their spatial and temporal resolution.

When comparing the non-invasive recording modalities, the choice always depends on the purpose of the BCI and its availability. If the BCI is to be used by the industry and has to assist people with their tasks, it has to be portable and as inexpensive as possible. On

that front, EEG is the primary choice and is the most used recording device, thanks to its great temporal resolution, portability and cost. The fNIRS suffers from the lower temporal resolution and higher cost, but with the further research might prove much more useful as it does not suffer from the artifacts as much as the EEG does.

For the medical applications where the research requires the information about brain structures deep in the brain, the fMRI is the primary choice. It is used extensively in the emotion control neurofeedback for patients with psychiatric disorders. The recording modalities can also be combined together to complement each others weaknesses. The combination of the EEG and fMRI can bring unique insights, as it enables us to draw the correlations of the activity measured on the surface of the scalp with the information about activation deep in the brain [108].

For the purposes of this thesis, the EEG was chosen as the recording modality. Ideally, the user should use the BCI independently of the situation, which renders the non-portable measurement devices inconvenient. Additionally, the temporal resolution of the EEG is so precise, that it is possible to measure events in the range of milliseconds of them happening, which is suitable for any tasks requiring fast reaction times.

Chapter 3 gives a detailed overview of the EEG, what does it measure and what are the techniques commonly used to infer neural information from it.

2.3 EEG based BCI

EEG based BCIs can be built upon several paradigms, depending on the spontaneity, synchronicity and the purpose of the BCI.

2.3.1 Motor Imagery

Motor Imagery (MI) refers to the mental simulation of the body movement. The primary area activated during the movement is motor cortex, located on the frontal lobe, which is associated with planning, control and execution of voluntary movement [178]. The motor cortex can be further divided into primary motor cortex, premotor cortex and supplementary motor area. The primary motor cortex is mainly responsible for the execution of the movement, while the premotor cortex is associated with the planning of the movement and supplementary motor area with movement coordination and sequence planning. On the primary motor cortex, there are small areas all designated for very specific movement of the different body parts. The motor area and slice of the primary motor cortex revealing the body parts represented is depicted in Figure 2.6. The slice view represents only one hemisphere, but the primary motor cortex is present at both hemispheres, with right hemisphere controlling the left side of the body and vice versa.

The most crucial finding for the BCI was that the movement that person only imagines doing, without executing the movement activates the same areas in the brain as the actual movement [35]. This enabled the creation of the MI based BCI, where user is asked to imagine moving his limb and control some external device. Usually, these BCIs are build upon imagining hand or arm movements and that is because of the proximity of these on the primary motor cortex to the scalp. It is evident from the Figure 2.6 that thumb, fingers, hands and arms have relatively large designated areas, close to the skull, whereas toes and feet are folded inward, which makes these much harder to measure, especially with EEG.

MI based BCIs are used extensively for the rehabilitation to regain the body movement, but have a lot of potential in any device control. They require a lot of training to master
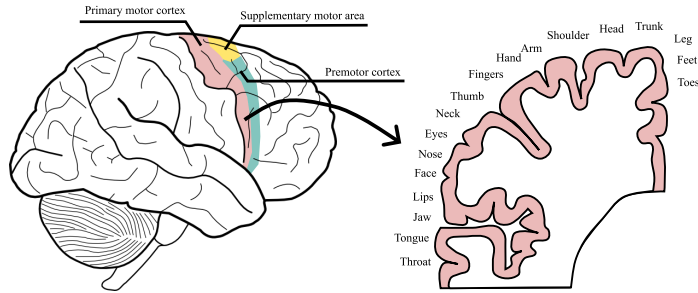
Figure 2.6: Motor area and respective body parts present on the primary motor cortex.

the control. If done right, however, they would be an ideal way to for the implementation of the asynchronous BCI, which would be an ideal case.

2.3.2 Steady-State Evoked Potentials

Steady-State Evoked Potentials (SSEP) are signals that are responses to a stimulation at specific frequencies. This stimulation can be visual (SSVEP), auditory (SSAEP) or somatosensory (SSSEP). In case of the SSVEP, when a person is looking at an object flickering at certain frequency, it creates oscillations in the brain which are the same (or multiple of) frequency as the flickering object. This can be very reliably detected using the EEG and inspecting the spectrum of the recorded brain signal in the occipital lobe - the area associated with visual processing. An example of the SSVEP is pictured in Figure 2.7. The same principles hold for the auditory or somatosensory SSEP, but with hearing the frequencies or feeling the frequencies physically.
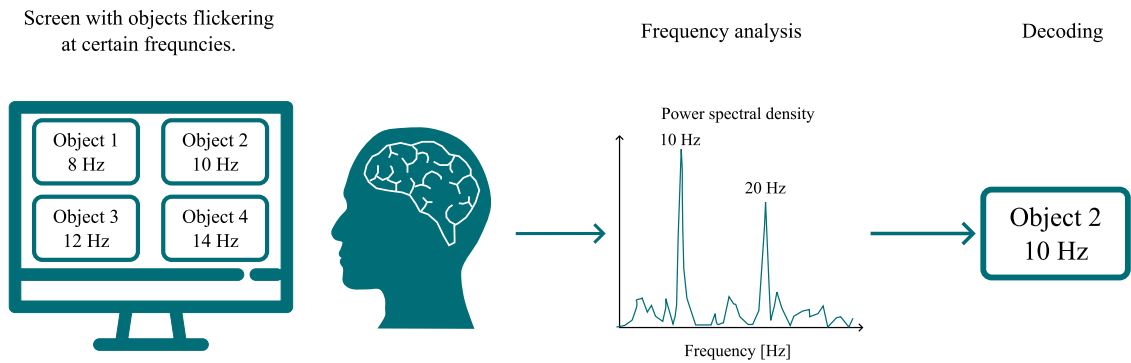
Figure 2.7: Example of the SSVEP based BCI.

Usually SSVEP based BCI are used as spellers, so that paralyzed people are able to communicate, but can be utilized for various applications, such as a wheelchair control [159].

SSEP based BCI have very high accuracy and virtually no training time is needed for a user to be successful [62]. Moreover, SSVEP spellers have the highest information transfer rate out of all non-invasive BCI spellers [30]. Disadvantage is the maximum number of targets that can be presented to reliably distinguish between them, which is about 60, but in some cases can be as high as 80 [56]. Another drawback is high visual fatigue and possibility of an user getting epileptic seizure from the flickering [86].

2.3.3 Event Related Potentials

Event Related Potentials (ERP) represent a time-locked neuronal response to the specific task. They are described in more detail in section 3.3.2.

The most common usage for the ERPs in the BCI are the spellers. When a person encounters something unexpected, it elicits a response in the brain that is already well defined by the years of research and can be detected. As different letters are presented to the subject on the screen, when the target letter appears the brain's response can be decoded.

Besides spellers, another exciting application of the ERPs in the BCI is detecting errors. When the signals are incorrectly classified as some action and the user realises that, it elicits a response in the brain that produces Error Potential (ErrP). This can be utilized to make a correction accordingly, such as repeating the last incorrectly classified letter in the speller [33]. ErrPs bring a potential of reinforcement learning to the BCI, where machine could learn the intention of the user over time [102].

The advantages of ERP based BCI is that a user does not have to be trained for the task and the results can be very good only after a few trials. However, in case of detecting an ERP, the EEG signal is considered as noise, and is much more prevalent than small ERPs. In the ERP research, this problem is tackled with averaging tens of trials to zero-out the noise [101]. In BCI, unfortunately, the ERP wave has to be detected on a single-trial basis and therefore sophisticated processing and detection techniques have to applied to infer the ERP for correct classification [28].

2.4 Areas of Application

The areas where the BCI are predominantly used can be divided into two categories - medical and non-medical [133]. Because all of the measurement modalities were at first used in a clinical setting for various diagnoses, the medical applications of the BCI are dominant, with utilization ranging from diagnosis to treatment and rehabilitation.

2.4.1 Medical Applications

Diagnosis

Studying and evaluating brain responses to various tasks, such as in BCI, brings an unique insight into the underlying processes happening in person's brain and consequently, might reveal abnormalities that contribute to diseases and disorders. These functional abnormalities might not be evident from simple structural scan, for example depression or other psychiatric disorders. The usage of BCI might therefore be beneficial to diagnose disorders that are a challenge even for the professionals. For example autism diagnosis [7], where professionals are scarce, the automatic diagnosis could help.

Another example is a Disorder of Consciousness (DoC). DoC refer to state where consciousness has been affected by damage to the brain and the patient might not be awake or aware (coma or vegetative state). Conventional methods to assess the patient's consciousness are highly dependent on the patient's motor ability, and might lead to misdiagnosis [130]. Preliminary research shows that it is possible to use BCIs to assist in consciousness detection, auxiliary diagnosis, prognosis, and rehabilitation of patients with DoC [130].

Rehabilitation

After the brain injury or damage, brain areas can cease to function properly, resulting in patient's losing the ability to perform certain tasks, such as movement or the speech. Neuroplasticity refers to ability of a human brain to modify, change, and adapt both structure and function [170]. Brain can be trained to make new neuronal connections and replace the damaged areas by substituting them in the different part of the brain. The rehabilitation to regain the lost functions is a very promising field in the BCI application and has been utilized for various nervous system injuries [24].

Spinal cord injuries are a form of injury that damages the spinal cord resulting in partial or, in worse case, total paralysis. Restitution of movement for these cases takes years and is expensive. Rehabilitation sessions utilizing BCIs in the virtual reality settings or with exoskeletons (such as shown in Figure 2.8) and neuroprosthetis bring notable benefits, however it still requires a lot of trained professionals to guide the rehabilitation and expensive hardware [110]. The goal is to work towards a fully autonomous BCI that would help with the rehabilitation at home, such as in [25].
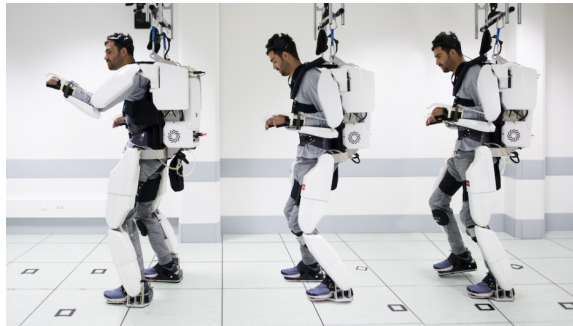
Figure 2.8: Use of an exoskeleton by a paralyzed man. Picture taken from [1].

Stroke is a leading cause of long-term disability and reduces mobility in more than half of stroke survivors [2]. It is a result of a cut-off of a blood supply to some part of a brain, which causes brain damage and subsequently loss of function. This loss can be permanent and include speech impairment, comprehension, memory problems or paralysis. Therefore, multiple BCIs for various body parts are being developed, utilising robotic replacement controlled by the brain to elicit a perception of a movement for these patients resulting in improvements in regaining the control over their body[12][31][99]. This movement restoration BCIs can also help patients with epilepsy, as their brain areas also get damaged. Additionally, it is also crucial to enhance the quality of life for post-stroke patients in case the stroke resulted in irreversible damage, for example controlling simple tasks at their home by the use of the brain signals [32].

Another use is stimulation of certain brain areas based on the information within the brain. Such BCI is proving to be crucial for treatment of patients with Parkinson's disease, which is usually accompanied by severe tremors [138]. One of the possible treatments is Deep Brain Stimulation - the electrodes are implanted into patient's brain, sending electrical impulses into the brain area to stimulate it. The already implanted electrodes can be used to also provide a feedback to control the timing of the stimulation, improving efficiency and efficacy [98].

Neurodevelopmental Disorders

Neurodevelopmental disorders affect the development of nervous system, which has an effect on emotion, learning abilities, self-control, memory and in some cases motor functions [115]. These disorders usually last lifetime. For these patients, BCI is used mainly for training - preparing patients for social situations, training their attention or improving their motor functions.

Children and adolescents being diagnosed with Attention Deficit Hyperactivity Disorder (ADHD) suffer from the lack of attention, excessive motor activity and impulsiveness [87]. BCI systems are already established as an effective complementary treatment for ADHD patients to offset several problems patients are facing [180]. BCI games to improve the attention of ADHD children were shown plausible, improving the attention span of patients over numerous training sessions [96]. With the addition of the virtual reality, these types of game-based trainings for various attention deficit disorders might over time prove very effective [145].

Autism Spectrum Disorder (most commonly known as autism), is neurodevelopmental disorder that can mostly be defined by the problems with social interactions, communication and restricted or repetitive behaviors [3]. BCIs are being utilized in conjunction with the virtual reality settings to assess the emotional levels and engagement levels for better autism intervention [50]. It is important, however, for these BCIs to not be reliant on any training, such as in motor imagery tasks, due to the low attention span of autistic patients [11]. It might be also possible to improve social skills of autistic patients [8].

Communication

Locked-in syndrome is a rare neurological condition, where a patient is completely paralysed and unable to voluntary control muscles, except for the vertical eye movement. The cognitive functions, however, remain undisturbed, meaning patients can perceive their surroundings, think and reason with usual capabilities [160]. BCI provides the means of communication, creating a direct path from the brain to an external world.

The conventional methods for these patients take advantage of the eye-movement and gaze tracking [179]. BCI spellers, were successfully utilized and provided faster information retrieval than conventional eye-movement ones[166]. BCIs for these patients are invasive, as their quality of life is so severely impacted, that having as precise signal as possible is a must [167]. There is a research in non-invasive BCIs for locked-in patients, but they are usually less accurate [65]. Non-invasive communication BCIs usually utilize spellers based on the P300 ERP and SSVEP paradigms.

2.4.2 Non-Medical Applications

BCI is still used predominantly in the medical applications, but it is evident, that industrial applications could also benefit enormously from the brain-controlled devices. There are several reasons why such applications cannot yet be seen on a day-to-day basis. Firstly, most commercially available BCI sets require a lot of electrode calibration prior to the recording, which takes a huge portion of experiment time. This is not an issue in medical setting, but it is a problem for inexperienced user who, ideally, should be able to use BCI device on his own. Secondly, only portable BCI devices are EEG and fNIRS ones. EEG is very sensitive to any electrical noise and most experiments are conducted in electrically shielded rooms. Moreover, EEG is also very sensitive to movement, which places a huge

constraint on the real-world applications. fNIRS might be the answer to these problems, but the research is still relatively young. Thirdly, it is a low accuracy and low transfer rate that might frustrate end-users. All of these points are reasons why it will take some time before any real industry used BCI [10] [27].

Gaming

The aim of the BCI within a game industry is to enable user to control movement-based actions through mental commands. There are already multiple games developed for the BCI, including classics, such as Pacman or Tetris [5]. A popular one, shown to the public many times, is a mind game Mentalista Foot, where two participants are instructed to move the ball into opponent's cage by concentration [2]. The games range from single player games to multiplayer, cooperative, logical or fighting - safe to say the BCI can be used in any game settings [3].

According to [6], the gaming industry will be the first one to use the BCI on a large scale when it will become industrially viable. However, in the current state, the BCI is not yet mature enough to be used in gaming widely. Along pitfalls mentioned in the section above, the BCI games suffer from the lack of appropriate game design, where ease of use is one of the most important aspects for gamers [27].

Industry

In the recent years, BCI started to draw attention of the various industrial areas to enhance work safety, train the employees more effectively or control devices [46]. Passive BCIs aim to monitor the mental state of a person from the brain signals, assessing their arousal levels or cognitive workload. This is crucial for work positions, where operator must be in excellent condition to make decisions, such as pilots [36], air traffic controllers or drivers [10]. The BCI could monitor driver's drowsiness level and mitigate traffic accidents [81].

Military

There are multiple areas in the military which would benefit from the mind-controlled devices. For example making complex multitasking operations more efficient, such as in [14], where the BCI is used to control drone-robot interactions, or controlling drone swarms, which might be a non-trivial task [90]. Other usages could be smart helmets with integrated dry electrodes for simple usage, for mental load monitoring and performing small tasks according to the intentions read from the helmet [83].

2.5   Challenges and the Future of the BCI

The BCI applications still have a long way to go and there are several pitfalls to overcome before the reliable and publicly accepted BCI.

Because each human brain works differently, there is a significant intra and inter-individual variability between different brain signals [147]. The BCIs are therefore all subject-specific and each subject must undergo training sessions. Long training times required for the successful completion of the task are tedious and users might lose motivation and interest.

---

[2]https://studio.mentalista.com/foot
[3]https://bcigamejam.com/pages/showcase2021.html

23

Moreover, it seems that some users cannot learn to control the BCI even after numerous trainings. This phenomenon is known as BCI illiteracy and affects a lot of MI research [165]. Another limitation to this might also be the mental state of the BCI user, which might negatively impact the performance. Fatigue and frustration were shown to lower the performance as well as attention [121].

For the medical applications, the BCI should ideally lower the number of trained professionals to guide the rehabilitation or training. As of now, however, the time and the resources put into this training in the medical centers are huge, which places a huge constraint on the availability. In the ideal situation, the patient would use this BCI at his home, without requiring any professional assistance and rehabilitate at his own pace, which might take months or years [157]. This long training times are also posing a problem, as the patients might, again, lose the motivation and determination to improve.

Although the EEG is the most popular modality for the BCI for now, there are numerous challenges that EEG has to overcome. Mostly, it is its susceptibility to the movement, where even the slightest movement can produce spikes in the signal, rendering it unusable. For any user-friendly BCI it is crucial to implement algorithms and techniques that mitigate movement artifacts [154].

Some ethical factors also play a role in the future of the BCI. As was mentioned above, the BCI for the locked-in patients enable them to have a connection with an external world. However, how do we obtain the informed consent to participate in the BCI in the first place [66]? In [66] it was also noted, that media creating catchy headlines regarding mind-reading or zero training BCIs might create false expectations within the public. It is important for the researchers to state the abilities and limitations of the BCI clearly as to avoid any misunderstandings.

When the BCIs become more popular, another problem might come up, such as privacy of the user or identification of a user through his unique brain signals [16]. If we can control the tremors of the Parkinson's disease now by implanting electrodes into the brain, what can stop us from the controlling the emotions one day? Or even person's actions altogether?

Emotional control and mind-reading, is, of course, seemingly far in the future as to not bother the researchers now. In the present, it might seem that the biggest challenge is that the researchers are sacrificing the easiness of the use in exchange for the results and performance [27]. The primary challenge for the future is to eliminate the above mentioned problems, such as users not being able to use the BCIs alone without the assistance of trained professionals and make the BCI more robust, so that it could be also used in the industry. The industrial use of the BCI is the most exciting one, because it offers many possibilities, but also places the most constraints. The devices must be comfortable to wear, must be portable and must be reliable to deliver the results it promised outside of the laboratory settings [46].

Chapter 3

Electroencephalography

Non-invasive Electroencephalography (EEG) is a way to measure brain's electrical activity by placing electrodes on a scalp that can detect it. It is a non-invasive method, that has an excellent temporal resolution, but suffers from the poor spatial resolution. Mostly thanks to the temporal resolution and relative low cost of the equipment, it is the most popular modality used for the BCI applications and also chosen as a modality for this thesis.

The aim of this chapter is to give a general overview on the EEG. It will explain how to record the signal and what are the general processing steps to acquire a signal without artifacts. The chapter will also talk about various types of analysis used in the field, their most popular methods and usage.

3.1   Signal Acquisition

To measure the electrical brain activity from the scalp, the appropriate recording setup is required. The EEG setup consist (mainly) of electrodes, amplifiers, A/D converter and a recording device. Electrodes capture the electrical signals, which are then amplified by amplifiers to bring it into the ranges suitable for accurate digitization. The A/D converter converts the analog signal to the digital signal, which is then stored on a recording device (for example a computer). This setup is depicted in Figure 3.1.
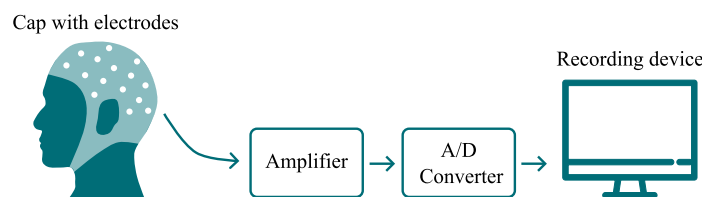
Figure 3.1: Data acquisition setup for EEG.

This section will first give an overview of the electrodes and their placement on the scalp and then it will talk about montages, which are essential for understanding what exactly the EEG signal represents.

3.1.1   Electrodes

Multiple electrode types exist and their usage depends on the defined task. The classical EEG electrode is a small disc made of silver and silver chloride. For these electrodes to

acquire a good signal a lot of effort needs to be put into their setup. Firstly, the skin under the electrode needs to be cleaned of imperfections and sanitized. Then, the electrolyte gel that facilitates the transfer of electric currents between the scalp and the electrode needs to be applied to the area, leaving the substance in the hair even after recording. The experimenters need to manually adjust the electrodes and reapply the gel to get a low electrode-skin impedance and good signal. This is a very time-consuming effort, more so with many electrodes, and is only suitable for clinical applications.

To mitigate this problem, dry electrodes were invented, that do not require any conductive substance and have a much quicker setup time. This is ideal for BCI applications, since the user should be able to set up a recording all by themselves. However, it suffers from the poor signal-to-noise ratio and therefore for clinical application, the gel electrodes are still considered to be the gold standard [69]. A good review of different electrodes and their usages can be found in [40].

Electrode Placement

For any results to be comparable between experiments, it is crucial to have an unified way to place the electrodes on the scalp. The widely used placement is called 10-20 placement, because it divides the scalp into a 10% and 20% sections, where the electrodes are placed relative to the other electrodes. This relative division ensures that the electrodes are placed over the same regions of the brain even when the head sizes of the people differ. The 10-20 electrode placement is shown in Figure 3.2. By the convention, the electrode name starts with the first letter of the lobe that the electrode is placed above and a number indicating the hemisphere and distance from the central line. Electrodes on the left hemisphere have odd numbers, while electrodes on the right hemisphere have even numbers. For instance, the electrode T8 would indicate the electrode placed to record activity from the temporal region in the right hemisphere.
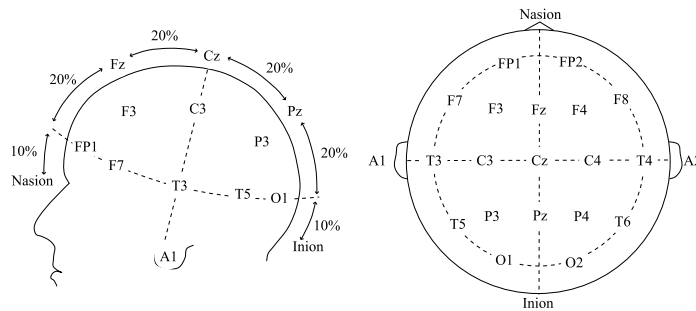
Figure 3.2: 10-20 electrode placement.

Adding more electrodes requires placing them proportionally in the empty spaces, resulting in the 10-10 systems or even 10-5 systems. The number of the electrodes to use depends on the experimental design and purpose. In research settings, researchers opt to use 64 or even more electrodes. It is debatable, what is the ideal number, although research indicates that 32 might be enough [114]. Naturally, more electrodes require larger setting time and therefore, for the BCI settings, researchers tend to use as few electrodes as possible, focusing their position over the brain areas associated with the task.

3.1.2 Montages

To successfully interpret the EEG signal it is important to understand that because of the amplifiers, the EEG signal is always recorded relatively to some other signal, called reference. This is depicted in Figure 3.3.
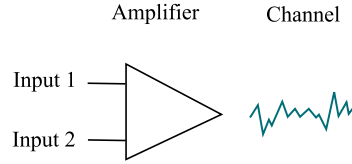
Figure 3.3: Resulting channel signals is a result of two different signals.

The montages define to what referential signal the electrode signal is relative to. Based on the montage, the EEG data interpretation can vary and so it is crucial to study the different results they can produce. The montages can be divided into two major categories - bipolar montages and referential montages.

Bipolar Montage

In bipolar montages, the electrode signals are referenced in pairs. Every electrode is connected to a different one to produce the resulting data. The most widely used bipolar montage is called double banana, for the characteristic chains on both hemispheres. Each electrode is referenced to the electrode that is next in chain, as is shown in Figure 3.4.
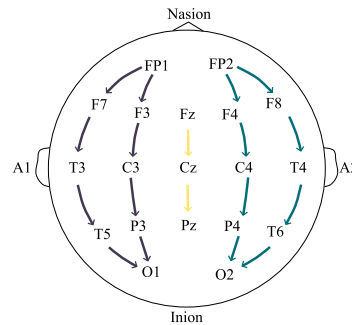
Figure 3.4: Double banana montage.

The main reason for using bipolar montages is a phase reversal. In case the first electrode recorded more positive signal then the second, the resulting signal is a downward deflection. Consequently, if the signal recorded on the first electrode is less positive than on the other electrode, the resulting signal would be an upward deflection. These deflections of different polarities are called phase reversals and because they are easy to spot in the recordings, they are the main reason the bipolar montages are used in the clinical studies as large deflections might represent areas of abnormalities.

The biggest disadvantage of the bipolar montages is the possible phase cancellation. If the electrodes contain very similar signal, they might cancel each other out, leaving no information from the area. That is one of the reasons the bipolar montages are not used in the BCI setting and referential montages are used instead. Another reason is their challenging interpretation as each electrode is referenced to a different signal and the fact that the first and last electrode in the chain might not have a reference at all.

Referential Montage

The referential montage compares all of the electrodes to one single reference, which can be one designated electrode or average of many electrodes. It is easier to interpret, since there is no phase reversal and the electrode with the highest amplitude waveform is really the one with the greatest voltage.

Referential montages aim to reconstruct the true EEG potentials from the scalp electrodes. For that, ideally, the reference signal should be zero. However, there is no single point on the body where the potential would be zero and therefore the reference will inevitably bring a noise into the data. This zero potential reference problem is shown in Figure 3.5.
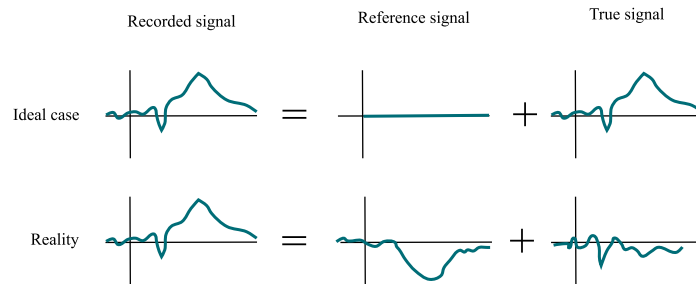
Figure 3.5: Recorded signal is a composition of the true signal and the reference signal subtracted from it [41].

Common Reference Common reference utilizes one designated electrode as a reference one. The referential electrode is placed on a body far enough from the recording site as to not pick up the signal of the interest. As was stated before, there is no place on a body with zero potential, so the reference will definitely bring some bias, but it will do so uniformly across the electrodes.

The placement of the referential electrode on a body can in theory be anywhere and a lot of researchers even opt to designate a one of the scalp electrodes as one. It is acceptable to do so if the reference signal is not in the area used in the analysis. It is also not recommended to use single electrode placed on one hemisphere, as that might bring uneven bias to the electrodes located on the other hemisphere. Electrodes from the central areas are the most ideal (Cz, Pz or Fz).

Most commonly used reference is called Linked Mastoids (LM), which is calculated as an average of signal from left and right mastoids. The idea behind LM reference is that it should pick up minimal signal from the body (either neuronal or other, such as ECG). In reality, however, it was proven to contain muscle artifacts, which distort the signal [177]. Still, its independence from the number of electrodes used in the recording makes it easy to compare different experiments between each other [174] and is therefore still a popular reference to use.

Average Reference The first attempt (in 1950 by [59]) in a zero-potential reference is an average reference (AR), which is calculated as an average of the sum of all electrode potentials. If there is a noise affecting all of the electrodes the same way, it should be reflected in the average reference and then subtracted from the data to obtain (in theory) the dereferenced solution.

However, this only holds true if we assume a sufficient electrode density with full head coverage, which means a large number of electrodes, otherwise the bias of the reference will still be present in the signal [41].

The AR reference is still most widely used in the clinical studies as a good approximation of the zero potential reference, as the number of electrodes used in those experiments is not a problem.

Reference Electrode Standardization Technique   Reference Electrode Standardization Technique (REST) developed in 2001 by [176], is an approach to reconstruct the EEG potentials with the theoretical zero reference. It has gained popularity as a re-referencing method (it cannot be used as a reference during the actual recording).

It aims to find a reference point at infinity, which is far from all the possible neural sources and thus has a theoretically neutral potential, which is used as an approximate of zero potential [44]. It was proven to be the best dereferencing method to study ERPs or EEG spectrum [93].

The REST method relies heavily on the head model, which might be biased because of the tissue conductivity or inaccurate segmentation [127]. It is not recommended to use it with insufficient number of electrodes (64 or more).

Choosing the Reference

To this day, the researchers cannot agree as to which reference should be accepted universally, which brings problems in the form of result interpretability, comparability and reproducibility across different experiments [177]. The resulting EEG data will differ substantially based on the reference used and it is therefore important to disclose the reference used when publishing any EEG results [144].

It is a normal practice in the EEG research to change the reference method after the recording when analysing the data, since the EEG data acquisition systems usually have a predefined reference that might not be suitable for the experiment type.

In the BCI applications, the reference used is either common or average one, depending only on the researchers. For clinical applications, average and REST references are considered a gold standard for majority of the use cases. In this thesis, average reference is used as a sufficient reference for the BCI applications.

3.2   Preprocessing of the EEG data

The true neuronal signal as generated by the action potentials is a very weak signal, easily disturbed by any interference. The signal that reaches the recording device is a sum of this true neuronal signal and noise, which can be a result of the environment or physiological processes affecting the body.

To study the brain, EEG data should be cleaned as thoroughly as possible to analyze it (which is the case for classical EEG analysis, not for deep learning approaches). To clean the data, multiple methods were developed to detect the unintended artifacts in the data and their subsequent removal.

3.2.1 Artifacts

EEG data is prone to many kind of artifacts which disrupt already weak neuronal information. In the clinical settings, the researchers usually try to minimize chance of anything interfering with the EEG data by conducting the experiment in the noise-proof environment and placing multiple constraints on the subject with respect to their behavior and movements. In the BCI settings, the artifacts have to be removed and, ideally, all of the neuronal information must be preserved.

EEG artifacts can be divided into two groups based on the source of the artifact - non-physiological or physiological.

Non-Physiological Artifacts

The artifacts that are due to the environment noise, poor grounding or bad electrodes are relatively easy to detect and correct, and usually lie outside of the frequencies of the useful EEG data and therefore can be simply filtered out.

The most common one is a line noise artifact, which is represented as a spike in frequencies of either 50 or 60 Hz (depending on the location). The line noise and its characteristic peak frequency is depicted in Figure 3.6. In most analyses, the researchers do not take into account frequencies above 40 Hz, as it does not probably contain much useful data (which will be talked more in Section 3.3.3) and thus effectively disregard the line noise altogether. In other case, a notch filter will reliably remove unwanted frequencies around power line frequency.
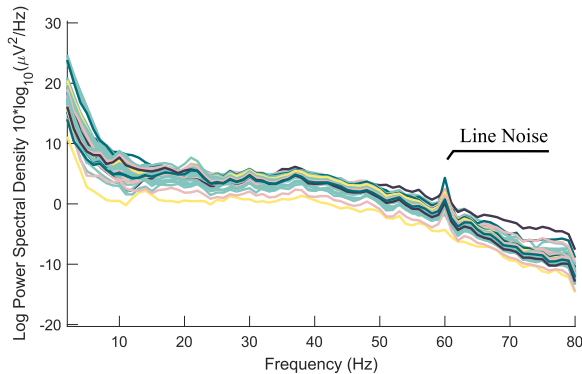
Figure 3.6: Frequency spectrum of multiple channels. The line noise of 60 Hz can be clearly visible, affecting all channels.

Electrode movement can drastically alter the signal, abruptly changing amplitudes. The electrode movement can happen because it loosened up from a cap, because some external object moved it or simply by just head movement and cap sliding. This poses several problems. Firstly, it renders the portion of the signal where the movement happened almost unusable. Secondly, electrodes changed the position (albeit slightly). This is crucial for BCI applications, as they should be prone to such noise. There is, however, no single solution to solve all motion artifact issues [154]. In the clinical settings, this problem is resolved by placing a constraint on a participant to move as little as possible and designing experiments in a manner that requires no movement whatsoever.

Another problem related to the electrodes is when its signal properties suddenly change, simply because the electrode lost connection to the acquisition device, resulting in the zero

signal, or because it lost connection with the skin resulting in the abnormal voltages. Apart from visual inspection to identify these bad channels several automatic methods are used to detect them without any human interaction. The bad channels can be identified by their abnormal amplitudes, lack of correlation with other channels, lack of predictability by other channels and presence of high frequency noise [17]. These channels can then either be omitted from the analysis, or can be interpolated from the signal of the neighbouring good electrodes. However, these interpolations do not bring any new information to the EEG data, as they are only reconstructed from already existing signals and therefore it is not recommended to interpolate more than 15% of the channels used.

Special kind of artifact to mention is a Gradient Artifact (GA), which is present in the simultaneous fMRI-EEG recordings. GA is a result of the MRI's machine magnetic field gradients, which induce current in EEG electrodes hundreds times larger than neural activity. As can be seen in Figure 3.7, the artifact renders the raw EEG signal completely unreadable, and must be removed from data. As its frequencies coincides of those the EEG, it cannot be simply filtered out. Because the GA is time-locked to the repetition time of the MRI machine, the most popular method is a template method, which creates an estimation of the artifact, that can be simply subtracted from the original data [23].
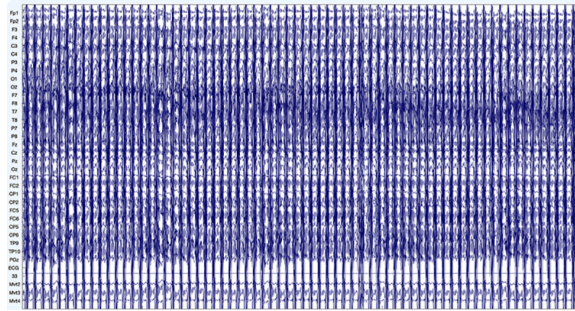
Figure 3.7: Gradient Artifact. Figure taken from [23].

Physiological Artifacts

One of the reasons why EEG is still not used widely in the industrial settings is also its susceptibility to physiological artifacts, inevitably created when performing tasks. Any kind of head or eye movement is visible on the recording, rendering any analysis potentially flawed. These artefacts sometimes coincide with the signal in a way that it is challenging to even detect them and over the years, various methods and algorithms were proposed to remove them from the data automatically. In the classical EEG research, many researchers choose to simply remove the corrupted segments of the data from the analysis and use visual inspection to detect them. This is impossible to do in the BCI settings as the BCI should be able to decode the brain signals in any situation automatically. Here, most common physiological artefacts are mentioned, along with possible solutions for their removal.

Eye Two types of the eye artifacts can be observed from the EEG signal - eye blinking and eye movements.

Eye blink artefacts are most common in any type of task-related EEG recording. They are visible as prominent high amplitude peaks of low frequencies, mostly occurring in the signal of frontal channels and slowly diminishing as the channels get further to the back.

Because they overlap the frequencies used in the EEG analysis, they cannot be simply removed from the signal by high-pass filtering. The artefacts as present in the EEG recording are shown in Figure 3.8a. It is evident from the picture, that the biggest amplitude changes are present at the electrodes FP1 and FP2, which are located at the very front of the head and therefore capture most of the artifact.
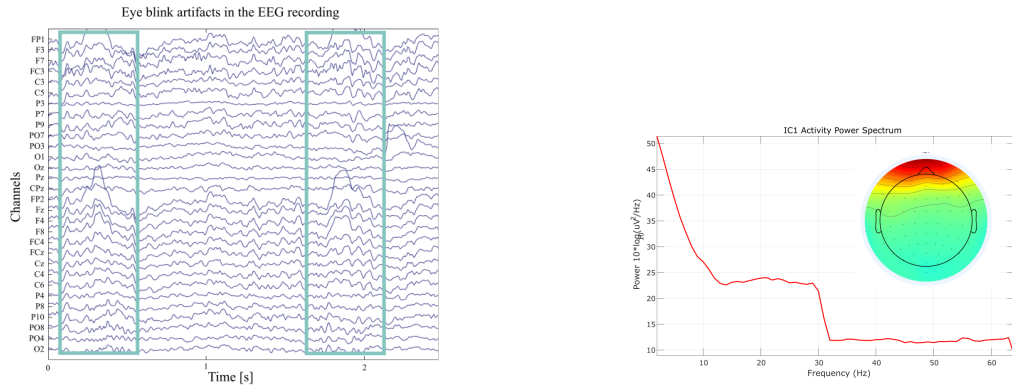
(a) Eye blink artifacts present in the recording.

(b) Independent Component Analysis on the EEG data - component representing the eye blink artifact, its frequency spectrum and topography.

Figure 3.8: Eye blink and its characteristics in the EEG recording.

There are multiple ways to remove the eye movement and blinks from the data. Multiple experiments utilized Electrooculogram (EOG). The eye acts as a dipole where the anterior pole is positive and posterior pole is negative. When the person is looking left, the cornea moves closer to the outer corner of the eye, which result in the negative potential difference being recorded. On the contrary, the right gaze, when the cornea moves closer to the inner corner of the eye, results in the positive potential difference. This potential differences are measured by placing electrodes around the eyes. For the eye blink artifacts, the electrodes are placed above and below the eye, and the sudden spikes represent the eye blink.

With the information from the EOG, the eye artifacts can be removed in regression based approach where the EOG channels are correlated with the EEG channels and subtracted from the data [70].

Naturally, adding more channels to specifically record one artifact goes against the principles of the BCI, which should ideally utilize as little channels as possible. Other popular method for artifact removal is based on the Blind Source Separation (BSS) approach, utilizing Independent Component Analysis (ICA) to separate the linearly mixed sources present in the sensor data. ICA does not assume any prior knowledge about the sources that make up the final signal. It is used heavily in the research community for artifact removal of the EEG, but relies on the visual inspection of the components, which even trained professionals might make a mistake in, and their manual removal. Furthermore, the components will never be perfectly separated, and some neuronal activity will inadvertently be removed. This is especially the case with the ERP research, where the removal of ICA components regarded as artifacts can potentially alter the ERP amplitudes and latency [139]. The component representing the eye artifact as a result of the ICA can be seen in Figure 3.8b. The topoplot shows high activity at the frontal regions, characteristic for the eye movements.

Other BSS methods were also utilized for the EEG artifact removal, such as Canonical Component Analysis (CCA) or wavelet based Independent Component Analysis (WICA).

Adaptive filters [29] or Wiener filtering [76] were proven to work well in removing the eye artifacts. Different machine learning based algorithms can also help to distinguish between the artifacts and the neuronal data, such as using Support Vector Machines (SVM) and BSS methods to help classify the eye artifacts [156] or simple K-Means to detect artifact patterns [103]. Deep-learning approach to artifact removal are still in the early stages of the research, but the already published results show promise in generalization ability, being able to remove noise successfully even among different trails [173].

Heart   Cardiac artifacts are generated by the electric activity of the heart and are represented by the Electrocardiogram (ECG). In the signal, they are present as a spiky artifacts, usually of low amplitude, but that also depends on the subject's body physique [73]. If the ECG is recorded simultaneously with the EEG, the ECG signal can be extracted from EEG by simple subtraction of averaged signals around spikes, however, this might potentially disrupt the signal. Another option is to use BSS methods as with any other EEG artifacts.

In the typical EEG recording, the heart artifacts are not very prominent and usually do not disrupt the neural data. They can be more visible in the recordings that use referential montages using earlobe electrodes A1 and A2. The one special case is the simultaneous fMRI-EEG recording, where the heart artifacts (in this case called Ballistocardiogram) is very prominent and interferes with the neuronal data. This is because of the changes in magnetic properties of the blood flow, which is influenced by heart [23]. Usually, the ECG is recorded along with the EEG and MRI data, to have a location of these artifacts. Then, either template methods similar to those used in the GA are utilized, or classical BSS methods, such as PCA or CCA [23].

Muscle   Muscle artifact is a high-frequency and high-amplitude artifact, that is present in the signal as a sudden burst of high frequencies (20-100 Hz) 3.9. Usually, it is caused by clenching or tightening of jaw muscles and is most evident in the signal from the electrodes in frontal and temporal region.

Because of their bursts, they are easily detectable in the signal by simply either temporally by their sudden change in the amplitude, or spectrally, by sudden change in the power. Most common methods to remove them are BSS methods [55].
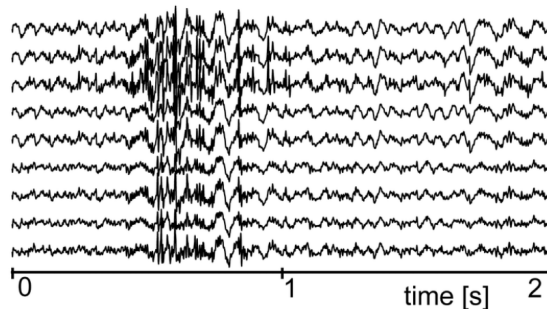
Figure 3.9: Muscle artifact in the EEG recording. Figure taken from [152].

3.3 Analysis of the EEG Signal

With the EEG data cleaned of any noise, it is possible to look at its signal properties to infer its characteristics. The EEG signal can be studied from various perspectives. Apart from the classical signal analysis in time domain, frequency domain and time-frequency domain, the EEG signal offers to also analyze the relationships between the signals from the different channels. It is also possible to construct models that would estimate the areas inside the brain that generated the resulting EEG data. The next sections provide a non-exhaustive review on the analyses that are used in the field of the EEG most frequently.

3.3.1 Source Localization

Source localization refers to the problem of finding true brain sources that generated the signal recorded by the EEG electrodes. It is important to understand that the signal captured by the EEG electrode did not originated at the exact location of the electrode. It is, in fact, a sum of many potentials originating from various sources, some even deep inside the brain. If it would be possible to reliably reconstruct the underlying brain sources, it would allow non-invasive and inexpensive insight into the real brain activity. This would prove crucial in localizing the epilepsy centers for instance.

Identification of the underlying sources requires a source model, a head model and the resulting EEG data. The source model is simply positions of sources in the 3D space. The head model defines how these sources end up generating the EEG data and that depends on two factors - the geometry of the head and the conductivity of various tissues. The estimation of the source model given the EEG data is called an inverse problem. In the forward problem, the source model of the brain signals is known and from it, the EEG data can be calculated. But source localization poses a problem inverse to that - the EEG data are available, but the true sources are unknown. This problem is considered ill-posed, since there are many solutions to this - multiple unknown sources contribute to the channel signal and also one source can contribute to many channel signals.
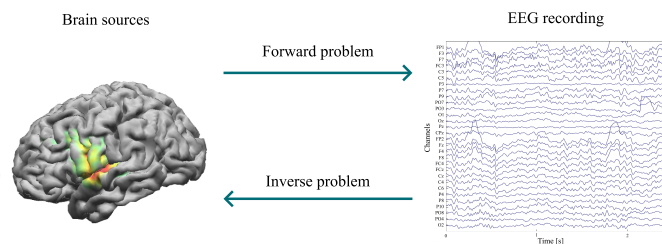
Figure 3.10: Forward and inverse problem in the EEG source localizing.

The methods to solve the inverse problem can be divided into two categories - parametric and non-parametric. The parametric methods assume the fixed number of dipoles apriori. Non-parametric methods do not make any underlying assumptions and use the data to infer the sources. Generally speaking, the parametric models are faster and require less data, but the result will contain some error because of the approximations. On the other hand, the non-parametric models might find the sources very precisely and reliably, but it will be a slower process requiring more data.

In parametric method, the apriori assumption is that only one or a few areas in the brain can generate specific signal measured by the electrodes. With this assumption, the dipole parameters that best explain the observed data can be determined by using different

optimization methods. The problem with parametric method is that in case the number of dipoles is underestimated, the source locations will be biased by the missing dipole. If the number of dipoles in overestimated, it might result in the estimated sources that in reality are not there [111]. The example of the parametric method is Multiple Signal Classification (MUSIC) [116], with its derivatives such as Recursively Applied and Projected MUSIC (RAP-MUSIC) [117] and truncated RAP-MUSIC (TRAP-MUSIC) [104].

The non-parametric methods for source localization mostly replaced the parametric ones. They do not make apriori assumptions about the number of dipoles. The first one was a Minimum Norm Estimate (MNE) [64], which estimates the amplitude of brain sources by finding a solution that best fits the observed data with minimum overall amplitude of brain activity. Among the derivatived of the MNE solution are Low Resolution brain Electromagnetic Tomography (LORETA), standardized LORETA (sLORETA), exact LORETA (eLORETA) and Local Autoregressive Average (LAURA).

3.3.2 Event Related Potentials

Event Related Potentials (ERP) are time-locked neuronal activity related to the onset of a specific task. They reflect the postsynaptic activity of multiple neurons in the same area that fire synchronously [163]. These activities are recorded with the EEG as very small waves, usually in the range of $\pm 10 \mu V$ and have to be extracted from the EEG recording. Sensory ERPs refer to the ERPs present approximately up until 100 ms and are usually vision or auditory related responses. After 100ms, the ERPs are linked with cognition and represent higher functions of the brain, such as reasoning or decision making. ERPs are defined by their amplitude and the latency, which refers to the time onset after the event. Based on these parameters, they are named either P (positive wave deflection) or N (negative wave deflection) plus their time onset. P300 which would mean a positive deflection at around 300 ms after the stimulus. The ERPs and their characteristics are shown in Figure 3.11.
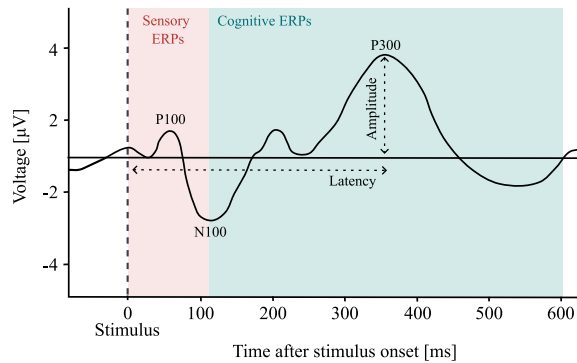
Figure 3.11: Different event related potentials and their characteristics.

The most commonly utilized ERP in the BCI is the P300. It has been linked to participant's engagement in the task of detecting targets and its latency and amplitude varies depending on the difficulty of recognizing the target [134]. There are multiple BCIs utilizing the P300, most common ones are spellers, where the participants are presented with a grid of letters an numbers. These symbols are then randomly highlighted on a screen. Highlighting of the letter that the participant wants to spell results in the P300 peak, whereas

highlighting any other symbols does not. The example of such speller is pictured in Figure 3.12.
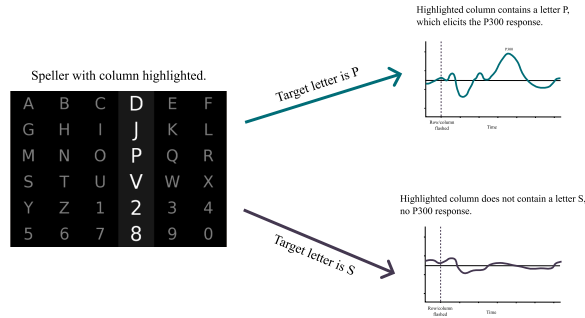
Figure 3.12: Example of a speller based on the P300 ERP.

In clinical settings, the ERPs have been used in the studies of drug addiction [47], reward processing [60], emotion processing [48], diagnosis [140] and countless other use cases.

3.3.3 Frequency Analysis

Frequency analysis of the EEG is one of the most popular and also very mature fields of the EEG analysis. It was observed very early on (1929) that certain frequencies present in the EEG signal can be mapped to specific brain functions, which has led the researchers to split the EEG frequency range into separate frequency bands. These bands will be explained in the next section.

Frequency Bands

When the large groups of neurons fire synchronously, the oscillations of certain frequency and amplitude can be observed from the EEG recording, which is evident from the rhythmic pattern of the signal [124]. These oscillatory patterns were discovered between the years 1929-1938 and were studied extensively since then. There are five major frequency bands all named after the Greek letters (Delta, Theta, Alpha, Beta and Gamma) and one which is crucial for analysis of the motor movement and MI (Mu).

Frequency bands are one of the most important characteristics of the EEG. They are studied heavily for their relationships with different task or for their characteristics in multiple diagnoses. Therefore in many publications and research, only specific bands are analyzed, disregarding the information in the other bands.

It is important to note that the frequency boundaries mentioned here are not fixed and many researchers use different boundaries, although usually they differ mostly $\pm$ 1 Hz.

Delta Delta waves represent oscillations with the lowest frequency but with the highest amplitude. They are defined by the frequency range lower than 4 Hz. Most commonly, they are associated with the deep sleep in the adults, where they are present in the frontal regions of the brain and are found posteriorly in babies. The presence of the delta waves during waking state in the adults is considered abnormal and can be an indicator of lesions in the brain [57]. The delt wave is depicted in Figure 3.13.

Theta Theta wave, as shown in Figure 3.14 represents the frequency range of 4-8 Hz and can be seen normally in young children. In adults, theta frequencies are present in a drowsy
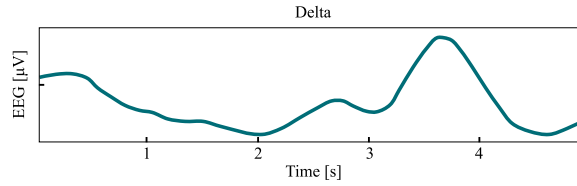
Figure 3.13: Example of the delta wave.

state, but can also be observed in meditation. The abnormal presence of the theta wave can be an indicator of lesions or even some brain disorders, such as depression [105].
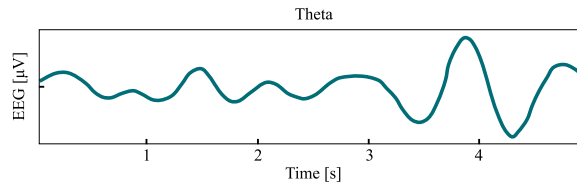
Figure 3.14: Example of the theta wave.

Alpha   Alpha frequencies (8-13 Hz) are very prominent during the resting state and relaxation. They mostly resemble sinusoidal signal, as can be seen in Figure 3.15. When relaxing with the closed eyes, the alpha frequencies are prominent posteriorly, mostly in the area of the occipital lobe. Opening the eyes diminishes these frequencies, but they can still be observed if the person is relaxing. They disappear during the task execution. Higher level of arousal were also reported to lower the power of the alpha frequencies

Studying and understanding the resting state of the healthy brain and comparing it to the resting states of the human brain with disorders can reveal important biomarkers, which could help with the diagnosis of the disorder. For example, the lower power of the alpha frequencies as compared to healthy subjects were found in the patients with depression [78]. In dementia, the alpha waves are replaced by the theta waves [148].
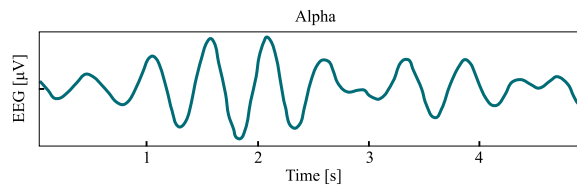
Figure 3.15: Example of the alpha wave.

Mu   Mu band's range is within the alpha range and is sometimes classified as only a sub-band of the alpha frequencies, usually between 8-15 Hz. However, it plays a different role in the EEG analysis. It is studied during the motor execution or MI tasks as it emerges when the hands and arms are idle and is supressed during the execution.

Beta   Beta frequencies (13-30 Hz) are symmetrically distributed over the brain and are usually observed over the frontal areas. They are associated with cognition, thinking, problem solving and active concentration. Prior to and during the movement, these frequencies are suppressed.

Asymmetry in the beta range, especially if the asymmetry is more then 50% may be considered abnormal (if also other indicators are taken into consideration). Excessive beta activity can be a indicator of ADHD, anxiety disorder or epilepsy.
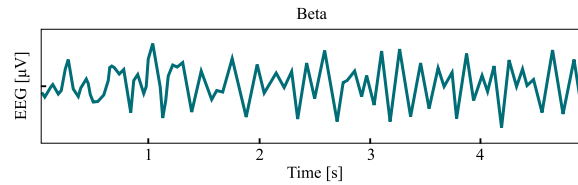
Figure 3.16: Example of the beta wave.

Gamma   Gamma waves are characterized by their low amplitude but high frequencies of over 30 Hz. There is still a debate whether the gamma activity represents any neuronal activities, although it has been linked with cognition, working memory and information transfer between different regions [107].

Frequency features

To transform the EEG signal into its representation in a frequency domain, the Fourier Transform (FT) and its algorithm Fast Fourier Transform (FFT) is utilized, resulting in a distribution of power spectrum over different frequencies.

When in frequency domain, the usual frequency features, such as total power can be inferred. Usually, the different frequency bands are compared to each other in terms of their total power or relative power. Below are the most common features and their example for the frequency analysis.

Peak Power and Frequency   Peak frequency is a frequency at which the maximum power of the signal occurs. This peak frequency can be calculated separately for each frequency band. For instance, it was shown, that the peak frequency of the alpha band lowers with aging [149]. While the people under 40 years of age have a peak alpha frequency somewhere around 9.8–10.5 Hz, older people tend to have an alpha peak frequency around 8.5–9.7 Hz.

Absolute and Relative power   Absolute power is the total power of the EEG frequency band, independent of the power of other bands. Relative power, on the other hand, is a ratio of the total power in a band compared to the other bands. For instance, when inspecting the resting-state EEG of a person with closed eyes, it is expected that the alpha band will be the most dominant one, having the highest relative power. Another example are patients with depression, as their absolute power of the alpha frequency in the occipital region is lower then in healthy patients [78].

Spectral Edge Frequency   Spectral Edge Frequency (SEF) refers to the frequency below which 80-95% (depends on the publication) of the total power is located. The SEF is an established feature to measure the state of the anesthesia. When the person is awake and resting, the usual values of the SEF fall between 18-20 Hz. During the deep stage of anesthesia, the SEF values fall between 12-14 Hz [151].

Brain Symmetry Index Brain Symmetry Index (BSI) compares power of the left and right channels. The perferct symmetry is obtained if BSI=0, the perfect asymmetry when BSI=1. Brain assymmetries were found for instance in relation to the dominant hand of a person - greater right alpha power as compared to the left alpha power were found in a right-handed people and vice versa [128].

Naturally, there are many other frequency features used in the field of frequency analysis. Usually, the frequency features are compared to the other bands, between different tasks or between healthy and diagnosed subjects.
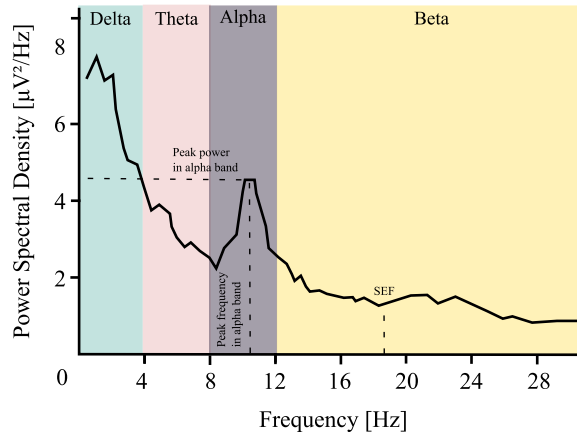
Figure 3.17: Frequency analysis of the EEG signal - frequency bands and features.

3.3.4 Time-series Analysis

The EEG signal can also be analyzed in a time series analysis, which helps to understand its statistical properties over the time. Mostly, they define the complexity of the data.

Entropy The entropy can be defined as the degree of disorder or uncertainty in a system. Measure of the entropy in the signal processing assesses the complexity of the signal. Higher values of entropy indicate less predictability of the signal, while low values indicate completely predictable signal. Entropy measures in the time domain generally break up the signal into segments that are then compared for similarity. There are numerous methods to calculate entropy of a signal, for instance sample entropy, approximate entropy or Composite Permutation Entropy Index (CPEI).

Entropy measures were used in the anesthesia studies to detect the stage of the anesthesia [95], to characterize the depth of a sleep [77] assessment of the cerebral injuries [34] or detection of epilepsy seizures [175].

Other measures that quantify the complexity of the EEG signal are Fractal Dimension [4], Hjort complexity [63] or Hurst exponent [142].

3.3.5 Time-Frequency Analysis

Combination of frequency information with respect to the time brings more in-depth insights into the underlying function of the brain. The frequency analysis alone gives an information about the underlying frequencies of the whole signal, but the signal from brain is non-stationary, so it changes over time.

The first attempts at localizing the frequency at the given time moment came as a Short Time Fourier Transform (STFT). STFT segments the signal into a series of (overlapping) windows, calculating the Fourier transform for each window. The question arises as how to choose the appropriate window. If the window chosen is too big, the frequency information would be precise, but the time information would be lost. Conversely, if the window is too small, not all frequencies of the frequencies can be captured, although, they could be pinpointed precisely at time. The result of the STFT is a spectogram, from which frequency at each time point can be observed.

An alternative approach is the Continuous Wavelet Transform (CWT), which decomposes a function into a set of wavelets. Wavelet can be defined as a wave or oscillation that is localized in time. It has two properties - scale, which is related to frequency and location, related to time. Just like a Fourier Transform is convolving input signal with complex sinusoids of different frequencies, in CWT, the input signal is convoluted with the wavelet of different scales and locations. The result of the CWT is scalogram.The difference between the spectogram and scalogram can be seen in Figure 3.18. The Discrete Wavelet Transform (DWT) differs from the CWT in terms of scale and position parameter. In CWT, this choice is arbitrary, while in DWT it is not.

(a) STFT and complex exponentials.

(b) CWT and wavelets.
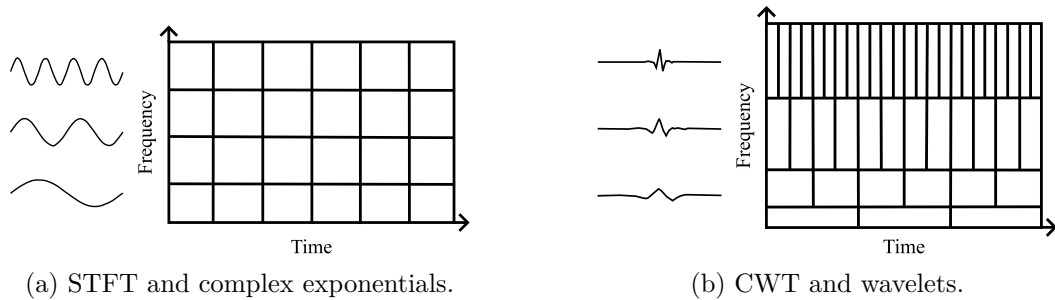
Figure 3.18: Difference between STFT and CWT for time-frequency analysis.

There are numerous wavelets to choose for the analysis, each suitable for different analysis. Most used ones according to [51] are db4 and Morlet wavelets, both shown in Figure 3.19.

(a) db4 wavelet.

(b) Morlet wavelet.

Figure 3.19: Two most used wavelets in CWT and DWT.

Time-frequency analysis has been used extensively in detection of the seizures [88] and epilepsy [51], as both of these are characteristic for their abrupt changes in the signal frequency. It also has been utilized in sleep analysis, for example for detecting sleep spindles [182].

3.3.6 Connectivity Analysis

Connectivity analysis explores the communication between different brain regions. Executing any task requires a coordinated flow of information between areas that are functionally connected. For instance, to grab an object a person must first look at the object and gain a visual perception of it, which would activate primary visual cortex area. To grab the object, the execution of the movement would activate a primary motor area and so on.

The connections between different areas were discovered as early as in 19th century, when Broca and Wernicke identified areas responsible for language. Modern neuroimaging techniques facilitated the discovery of many networks. Seven of these networks are considered major ones, but there are multiple others as no simple task has a single designated area in a brain, but rather requires cooperation of different ones. The major networks include the visual, sensorimotor, dorsal attention, limbic, default, central executive and salient one.

The main purpose of the connectivity analysis is to understand how the brain operates under different conditions. This might be helpful in the diagnosis, as different medical conditions might alter the functioning of the brain, which can be apparent from the modified interaction between areas during specific task.

With respect to the EEG, the connectivity analysis represents the comparison of signals recorded from different areas and finding influences or synchronizations that would reveal communication flow between these areas. This can be done on a source level or sensor level, depending on whether the relationship between areas is calculated for the already localized sources or if its calculated from the channel signals directly. The advantage of sensor level connectivity analysis is the saving of the computational power over the source level analysis, but in return might provide less accurate results.

On the highest level, the methods can be divided into two categories - functional connectivity and effective connectivity. Functional connectivity defines a non-directed relationship between signals. It is possible to conclude from the functional connectivity that there is a certain relationship between the signals, but it is impossible to say whether it is one signal influencing the other or vice versa. Effective connectivity, on the other hand, defines a directed measure of influence between the signals.

In the next section, some methods for connectivity evaluation are mentioned, but this is by no means an exhaustive list, as there are countless different approaches. A good review of the topic can be found in [13].

Functional Connectivity

The simplest measure of the functional connectivity can be a Pearson's correlation coefficient, which measures the linear correlation between two sets of data. The relationship between two EEG signals can hardly be explained as linear, and therefore mutual information or Spearman's Rank Correlation might be a better measure, since it explains also non-linear relationships and interdependence between signals [13]. All of these measures ignore the temporal information of the data and the results would be the same if the samples of the signals were mixed up.

To retain the time information, cross-correlation is used more frequently. It compares two time-series data and measures how well these two signals match with each other and when in time is this match mostly pronounced, thus inferring the information about the time delay between the signals.

In frequency domain, coherence measures the frequency dependent correlations of brain activity measured by two or more brain sensors [19]. It determines how similar the power spectra of two signals are.

Coherence is however, heavily affected by the effects of the volume conduction. When one true source inside of a brain is effecting two different sensors in the same way, the similarity between the signals might be high, even though in reality, there might not be any connection at all. One way to tackle this problem is to look at the phase information of the coherence. Ideally, when the regions communicate between each other, some time passes between the processing in one region and then sending signal to the other one. Zero phase delay would indicate instantaneous information flow, which is usually suspicious and is attributed to the volume conduction.

Another way to solve this problem is to calculate the coherence from the sources and not from the sensors [111]. Taking only imaginary part of the coherence into consideration as it was shown that the volume conduction strictly affected only the real part of the coherence [125].

Effective Connectivity

Granger causality is one of the most popular methods for evaluating directed relationships between sensors. The idea is that if one signal has some relationship with other signal, its future values can be predicted by that other signal.

Firstly, the future values are predicted solely as a weighted sum of the past values of the first signal S_1 and compared to the actual future signal, resulting in some error, e_1. Secondly, the future values are predicted not only based on the past values of the S_1, but also based on the past values of a different signal, S_2, resulting in e_2. Variances between the two errors are compared. If the variance of e_1 is smaller than the variance of the e_2, the S_1 can be better represented only by its own past values, indicating no relationship with the S_2. If the variance of the errors is smaller for e_2, the S_2 signal does contribute to the S_1, therefore revealing its influence over the S_1.

Granger causality can be implemented for both time domain as well as frequency domain. The interpretation of the Granger causality is dependent on the experiment. It is argued, it is more suited to compare the connectivity of different regions between experimental conditions, rather then revealing the connectivity itself [155] [161].

Pitfalls of the Connectivity Analysis

Connectivity analysis has many pitfalls, which renders it tricky to use. Volume conduction, processing steps and different types of analysis make it challenging to compare results between the studies [113]. The reference chosen for the EEG analysis is crucial. When common reference is used, the same signal is subtracted from each electrode, possibly compromising all of the channels the same way. This has a huge impact on the connectivity analysis, which might find a non-existent relationship between locations [13]. There are multiple other problems linked to noise, sample sizes or system dynamics [13]. It is important to note that even though there are many variables affecting the connectivity analysis, it is not useless or unimportant, it just has to be interpreted very carefully.

3.3.7 Microstate Analysis

Microstate analysis is one of the newer fields of the EEG with a lot of unexplored potential. It gained attention thanks to the work of Koening and Lehmann in 1999 [84], when they studied the dynamics of the brain potentials at rest in healthy and schizophrenic patients. Both of the authors are still prominent figures in the microstate analysis field. Its popularity surged when the notions about the resting state of the brain started to be challenged. Previously, it was believed that the brain remained inactive during the rest and only an incoming stimuli would prompt an action. However, further research showed that the brain is active even in the resting state to optimally respond to the incoming stimuli [54]. This led to a lot of research in identifying the resting state networks and their characteristics.

The microstates can be defined as transient, patterned, quasi-stable states or patterns of a multichannel EEG potentials [112]. These states remain prominent in the brain for about 60-120 ms before rapidly transitioning to another state. It might seem that the topographies at different times during a spontaneous brain activity are random, but multiple research proved that only a handful of states are actually present among topographies (usually only 2 - 7 microstate maps are enough to explain 90% of the analysis time [171]). Therefore, from the microstates it can be observed that the topographies of the brain electrical activity do not change randomly and continuously, but rather remain stable and then change abruptly.

There are multiple steps to identify the maps and they will be described in the next sections. When the maps are already derived, multiple features can be extracted from them.

Global Field Power

The first step is to obtain the input topographies that would be then used to infer the global states. Most of the research opt to extract only topographies that are based on data observed at Global Field Power (GFP) peaks, where the signal-to-noise ratio is optimal and topographies are considered stable. The GFP is defined as:

$$GFP = \sqrt{\frac{(\sum_{n=1}^{M}(V_n(t) - \tilde{V}(t))^2)}{M}} \tag{3.1}$$

where M is number of channels in the recording, $V_n(t)$ defines recorded potential in time t and channel n and $\tilde{V}(t)$ represents the average potential of all channels at time t. The topographies at the peaks (local maxima) of GFP, where the spatial variability across channels is highest, are further considered for clustering. The GFP is depicted in Figure 3.20 (1).

The choice of the reference can impact the microstate analysis as it might alter the GFP peaks. Usually, the AR is used, but the authors in [71] argued that using the REST reference produced more objective maps.

Clustering and back-fitting

After extracting the relevant topographies, global microstates are found by clustering. Multiple clustering algorithms across the research can be seen, but the most usual are modified K-means (and also different variants of K-means algorithm such as Fuzzy C-means) as defined in [131], Topographic Atomize and Agglomerate Hierarchical Clustering (TAAHC) or Principal Component Analysis (PCA).

The modified K-means has usual steps of a classic K-means algorithm. Firstly, n random topographies are chosen as representatives of a cluster. Then the solution is found

iteratively, performing two steps in each iteration - assignment of the topographies to the current global maps based on the correlation and then recalculation of the global maps representing the cluster. The TAAHC represents a bottom-up approach, where all of the topographies are firstly clustered into the pairs that are the most similar and in each iteration the clusters are again paired together until the desired number of clusters is reached.

With all of the aforementioned methods the number of clusters is determined by the researcher beforehand. In the resting state research, the microstates were already studied so heavily, that the 4 microstate maps are well established and used in most of the cases. As will be later evident from Section 3.3.7, 4 microstate maps are also standard in many other tasks, when researchers do not even consider a different number (which is advantageous for comparability between different research but might not be as much for the identification of the maps themselves). One can look at the GEV of the maps and choose the number of them that explains at least 70% (or other defined percentage) of the data. Other criterions, such as Krzanowski–Lai criterion and its normalised version, cross-validation criterion or dispersion can be used to infer the ideal number of clusters.

Resulting global maps are then used to back-fit all of the data. The input data need to be assigned the label and in case of the microstate analysis, the usual approach is a winner-takes-all. At each data point, the topography must be represented by exactly one global map. To calculate the similarity of the global map and instantaneous topography, usually the measure used is orthogonal squared distance between the vectors as defined in [131]. Minimizing this distance is equivalent to maximizing the squared correlation between the two maps. Therefore for each topography over time, the global map with the highest correlation will be chosen as a label for that topography. The clustering and back-fitting to the data is represented in Figure 3.20 (2) and (3).

To ensure that the global microstate maps are a good representation of the data, General Explained Variance (GEV) which measures the percentage of data variance explained by a given set of microstate maps is usually calculated. For instance, the K-means algorithm relies heavily on the initialization of the topographies and optimal maps might not be found. The common approach then is to run the clustering algorithm arbitrary number of times and choose the run with the highest GEV.

Features

After the clustering, microstates can be analysed in terms of their duration, occurrence, coverage or transition probabilities. The duration refers to the mean time in milliseconds that a microstate is active. This can be anywhere from 50 to 250 ms and can be different for multiple conditions. The occurrence is simply number of times a microstate occurred in the data and coverage refer to the percentage of all of the time the microstate was active.

Hidden Markov Models (HMM) are used to model the transition probabilities between the different states.

Applications

Microstates for the resting state are already well defined and consistent across multiple research, as can be seen from the review in [112]. These maps are shown in Figure 3.20 (2). They play a key role in a different application and have already been connected to the underlying brain activities in the simultaneous EEG-fMRI studies [119]. For instance, microstate D has been linked to the cognition and might be linked to dorsal attention
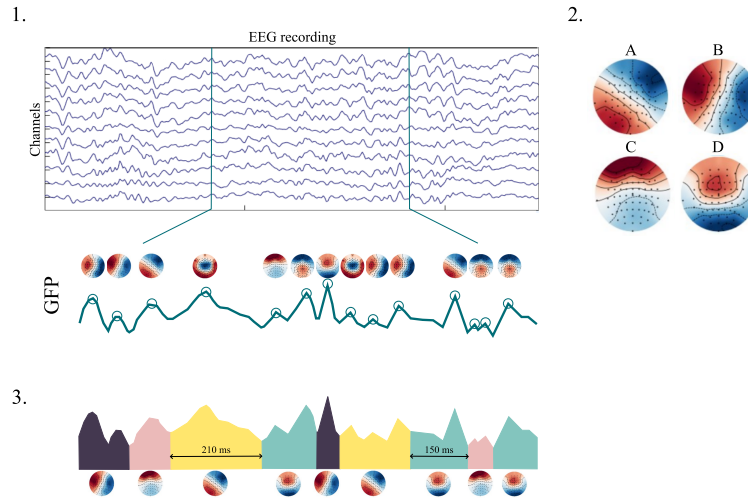
Figure 3.20: Steps of the microstate analysis. 1) Finding the GFP and extracting topographies at the local maxima. 2) Clustering of the topographies and finding the global microstates. 3) Back-fitting to the data.

network [20]. The microstate C was shown to be more prominent in the resting state than in any other states and it believed to be associated with the default mode network [153].

Microstate analysis has been used extensively in schizophrenia research [92], autism [18] or sleep [21]. Microstates have also been studied in relation with the working memory, where the studies indicate that it is possible to predict a performance based on the microstate dynamics [120][164].

Not a lot of work has been done with regards to the task-related microstates apart from the memory or other cognitive tasks such as mental arithmetic. The microstates are advantageous in their temporal characteristics, as they can exploit fast-pacing processes happening on the whole-brain scale. The relationships between different microstate maps might reveal more information about how brain works not only in the resting state but in different tasks settings as well.

Microstate Analysis of Motor Imagery

There is a lot of research already done regarding the microstate analysis of the resting state, where it is utilized to identify the differences between the microstates of the healthy patients and the diagnosed ones. Regarding the microstate analysis of the motor movement or MI, it has not been so heavily studied and there is a great deal of room for improvement and for novel approaches. As of the time of writing this thesis, searching on Scopus revealed only 8 articles regarding the keywords EEG, microstate and motor movement or motor imagery. Their short description and microstate maps identified for them are present in the Table A.1.

Only in three of those articles, the authors were distinguishing between the left and right movement (two imagined movement and one real movement) and others were focusing on identifying the maps for different motor execution tasks or motor imagery tasks in general.

The most notable takeaway from the articles is that most of them identified the states comparable to the ones found resting state. In [137], the authors noted that states of

ongoing spontaneous activity are also commonly active during behavioral tasks, which was supported by multiple research.

For the work that focused on distinguishing between the left and right movement, the only distinction across research was the difference between transition probabilities [100]. However, none of the articles tried to find the maps specific to the left or right imagery as they only derived the maps from the whole recording using all of the electrodes. In [100], the authors only focused on the mu band, which is the frequency related to the ERD/ERS phenomena of the motor execution.

The very limited number of articles regarding the motor imagery and microstate analysis indicate that this field has a lot of potential in the research. The temporal resolution of the microstates in theory makes an ideal candidate to study a fast changes in the brain, which is ideal for the BCI applications. Hence, in this thesis, it is proposed that microstates and their combination with other features may be explored for the BCI application.

3.4 Summary

All of the aforementioned methods can be used in the BCI settings. For the preprocessing, the methods used in the BCI must be fully automatic and fast so that they could transform the data reliably in the real-time. Usually, various automatic BSS methods based on the ICA are utilized to detect and remove the artifacts from the data. Same constraints apply to the feature extraction and analysis methods. The summary of the analysis methods, their usage in the EEG-based BCI paradigms described in 2.3 and their advantages and disadvantages can be found in Table 3.1.

Table 3.1: Comparison of different analysis methods with regards to the BCI, their advantages and disadvantages.

Analysis Methods	BCI Applications	Advantages	Disadvantages
Time, Frequency and Time-Frequency Analysis	MI, SSEP	Very well studied field with lot of references and proven concepts.	Non-stationarity and non-linearity are the fundamentals of the EEG. Any changes in state or mood can significantly alter the studied signal and even after profound research on these methods, the BCI is still not robust enough.
ERP Analysis	BCI based on the P300, error detection in the BCI	ERPs represent spontaneous brain activity and ERP-based BCI require little user training.	Low accuracy, hard to detect the desired ERP component on a single trial basis.
Source Localization	MI	Determining the true sources proven highly informative for the MI BCI [181].	Not well studied in the BCI settings
Connectivity Analysis	MI, evaluation of the performance	Robust to artifact and inter-subject amplitude variability.	Inconclusive results between the studies [91], not researched enough in the BCI settings.
Microstate Analysis	/	Microstates show a consistent results across different tasks and in between participants.	No prior BCI attempts.

The time-frequency (and subsequently time and frequency) analysis has been the most extensively used in the field of the BCI so far. In the recent years, other methods, such as source localization and connectivity analysis have also proven to be informative and can reveal features discriminative enough to distinguish between different states (mainly in the context of the MI task). Microstate analysis have not yet been explicitly used in the BCI application. Microstates have already been replicated across different tasks and individuals, which might indicate their robustness and their great temporal resolution is beneficial for the BCI. Therefore this thesis focuses on microstates and their combination with different features as a proposed solution to the BCI.

Chapter 4

Proposed solution

The aim of the thesis is the construction of the EEG based BCI for the motor imagery task. The general proposed solution is depicted in Figure 4.1 and is comprised of the appropriate dataset selection, data preprocessing methods, data extraction methods and the classification of the MI based on the microstate analysis, frequency analysis and time-domain analysis. The novelty of the proposed solution is in optimizing microstates for the classification of the MI task.
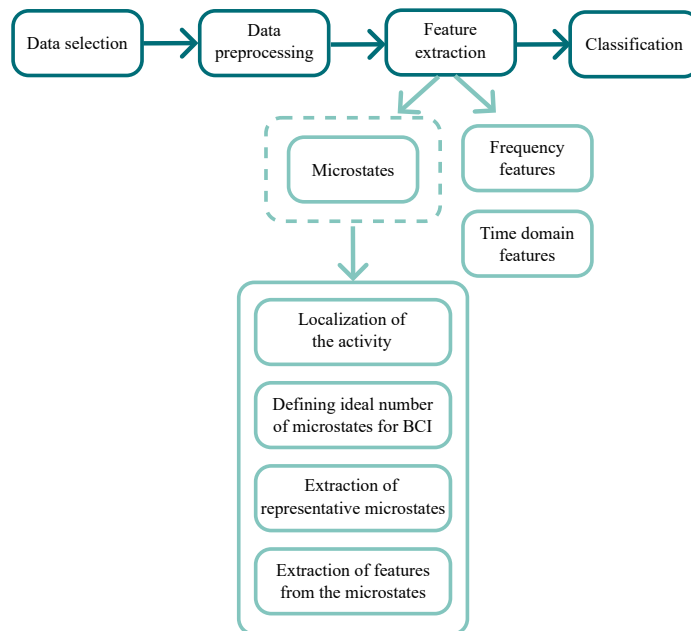
Figure 4.1: Thesis proposed solution.

Data selection For the purposes of the thesis, the dataset selected needs to contain the instances of the left/right MI and the instances of the rest in between the tasks, collected from multiple subjects to test the proposed solution on multiple participants.

Preprocessing The data preprocessing is a crucial step in the pipeline and for the BCI applications in general, all of the preprocessing methods need to be fully automatic and able to work in a real-time settings. The proposed solution consists of the data re-referencing,

data filtering and artifact removal to obtain clear EEG data. The reference chosen is an average one, as it is considered a gold standard for most of the EEG applications. For the data filtering, simple band-pass filter between 8 - 30 Hz is proposed as this includes all of the meaningful EEG frequency bands commonly found during the motor tasks. For the artifact removal, the thesis proposes the utilization of the BSS methods, such as automatic wICA for the real-time removal of the artifacts. Additional bad channels or bad segments of the data will be handled using statistical methods for the bad channel/EEG data detection.

Microstates   The thesis proposes a novel method of the feature extraction for the BCI and that is a microstate analysis for the MI task. This includes multiple steps: localizing the activity during the MI task, determining the optimal number of the microstate maps, clustering the derived microstate maps and then extracting the meaningful features out of them. This pipeline is depicted in Figure 4.2.
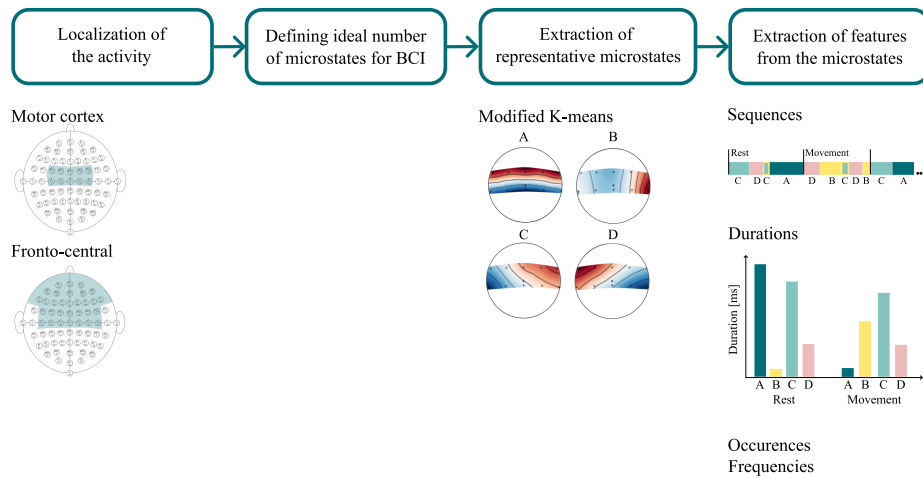
Figure 4.2: Proposed pipeline for the microstate analysis for the BCI application.

Localizing the activity means finding the maps only from the region that is associated with the motor execution and MI. For this reason, three different regions are proposed and compared with each other.

For the establishment of the ideal number of the maps, the thesis proposes the classification accuracy as an indicator of the number of the maps required. Additionally, the maps have to have reach at least 70% of the GEV to be even considered for the classification purposes.

For clustering of the maps, the widely used modified K-means algorithm will be implemented, as it is faster then TAAHC, which is crucial for the BCI application. The thesis proposes that the different tasks (left/right hand MI and rest) will be differentiated based on the features extracted from the microstate sequences.

Feature Extraction and Selection   The features extracted from the data are proposed to be: microstate features, time-domain features and frequency features as all of those were previously used for motor imagery classification. For the microstate features, also ones that are not usually used in the literature, such as microstate transitions recurrences are considered as well.

Classification The classification is proposed to be done on a subject-level. The data from one user from one experimental run will be split into the training data to extract the microstate features and then classify the intent from the rest of the data. This mimics the usual BCI usage pipeline, where the classifier is trained for each subject and this classifier is then used to predict the intentions of the user in during the next sessions. Additionally, two separate classifiers are proposed - one for the classification of the rest versus activity segments and one for the classification of the left and right motor imagery segments.

4.1 Dataset Selection

To analyze the MI of left and right hand and their respective microstates, the dataset collected by [150] was used. It contains data from 109 participants each performing 14 test runs:

- 1 minute of baseline task with eyes open
- 1 minute of baseline task with eyes closed
- 3 x 2 minutes of opening and closing of the fist (either left or right)
- 3 x 2 minutes of imagining opening and closing of the fist (either left or right)
- 3 x 2 minutes of opening and closing either both fists or both feet
- 3 x 2 minutes of imagining opening and closing either both fists or both feet

Participants were seated in front of a monitor with their arms resting on the arm rest. In the task regarding the fist clenching, the targets appeared on either the left or right side of the screen and participants were instructed to open and close the corresponding fist for the duration of the cue. In fist and feet task, the cues appeared either on top or the bottom of the screen. The task and rest periods alternated and thus each task data were divided into the 4 second sections of rest and 4 second sections of task. The experiment protocol can be seen in Figure 4.3.
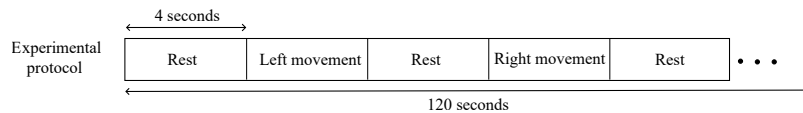
Figure 4.3: Experiment protocol - alternating conditions in the recording.

The data is a 64-channel EEG recording with the electrodes positioned according to the standard 10-10 system. The electrodes used and their locations are depicted in Figure 4.4.

4.2 Data Preprocessing

The data for the analysis are proposed to be preprocessed using the MATLAB toolbox EEGLAB [37] and PyPREP library [9] in Python. The data will be stored in the MNE [61] structures, which is a Python library for EEG and MEG data processing and analysis.

The data will first be filtered with a band-pass filter between 8 Hz an 30 Hz. Then, the channels will be re-referenced to the average reference.
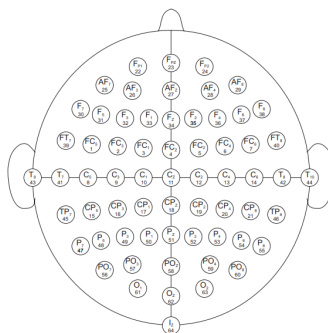
Figure 4.4: Electrodes and their positions used in the dataset. Figure taken from [150].

4.2.1 Wavelet Independent Component Analysis

Additional artifacts such as eye blinks and eye movements can be detected by the wavelet ICA (wICA). When performing a standard ICA on an EEG data, the components that are considered artifacts are rejected as a whole, assuming that the component contains 100% of artifact data. That is, however a false assumption, as there will always be some neuronal data present in the component and by rejecting the component, all of that data will get lost. The motivation behind a wICA is to filter out the actual artifacts from the components themselves and reconstruct the signal with the corrected components.

The component can be divided into the artifact (localized high amplitude) and neuronal activity (evenly spread out lower amplitudes). Wavelets provide and excellent way to detect the high amplitude artifacts in time-frequency domain. The steps included in the wICA are therefore following:

1. Application of classical ICA on a raw data EEG and obtaining N independent components.

2. Using wavelets to transform the components into a time-frequency domain.

3. Thresholding the wavelet coefficients - set them to 0 if they are higher then some threshold. This will eliminate prominent artifacts but keep the neuronal activity.

4. Reconstruction of the EEG from wavelet corrected components.

4.2.2 Bad channel handling

Some channels will always deviate from the others, which might pose problems with identifying the relevant maps. Therefore, automatic detection of the bad channels and their subsequent interpolation is proposed using the PyPrep library, which is a Python implementation of the MATLAB software described in [17]. Bad channels are detected using 4 different criteria - deviation criterion, correlation criterion, predictability criterion (using RANSAC [53]) and noisiness criterion. In-depth description of the methods can be found in [17]. The channels marked as bad were interpolated using the spherical spline interpolation as described in the [132] and implemented in the MNE.

Additionally, the data is proposed to be bandpass filtered between 8 and 30 Hz, which includes alpha, mu and beta band - all associated with different stages of motor movement or motor imagery.

4.2.3 Interpolating bad epochs

Muscle artifacts or sudden movements might render some parts of the EEG signal completely unusable and the high noise might completely overshadow any neural activity. In research it is a common practice to identify the bad epochs manually just by visual inspection, but this process is very ineffective, even if it usually yields more clean data (or at least that is a general consensus after discussing this topic with several people in the field of EEG). However, this practice is not scalable and also very often not reproducible.

In this thesis, the automatic rejection and interpolation pipeline for Python called autoreject [74][75] is proposed to be utilized. The goal of the autoreject is to identify the epochs that are deviating from the rest of the data and possibly repair them by interpolation based on the electrode neighbors. This is achieved by defining an electrode-wise rejection threshold as opposed to a global rejection threshold (such as when comparing a peak-to-peak threshold from all electrodes to peak-to-peak amplitude of one electrode). This ensures that even if the electrode has a different amplitude then the rest of the electrodes (since the placement of the electrode over different areas might make a difference in the signal amplitudes), the data from it will not be automatically excluded.

For each data epoch, data from each electrode is separately marked good or bad. If there are more than k bad electrode data in the epoch, the epoch is marked as bad and should be excluded from the dataset, since there will not be enough good electrodes to interpolate the bad ones. On the other hand, if there is less than k bad electrode data, then interpolate the first ρ bad ones and keep the rest as is (as they are not the worst in the epoch, there is a possibility that they are just false positives). The example of the bad epoch interpolation/rejection is shown in Figure 4.5.
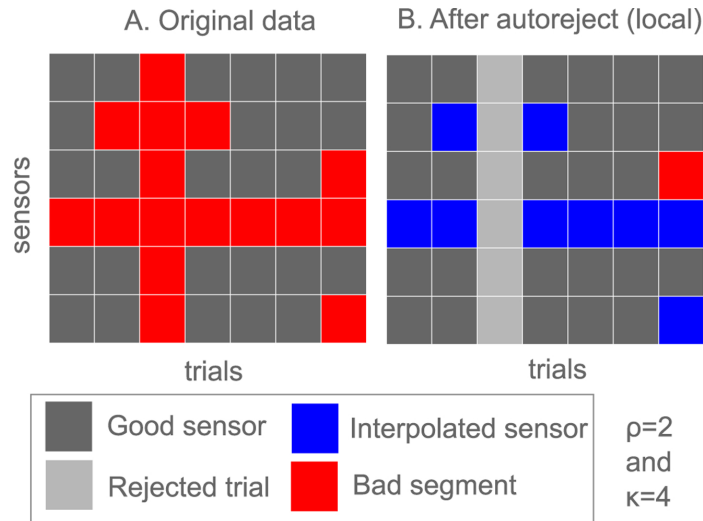
Figure 4.5: Segments of the epochs are either interpolated or the whole epoch is rejected, based on the parameter k (if there are more than k bad segments, reject the whole epoch) and ρ (interpolate ρ worst epochs). Figure taken from [75].

In the end, the data was divided according to the participant and task, creating epochs. For each participant, the data from MI and motor execution task was studied separately to identify any similarities between the two. Data of one task from one participant (for instance MI of left and right hand) was concatenated and separate epochs were extracted

that contained only rest data, left hand MI data and right hand MI. The resulting data for one participant were:

- 7 epochs of left hand motor execution/MI, each 4 seconds.
- 7 epochs of right hand motor execution/MI, each 4 seconds.
- 15 epochs of rest in-between the tasks, each 4 seconds.

4.3 Microstate Analysis

4.3.1 Localization of the Microstates

Three approaches for the microstate localization are proposed. Firstly, only the motor cortex area is taken into consideration, as that is the area primarily activated during the motor execution and MI task. The electrodes corresponding to this area are FC3, FC2, FC1, FC4, C1, C2, C3, C4, Cz, FCz and are shown in Figure 4.6a.

Second approach is to choose the electrodes on the motor cortex along with all of the frontal electrodes. The frontal lobe is responsible for decision making and it was proven to be also activated during the motor execution and MI.

Third way is to find the microstate maps from all 64 electrodes used in the recording, which might reveal more complex relationships between the brain areas.

The electrodes corresponding to the areas are shown in Figure 4.6b.

(a) Electrodes in the motor cortex area.

(b) Electrodes in the fronto-central area.

(c) All electrodes used.
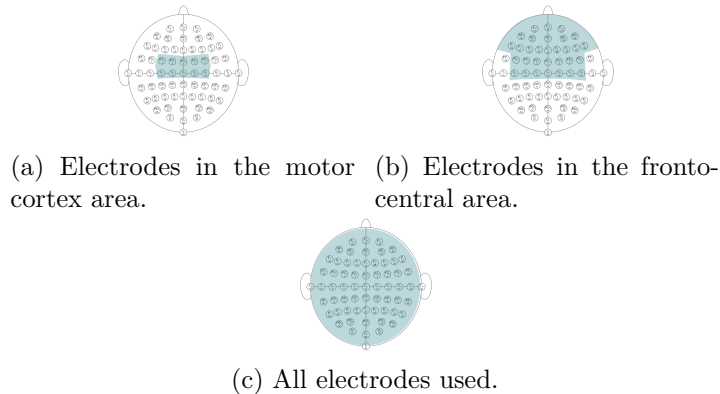
Figure 4.6: Proposed selections of the electrodes for the localized microstates.

4.3.2 Number of Microstates

The thesis proposes to define the ideal number of microstates with regards to the classification results on a subject level. In the literature, the ideal number of maps is usually chosen as a number of maps for which the GEV exceeds some arbitrary threshold value. However, the number of maps chosen this way might not accurately reflect the number of maps ideal for the classification.

4.3.3 Map Extraction

The pipeline of extracting the microstates and back-fitting them back into the data is depicted on 3.20. The clustering algorithm chosen for this analysis is a modified K-means

algorithm as proposed by the [131] and implemented in the Python library for EEG microstate analysis Pycrostates [52].

Equations explaining the modified K-means algorithm are based on the original work in the [131] and [169]. Modified K-means are based on the linear model of the EEG data, where each EEG topography X at some time i can be modelled as a linear combination of a global map A and some residual error ϵ:

$$X_i = \sum_l \alpha_{il} A_l + \epsilon_i \tag{4.1}$$

Solution can be found by minimizing the cost function:

$$\sum_i ||X_i - \sum_l \alpha_{il} A_l|| \tag{4.2}$$

Because the microstate analysis assumes that only one global map can represent the topography rather than their linear combination, the $\alpha_{iL_i} = 1$ and $\alpha_{il} = 0$ for $l \neq L_i$.

The minimum of the cost function is found iteratively. Assume n microstate maps to represent the EEG data. Firstly, n random topographies extracted from the GFP peaks are assigned as a prototype microstates. Then in each iteration, two steps are performed - assignment of the labels to the existing topographies and recalculation of the prototype maps. The labels are assigned based on the maximum correlation between the prototype map A_l and the topography X_i:

$$C_{il}^2 = (\sum X_{ij} A_{lj})^2 \tag{4.3}$$

where j represents a channel index. The corresponding labels for the topography L_i can then by found by:

$$L_i = \underset{l}{\operatorname{argmax}}(C_{il}^2) \tag{4.4}$$

Recalculation of the topographies based on the labels found this iteration is defined as:

$$A_l = \underset{U}{\operatorname{argmax}} U' S_l U \tag{4.5}$$

where the maximum is computed across all ch-dimensional column vectors U, where ch is number of channels, subject to $||U|| = 1$ and

$$S_l = \sum_{i:L_i=l} X_i' X_i \tag{4.6}$$

The convergence is assessed by the relative change in residual variance proportional to:

$$\sigma^2 \propto \sum_i \sum_j X_{ij}^2 - (X_{ij} A_{Lij})^2 \tag{4.7}$$

The stopping criteria can either be a convergence threshold (for instance setting a $\sigma^2 = 10^{-6}$) or fixed number of iterations. Usually, both of these condition are defined and the algorithm stops when either of them is met. Because the K-Means algorithm is prone to the initialization steps, namely choosing the first n topographies as prototype mas, multiple runs of the algorithm are usually performed and one with the highest GEV is chosen. GEV is calculated as:

$$GEV = \sum_l GEV_l \tag{4.8}$$

where

$$GEV_l = \frac{\sum_i \sigma_i^2 C_{il}^2 \delta_{l,L_i}}{\sum_i \sigma_i^2} \tag{4.9}$$

where $\delta_{l,L_i} = 1$ for $l = L_i$ and is 0 otherwise.

The proposed method to extract the microstate maps consists of two different approaches. The first approach is a subject-level extraction, where the maps are extracted only from one subject. This includes maps being extracted separately for each condition in the dataset (rest, left, right). For each condition instance, the maps are extracted and then grouped together with the maps found in the other instances of the same condition. The representative maps then go through the second round of the clustering to extract the representative maps. This multiple level clustering is a common practice when extracting the maps from multiple participants to find a topical maps representing some condition. The first two levels of clustering are shown in Figure 4.7.
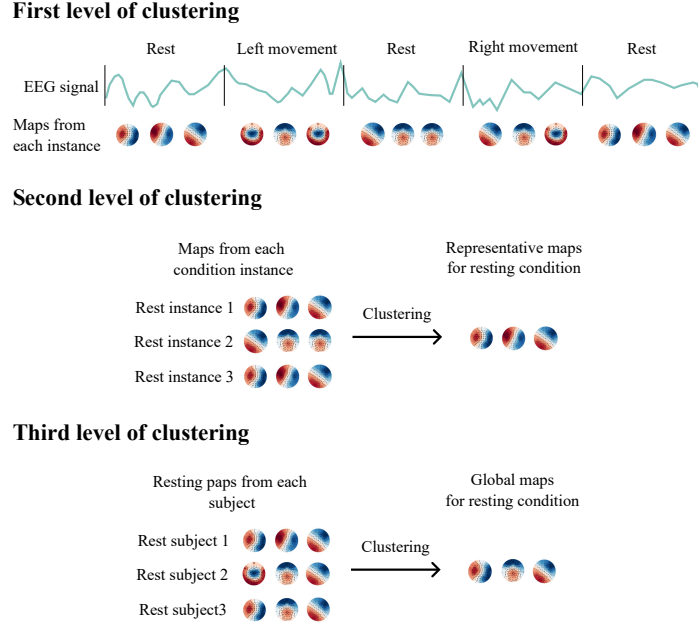
Figure 4.7: Levels of clustering in the process of microstate extraction.

The map extraction from each condition separately aims to find maps that could be specific only for the given condition and differentiate well between them. If the maps were extracted from the whole recording, the specific condition maps might not be as much represented when compared to others, and therefore when clustering they might be considered just as outliers. After the maps for each condition specifically are extracted, they are grouped together to form one set of maps for the experimental run. This is done because some maps are found consistently across different conditions and even across different subjects (such as resting state maps). The maps that have a spatial correlation higher than 0.8 shall be considered the same map. The example for clarification is depicted in Figure 4.8.
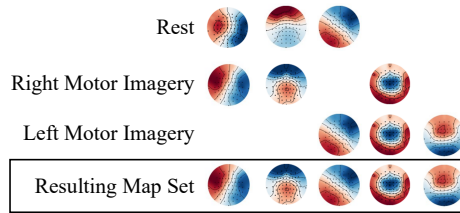
Figure 4.8: Resulting set of maps is derived from maps extracted from the conditions.

4.4 Feature Extraction

Multiple features are proposed for the classification between the experimental conditions. They include microstate features, frequency-domain features and time-domain features.

Microstate Features

After the microstate map extraction, the maps are fitted back to the data. At each time point of the recording, map with the highest correlation as defined in the Equation 4.3 is chosen as a representative of that time. This results in a sequence of map labels extracted from the recording.

Microstate Time Statistics   Each microstate map within a sequence can be quantified in terms of its time characteristics. Proposed time features are: maximum length of a microstate map found in the data, minimum length of a microstate map, mean length of a microstate map and standard deviation of lengths of microstate maps. All of the features can be seen in Figure 4.9. Mean, maximum and minimum duration were already used as a features in multiple studies.
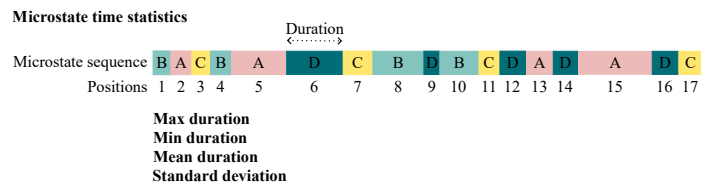
Figure 4.9: Time statistics of the microstate sequence.

Microstate Occurrence and Contribution   Microstate occurrence refer to the mean number of times a map occurs in one second. The contribution of a map is calculated as occurrence times mean duration. Contribution is more telling of how much map is really present in the recording then occurrence or mean duration. The occurrence and contribution is depicted in Figure 4.10.

Feature inferred from the occurrence is recurrence of an occurrence, which defines mean times between the map appears again in the sequence. Occurrence recurrence is depicted in Figure 4.11.

Microstate Transitions   Transition between the microstate A and B is defined as number of times A was followed by the B in the sequence, divided by number of times the A was followed by a different microstate, pictured in Figure 4.12.
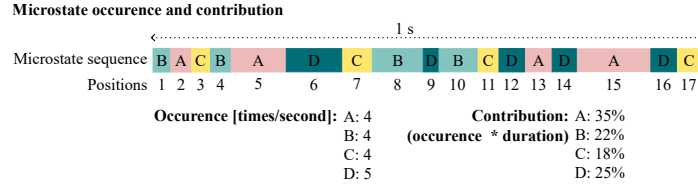
Figure 4.10: Occurrence and contribution of a microstate in a sequence.
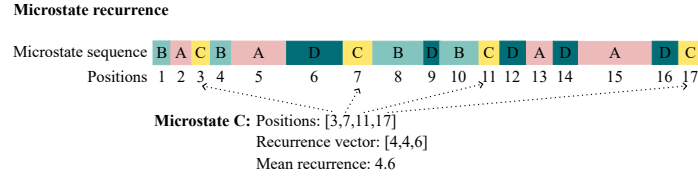
Figure 4.11: Recurrence of occurrence of a microstate in a sequence.

Similarly as with the occurrence, transition recurrences can be inferred from the transition probabilities - Figure 4.13.

Frequency-domain Features

Absolute Power   To estimate the Power Spectral Density (PSD) of the signal in the different frequencies, Welch's method is proposed, as it has been used extensively in the field of the EEG. Since the data is bandpass filtered between 8 and 30 Hz, it leaves only two bands for the analysis - alpha and beta. Power in alpha frequencies is dominant in resting states, but its mu sub-band can distinguish between movement and resting state. Beta frequencies are present in the EEG especially in the frontal lobe as an indicator of mental activity (which motor imagery is). The alpha (8-13 Hz) and high beta powers (20-30 Hz) are calculated for each channel separately, resulting in the 64 features respectively for each segment.

Relative Power   Relative power of a band can be calculated as PSD of the band, divided by the sum PSD from all bins for each frequency bin between the frequencies 8 and 30 Hz:

$$\text{Relative alpha} = \frac{\text{Alpha power}}{\text{Power across the whole spectrum}} \tag{4.10}$$

It expresses how much a frequency band is represented in the signal. The EEG signal, for instance, has a high relative alpha power in the resting state conditions. For the purposes of the thesis, relative alpha as well as relative beta are considered as features.

Asymmetry   Asymmetry (Brain Symmetry Index - BSI) can be expressed as a ratio of band powers between two areas and therefore calculated as:

$$\text{BSI} = |\frac{\text{Power A} - \text{Power B}}{\text{Power A} + \text{Power B}}| \tag{4.11}$$

The greater the power in two regions differ, the higher the asymmetry is (0 - the power in two regions is identical, 1 - the power between two regions is completely different). For the asymmetry, three different region splittings are considered:

57
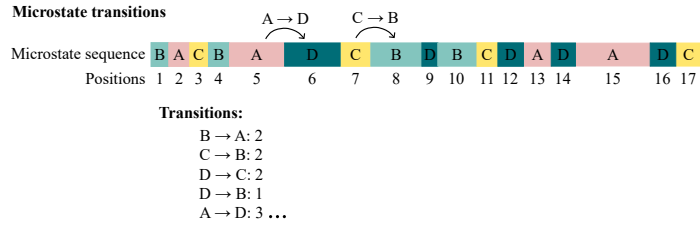
Figure 4.12: Transitions of the states within a microstate sequence.
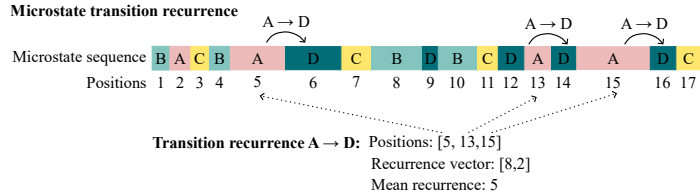
Figure 4.13: Recurrence of microstate transitions in a sequence.

1. Asymmetry between the hemispheres - the powers from all left or right hemisphere electrodes are averaged and compared.

2. Asymmetry between the areas (frontal, occipital, temporal, parietal, central).

3. Asymmetry between individual electrodes from left/right hemisphere.

Time-domain Features

Time domain features were extracted from the data utilizing the Python library Antropy[1].

Approximate Entropy Approximate Entropy (ApEn) examines the time series of a signal to find similar epochs - the more of a similar epochs the signal contains, the smaller the value of the ApEn is [136] since when the signal gets more predictable, its entropy should also be as little as possible. The similarity of the epochs is based on the distance metric as well as a threshold value. If the distance between the two pairs is smaller then some value, they are considered to be of a same template. This is depicted in the Figure 4.14.

The ApEn is then calculated as:

$$ApEn = \sum -log\frac{1 + A_i}{1 + B_i} \tag{4.12}$$

For applications, it is crucial to select the right values of m as well as the threshold value r. While m is usually set to be 2 (3 in some cases), the r varies on the application. It is recommended to be set as a $0.2 * (variance of data)$.

ApEn has some notable disadvantages (dependent on the length of the data and lack consistency across different datasets) and that is the reason why alongside ApEn, the Sample Entropy is also utilized.

Sample Entropy Sample Entropy (SampEn) is similar to the approximate entropy, but the equation to calculate it is:

---

[1]https://github.com/raphaelvallat/antropy

Template of length m+1

Series of samples
similar by some
threshold r

Template of length m=2
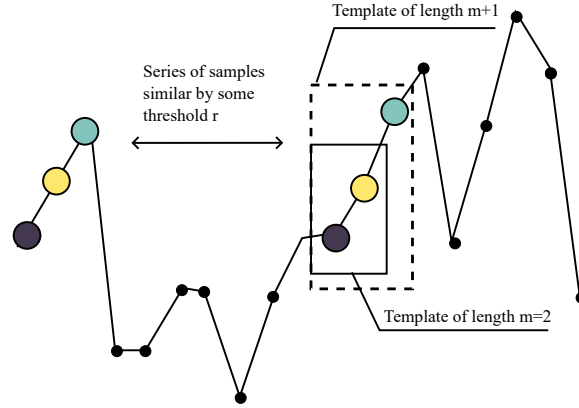
Ai - number of matches with template *i* of length m
B*i* - number of matches with the template *i* of length m+1

Figure 4.14: Approximate Entropy.

$$SampEn = -log(\frac{\sum A_i}{\sum B_i}) \quad (4.13)$$

It has two advantages over the ApEn:

1. Independent of the data length.

2. Easier to implement and computationally faster.

Hjorth's Parameters The Hjorth's Parameters are statistical properties of the signal in the time domain, used heavily in the field of the EEG. There are three parameters calculated:

1. Activity - simply a variance of the input signal $y(t)$:

$$Activity = var(y(t)) \quad (4.14)$$

2. Mobility - mean frequency or the proportion of standard deviation of the power spectrum:

$$Mobility = \sqrt{\frac{var(\frac{dy(t)}{dt})}{var(y(t))}} \quad (4.15)$$

3. Complexity - estimate of the bandwidth of the signal, indicating the similarity of the shape of the signal to a pure sine wave:

$$Complexity = \frac{Mobility(\frac{dy(t)}{dt})}{Mobility(y(t))} \quad (4.16)$$

Fractal Dimension Fractals are mathematical sets with a high degree of geometrical complexity that can model many natural phenomena [106]. The fractal dimension is therefore an index of complexity, which shows how a detail in a pattern changes with a scale at which it is measured and complexity of EEG signal measured by fractal dimension presents self-similarities across different scales [45].

There are multiple ways how to estimate the fractal dimension of a signal and for the purposes of this thesis, three are considered: Higuchi's, Katz's and Petrosian. In [49] it is argued that careful selection of the appropriate fractal dimension approximation is crucial, as for instance Higichi's fractal dimension is more sensitive to noise. Therefore all three were considered for the thesis:

- Higuchi Fractal Dimension [68] - given a signal X of length n and parameter $k_{max} \geq 2$, for each $k \in \{1, ..., k_{max}\}$ and $m \in \{1, ..., k\}$ define the $L_m(k)$ as:

$$L_m(k) = \frac{N-1}{|\frac{N-m}{k}|k^2} \sum_{i=1}^{|\frac{N-m}{k}|} |X_N(m+ik) - X_N(m+(i-1)k)| \quad (4.17)$$

The length $L(k)$ is then defined as average of all $L_m(k)$ values and the Higuchi fractal dimension is is defined as the slope of best-fitting linear function through the data points:

$$\{(log\frac{1}{k}), logL(k)\} \quad (4.18)$$

- Petrosian Fractal Dimension - for the time series of $x(1), x(2), ...x(N)$ and waveform signal consisting of $\{y_1, y_2, ..., y_N\}$ the sequence is first 'binarized' as:

$$z_i = \begin{cases} 1, & x_i > mean(y) \\ -1, & x_i \leq mean(y) \end{cases}, i = 1, 2, ...N \quad (4.19)$$

The total number of adjacent symbol changes in sequence is defined as:

$$N_\Delta = \sum_{i=1}^{N-2} |\frac{z_{i+1} - y_i}{2}| \quad (4.20)$$

And finally, the Petrosian fractal dimension is calculated as:

$$D = \frac{logN}{logN + log(\frac{N}{N+0.4N_\Delta})} \quad (4.21)$$

- Katz Fractal Dimension - the fractal dimension of a signal (x_i, y_i) is defined as:

$$D = \frac{log(N)}{log(N) + log(\frac{d}{L})'} \quad (4.22)$$

where N is a length of signal and and:

$$L = \sum N - 2_{i=0} \sqrt{(y_{i+1} - y_i)^2 + (x_{i+1} - x_i)^2} \quad (4.23)$$

$$d = max(\sqrt{(y_{i+1} - y_i)^2 + (x_{i+1} - x_i)^2}) \quad (4.24)$$

Katzd fractal dimension is a little slower to compute than Petrosian one, but still faster than Higuchi fractal dimension.

4.5 Feature Selection

The thesis proposes a to select the best set of features that can discriminate between different conditions based on the recursive feature elimination with cross validation (RFECV). The feature matrix with all of the proposed features are input into the RFECV and fitted to the selected estimator. Features are ranked based on their predictability and the least important feature(s) is eliminated. The new set of features is used to train a classifier again and the cross-validation accuracy determines whether the new feature set is to be selected as a resulting one or whether to continue eliminating more features. This process is shown in Figure 4.15
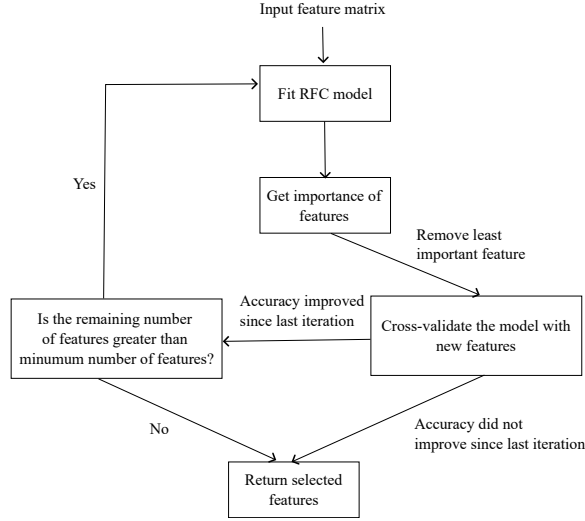
Figure 4.15: Recursive feature elimination with cross-validation.

The estimator chosen to eliminate features is Logistic Regression. To overcome overfitting issues, the L_2 penalty, known as ridge penalty is utilized:

$$\lambda \sum_{j=1}^{p} \beta_j^2 \tag{4.25}$$

4.6 Classification

Classification of the movement imagery or the resting state is proposed to be done on a subject level, which is a common practice for the BCI applications. Two levels of the classification are proposed:

1. Classify the condition instance as either rest instance or movement instance.

2. Based on the results of the previous classification, in case of movement instance classify the instance as left imagery condition or right imagery condition.

Multiple levels of the classification are proposed to differentiate between the motor imagery conditions. With regards to the microstate analysis, different number of maps as well as different areas of extraction of these maps might differentiate between the conditions better. The hypothesis is, that the maps that differentiate between the rest versus activity conditions might have patterns more in the frontal area as opposed to the motor cortex

61

area and conversely, there could be a map that has a distinct pattern in the motor cortex area for the distinction between the left and right motor imagery.

It is proposed to choose the classifier with the appropriate parameters by cross validation. The proposed classifier is Random Forests. Random Forest classifiers are an ensemble learning method widely used for classification tasks. They are built upon the concept of decision trees and operate by constructing multiple decision trees during training. Each tree is trained on a random subset of the original data and features, and the final prediction is determined through a majority vote of the individual tree predictions. This aggregation of predictions helps improve the model's accuracy and generalization ability compared to individual decision trees. One of the key reasons why Random Forest classifiers do not overfit is due to the random sampling of both data and features for each tree. This introduces diversity among the trees, preventing them from memorizing the training data too closely. Additionally, Random Forest classifiers incorporate techniques like bagging and feature randomization, further reducing overfitting tendencies by promoting model variance while controlling bias. As a result, Random Forests can effectively handle noisy data, high-dimensional feature spaces, and avoid overfitting, making them ideal for the thesis task, since number of features compared to the number of the training samples is disproportionately high.

4.7   Summary

The comprehensive summary of all the proposed steps is as follows:

1. Preprocessing

    (a) Bandpass filtering between 8-30 Hz
    (b) Reference: average
    (c) Artifact removal with wICA
    (d) Additional bad channel identification and interpolation with PyPrep.
    (e) Additional bad epoch identification and rejection/interpolation with Autoreject.

2. Feature Extraction

    (a) Time-domain Features
        - Sample Entropy
        - Approximate Entropy
        - Hjorth's parameters: Complexity and Mobility
        - Fractal Dimension: Petrosian, Katz and Higuchi fractal dimension approximations

3. Frequency-domain Features

    (a) Alpha/Beta absolute power (channel-wise)
    (b) Alpha/Beta relative power (channel-wise)
    (c) Alpha/Beta Assymetry (channel pair-wise an region-wise)

4. Microstate Features

    (a) Duration: mean/max/min/std duration

(b) Transitions, transition recurrences

(c) Occurrences, occurrence recurrences

(d) Contribution

5. Feature Selection - Recursive Feature Elimination with Logistic Regression

6. Classification - Random Forests

Chapter 5

Implementation

The implementation and testing was done in Matlab and Python. Matlab was utilized for the initial parts, specifically for the identification and removal of the artifacts.

5.1 Preprocessing and Feature Extraction

The preprocessing pipeline is depicted in Figure 5.1. The raw data (64 channel EEG) were first loaded into the EEGLab [37] structures, which make handling of the EEG data very easy. The primary reason why Matlab was chosen for some part of the preprocessing is the wICA implementation proposed in [26] provided in the Matlab code. First, the data were filtered using the Butterworth filter in the range of 8-30 Hz and rereferenced using the average reference. wICA was applied to the filtered data and the number of components for it was set to 64 (same as original number of channels).

Next step was the interpolation of the bad electrodes. The bad electrodes were identified and interpolated using the pyPrep library as discussed in the previous chapter. For that, the data from Matlab were loaded into the Python's MNE structures. The parameters for the pyPrep pipeline were kept at default.

After the interpolation, the data were epoched - each experimental run that included either motor imagery tasks or real movement tasks was segmented using rolling windows of length 1 second and overlap of 0.5 seconds. This resulted in the segments of the shape $(n, 160)$, where number of segments $n \approx 247$. The labels for the segments were given according to the conditions - 0 if the segment was from rest condition, 1 for left motor imagery (or real movement) and 2 for right motor imagery (or real movement). The segments that were in-between the different conditions were labeled as -1 and were excluded from training and testing.

Subsequently, the autoreject tool was used as discussed in the previous chapter to repair or reject epochs that may still (even after the wICA and filtering) contain some artifacts. The autoreject pipeline was run with the bayesian optimization and other parameters were kept at default as was recommended by the authors of the library. The output is a reject log as illustrated in Figure 5.2 with the resulting epochs (original epochs with interpolated ones and without the rejected ones).

From each epoch, the respective features as discussed in the previous chapters were extracted as shown in Figure 5.1. The scipy library was used to calculate the PSD for the
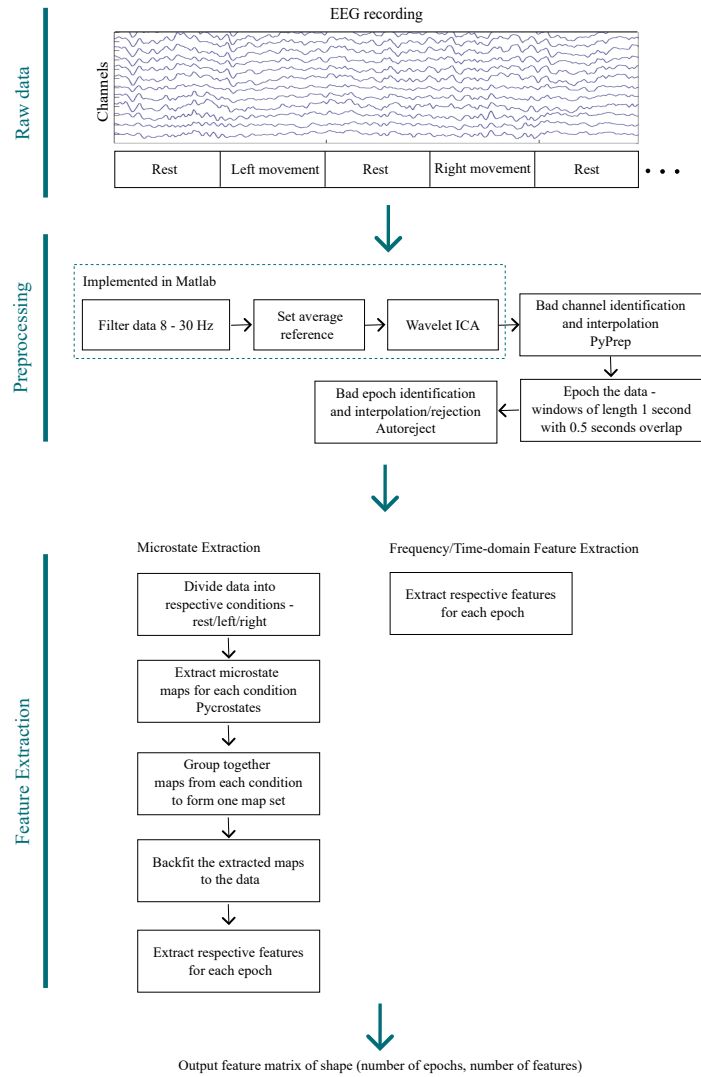
Figure 5.1: Implemented pipeline of the data preprocessing and feature extraction.

frequency features using scipy.signal.periodogram. The Antropy library was used to extract the time-domain features[1].

The microstates were extracted and backfitted using Pycrostates. The parameters for the clustering of the maps include number of initializations, which was set to 100 to make sure as much as possible that the algorithm will find a local minimum when it comes to cost function. The stopping criteria was set to a maximum number of iterations of 300 and convergence threshold was set to $1e - 6$. During the backfitting, the minimum map length was set to be 18 ms - if the map was present at one particular time for a period shorter than 18 ms, then the area was reassigned to the neighbouring maps according to the correlation.

---

[1]https://github.com/raphaelvallat/antropy
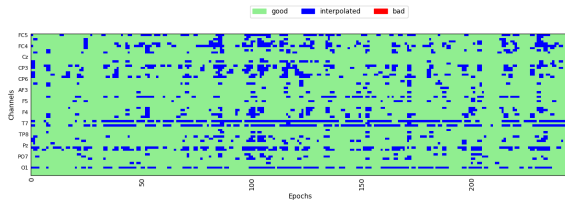
Figure 5.2: Example of the autoreject detection of interpolated and rejected epochs.

5.2 Classification

The process of classification include the selection of the appropriate parameters for the classifier, which include the selection of the model parameters, selection of appropriate number of maps as well as selection of the appropriate area from which the microstates were extracted from.

5.2.1 Cross-validation with Feature Selection

The cross validation was utilized to assess the model parameters as well as the ideal number of microstate maps along with the area of the microstates. All epochs from one experimental run were divided into the training and testing set in the 80/20% ratio total of 5 times, each time with a different training and testing set. The cross-validation is depicted in Figure 5.3.
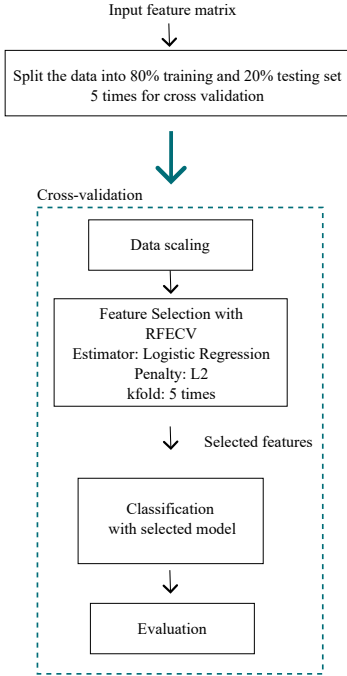
Figure 5.3: Implemented pipeline of the feature selection and cross validation.

The feature selection process was implemented as a Recursive Feature Selection with Cross-Validation (RFECV). The estimator for the feature selection was chosen to be Logistic regression with L_2 penalty and number of cross validations for the testing whether the accuracy of the model improved with the feature removal was set to 5. The number of features eliminated in one cycle was set to 10.

For the model parameters, the Gini and entropy were tested and number of nodes was set to be 1000 (since Random Forests do not suffer from overfitting). In the context of a random forest classifier, the Gini impurity and entropy are criteria used to measure the quality of a split when constructing decision trees. The Gini impurity, denoted as G, represents the probability of misclassifying a randomly chosen element in the dataset if it were randomly labeled according to the class distribution in the node. On the other hand, entropy, denoted as H, is a measure of the information content in the node, reflecting the level of uncertainty in the data. Both criteria are commonly employed to evaluate the homogeneity of the target classes in each split during the construction of decision trees within the random forest ensemble.

For the microstates, the models were tested with the number of maps from 5-9 and from the central, frontocentral and whole head topography.

5.2.2 Evaluation Metrics

In the context of binary classification tasks, several performance metrics are commonly used to assess the effectiveness of a model. Because the proposed models were trained on the rest/activity and left imaginary movement/right imaginary movement, the classification is binary. Three fundamental metrics are accuracy, precision, and recall. Accuracy measures the proportion of correctly classified instances out of the total number of instances in the dataset and is given by the formula:

$$\text{Accuracy} = \frac{\text{Number of True Positives} + \text{Number of True Negatives}}{\text{Total Number of Instances}}$$

Precision represents the ability of the model to correctly identify positive instances among all instances classified as positive and is calculated using the formula:

$$\text{Precision} = \frac{\text{Number of True Positives}}{\text{Number of True Positives} + \text{Number of False Positives}}$$

Recall, also known as sensitivity or true positive rate, measures the proportion of actual positive instances that are correctly identified by the model and is defined as:

$$\text{Recall} = \frac{\text{Number of True Positives}}{\text{Number of True Positives} + \text{Number of False Negatives}}$$

These metrics play a crucial role in evaluating the performance of classification models and are often used together to gain a comprehensive understanding of the model's behavior.

Chapter 6

Evaluation and Benchmarks

To evaluate and compare the models, accuracy, precision and a recall is reported for each experimental run and for each participant. Additionally, comparative test is performed to test the predictive power of the proposed solution as opposed to the usual classifiers.

6.1 Evaluation

For all of the participants the best topography for the microstate extraction was the whole head topography and the number of maps was 9. This is on one hand not very surprising, since the increase of the maps results in the increase of the input features from which the model can learn, but it makes he hypothesis that different regions can contribute differently for the respective conditions.

6.1.1 Imaginary movement

For the imaginary experimental runs, the results are reported in Table 6.1 and show the accuracy, precision and recall score for classifying rest versus activity instances.

The mean accuracy is 0.861, 0.842 and 0.853 respectively for each experimental run. Similarly, the accuracies for the classification between the left and right imagery movement were calculated and the results are shown in Table 6.3.

As expected the, accuracies between the left and right movement were were less when compared to the accuracies of rest versus activity classification. The mean accuracy for the first run classification of the left versus right motor imagery is 0.727. For the second run it is 0.729 and for the third run it is 0.734. Overall, participants did not get better at left/right imagery task as the experiment progressed as is evident from the classification accuracies.

6.1.2 Real Movement

Classification and evaluation through the same pipeline was done on the experimental run where participants were actually moving their left or right hands to compare whether the accuracy is higher or not, as it hypothetically should be.

The mean accuracy on classifying the instances of the rest versus the instances of the activity was 0.898, 0.876 and 0.885 for the three experimental runs respectively. The accuracy did increase as was expected and confirm that the proposed solution is valid.

Table 6.1: Performance Metrics for Rest vs. Activity Classification in Imaginary Movement Task

Subject ID	Run 1			Run 2			Run 3		
	Accuracy	Precision	Recall	Accuracy	Precision	Recall	Accuracy	Precision	Recall
1	0.838	0.836	0.842	0.811	0.808	0.82	0.833	0.826	0.833
2	0.8	0.799	0.801	0.842	0.846	0.842	0.868	0.878	0.868
3	1.0	1.0	1.0	0.919	0.938	0.906	0.963	0.976	0.929
4	0.784	0.816	0.788	0.757	0.771	0.771	0.816	0.817	0.814
5	0.737	0.73	0.73	0.75	0.75	0.748	0.737	0.734	0.734
6	0.947	0.947	0.952	0.842	0.847	0.839	0.868	0.864	0.869
7	0.811	0.81	0.812	0.861	0.862	0.856	0.938	0.944	0.938
8	0.895	0.894	0.894	0.974	0.972	0.976	0.892	0.882	0.899
9	0.865	0.867	0.874	0.861	0.862	0.856	0.842	0.842	0.846
10	0.838	0.835	0.835	0.811	0.808	0.82	0.784	0.81	0.833
11	0.947	0.947	0.952	0.842	0.846	0.842	0.842	0.842	0.846
12	0.892	0.897	0.89	0.789	0.776	0.803	0.921	0.922	0.921
13	0.868	0.896	0.868	0.676	0.683	0.673	0.868	0.869	0.868
14	0.816	0.814	0.817	0.865	0.862	0.866	0.789	0.793	0.789
15	0.895	0.894	0.894	0.974	0.972	0.976	0.892	0.882	0.899
16	0.838	0.835	0.835	0.865	0.865	0.859	0.919	0.918	0.902
17	0.865	0.867	0.874	0.865	0.863	0.855	0.865	0.866	0.864
18	0.784	0.78	0.78	0.865	0.865	0.865	0.789	0.803	0.789
19	0.865	0.867	0.874	0.816	0.816	0.817	0.842	0.838	0.838
20	0.892	0.891	0.891	0.946	0.96	0.929	0.842	0.842	0.846
21	1.0	1.0	1.0	0.816	0.816	0.817	0.816	0.817	0.814
22	0.842	0.84	0.84	0.947	0.938	0.958	0.842	0.842	0.846
23	0.865	0.866	0.864	0.842	0.842	0.858	0.784	0.778	0.786
24	0.865	0.862	0.866	0.838	0.841	0.839	0.838	0.856	0.835
25	0.895	0.894	0.894	0.789	0.78	0.78	0.865	0.874	0.867
26	0.784	0.787	0.785	0.811	0.812	0.81	0.784	0.782	0.787
27	0.816	0.828	0.832	0.838	0.835	0.856	0.919	0.92	0.92
28	0.865	0.867	0.874	0.838	0.839	0.841	0.784	0.81	0.833
29	0.789	0.789	0.789	0.838	0.841	0.853	0.947	0.947	0.947
30	0.842	0.842	0.846	0.842	0.839	0.847	0.865	0.865	0.859
Mean	0.861	0.868	0.875	0.842	0.841	0.847	0.853	0.859	0.853

6.1.3 Comparison

To compare the effectiveness of the model, the proposed solution is compared to the models utilizing only frequency features by using the very same pipeline. Generally, the frequency features are the most telling in terms of motor imagery or movement classification and offer a simple baseline to compare the proposed solution to. The results for the classification of the rest versus activity in imagined movement experiment is reported in Table 6.4.

As expected, the overall classification accuracy got significantly worse when using only frequency features, which can be evident when comparing the results of the accuracy from the table 6.4 with the accuracies from the table 6.1. This is in accordance with the hypothesis and proves that microstates do hold some informative power on the classification of the motor imagery task.

6.1.4 Performance and Hardware requirements

All of the training and evaluations were done on a PC with the following specifications:

- Processor - Intel(R) Core(TM) i7-7700HQ CPU @ 2.80GHz
- RAM - 8.00 GB

Table 6.2: Performance Metrics for Left vs. Right Hand Movement Classification in Imaginary Movement Task

Subject ID	Run 1			Run 2			Run 3		
	Accuracy	Precision	Recall	Accuracy	Precision	Recall	Accuracy	Precision	Recall
1	0.754	0.775	0.744	0.699	0.702	0.696	0.77	0.778	0.774
2	0.686	0.663	0.653	0.811	0.818	0.823	0.563	0.572	0.577
3	0.74	0.769	0.775	0.699	0.712	0.71	0.77	0.769	0.807
4	0.74	0.744	0.737	0.72	0.747	0.748	0.775	0.788	0.792
5	0.72	0.713	0.712	0.715	0.751	0.699	0.7	0.712	0.722
6	0.895	0.886	0.905	0.905	0.919	0.91	0.862	0.875	0.865
7	0.787	0.786	0.784	0.771	0.769	0.746	0.794	0.797	0.805
8	0.667	0.668	0.651	0.696	0.75	0.702	0.597	0.666	0.64
9	0.852	0.861	0.864	0.665	0.662	0.667	0.716	0.741	0.724
10	0.761	0.751	0.754	0.699	0.702	0.696	0.758	0.753	0.754
11	0.74	0.769	0.775	0.698	0.702	0.693	0.609	0.629	0.623
12	0.786	0.804	0.785	0.636	0.664	0.602	0.796	0.812	0.791
13	0.761	0.751	0.754	0.784	0.797	0.778	0.805	0.821	0.798
14	0.733	0.727	0.739	0.698	0.702	0.693	0.753	0.75	0.746
15	0.646	0.596	0.638	0.808	0.816	0.807	0.817	0.834	0.826
16	0.67	0.699	0.667	0.773	0.794	0.785	0.722	0.745	0.723
17	0.667	0.678	0.685	0.784	0.785	0.782	0.609	0.629	0.623
18	0.721	0.76	0.725	0.72	0.747	0.74	0.634	0.661	0.658
19	0.773	0.803	0.772	0.644	0.658	0.663	0.764	0.774	0.77
20	0.711	0.759	0.701	0.796	0.804	0.791	0.656	0.651	0.653
21	0.786	0.804	0.785	0.784	0.797	0.778	0.747	0.756	0.734
22	0.756	0.733	0.726	0.596	0.599	0.594	0.747	0.756	0.734
23	0.73	0.761	0.714	0.591	0.583	0.574	0.764	0.765	0.768
24	0.657	0.674	0.66	0.68	0.695	0.672	0.743	0.774	0.74
25	0.709	0.757	0.729	0.784	0.788	0.776	0.742	0.742	0.73
26	0.698	0.699	0.702	0.826	0.82	0.815	0.711	0.708	0.74
27	0.849	0.838	0.858	0.656	0.66	0.649	0.686	0.702	0.69
28	0.595	0.594	0.595	0.701	0.722	0.734	0.709	0.705	0.713
29	0.768	0.782	0.787	0.829	0.835	0.832	0.884	0.904	0.875
30	0.674	0.708	0.67	0.726	0.754	0.723	0.758	0.753	0.754
Mean	0.727	0.746	0.738	0.729	0.752	0.734	0.734	0.73	0.737

Table 6.3: Performance Metrics for Rest vs. Activity Classification in Real Movement Task

Subject ID	Run 1			Run 2			Run 3		
	Accuracy	Precision	Recall	Accuracy	Precision	Recall	Accuracy	Precision	Recall
1	0.895	0.89	0.89	0.806	0.812	0.81	0.917	0.919	0.91
2	0.846	0.844	0.844	0.794	0.854	0.794	0.865	0.878	0.835
3	0.97	0.978	0.955	0.968	0.977	0.95	0.933	0.955	0.9
4	0.892	0.889	0.913	0.895	0.9	0.909	0.895	0.897	0.897
5	0.892	0.898	0.887	0.842	0.846	0.842	0.794	0.794	0.795
6	0.868	0.868	0.869	0.917	0.917	0.918	0.895	0.892	0.892
7	0.943	0.95	0.941	0.973	0.975	0.972	0.919	0.92	0.92
8	0.892	0.893	0.896	0.919	0.912	0.935	0.865	0.866	0.864
9	0.921	0.917	0.935	0.886	0.89	0.887	0.833	0.819	0.836
10	0.868	0.868	0.869	0.895	0.9	0.909	0.919	0.921	0.929
11	0.921	0.917	0.935	0.944	0.944	0.944	0.974	0.974	0.975
12	0.947	0.95	0.95	0.784	0.785	0.787	0.889	0.875	0.917
13	0.868	0.891	0.875	0.857	0.857	0.85	0.865	0.871	0.871
14	0.939	0.947	0.938	0.967	0.967	0.969	0.933	0.931	0.931
15	0.921	0.935	0.917	0.895	0.895	0.899	0.974	0.974	0.975
16	0.842	0.842	0.846	0.816	0.813	0.807	0.857	0.859	0.856
17	0.895	0.892	0.892	0.944	0.944	0.944	0.895	0.899	0.895
18	0.914	0.917	0.911	0.919	0.925	0.925	0.921	0.923	0.919
19	0.865	0.864	0.866	0.946	0.95	0.947	0.919	0.921	0.929
20	0.842	0.839	0.847	0.829	0.825	0.825	0.765	0.768	0.765
21	0.846	0.844	0.844	0.829	0.825	0.825	0.833	0.819	0.836
22	0.921	0.935	0.917	0.857	0.857	0.85	0.895	0.897	0.897
23	0.939	0.947	0.938	0.829	0.825	0.825	0.974	0.974	0.975
24	0.895	0.892	0.892	0.842	0.846	0.842	0.895	0.897	0.897
25	0.895	0.892	0.892	0.857	0.857	0.85	0.919	0.92	0.92
26	0.868	0.891	0.875	0.895	0.895	0.899	0.919	0.921	0.929
27	0.842	0.839	0.847	0.895	0.9	0.909	0.794	0.794	0.795
28	0.842	0.842	0.846	0.857	0.857	0.85	0.895	0.899	0.895
29	0.895	0.892	0.892	0.829	0.825	0.825	0.865	0.878	0.835
30	0.947	0.95	0.95	0.816	0.813	0.807	0.889	0.875	0.917
Mean	0.898	0.899	0.898	0.876	0.885	0.874	0.885	0.884	0.893

Table 6.4: Performance Metrics for Rest vs. Activity Classification in Real Imaginary Movement Task with Only Frequency-Domain Features

Subject ID	Run 1			Run 2			Run 3		
	Accuracy	Precision	Recall	Accuracy	Precision	Recall	Accuracy	Precision	Recall
1	0.811	0.837	0.807	0.895	0.897	0.897	0.759	0.782	0.782
2	0.8	0.8	0.796	0.737	0.739	0.739	0.711	0.724	0.721
3	0.914	0.917	0.925	0.946	0.958	0.933	0.926	0.955	0.857
4	0.73	0.73	0.73	0.73	0.732	0.731	0.676	0.664	0.664
5	0.763	0.763	0.764	0.694	0.71	0.706	0.684	0.684	0.686
6	0.923	0.925	0.922	0.816	0.819	0.822	0.816	0.819	0.822
7	0.789	0.787	0.787	0.784	0.78	0.78	0.906	0.901	0.877
8	0.789	0.798	0.798	0.789	0.791	0.782	0.737	0.731	0.747
9	0.765	0.81	0.81	0.886	0.892	0.884	0.703	0.708	0.705
12	0.703	0.701	0.699	0.737	0.726	0.713	0.842	0.842	0.842
13	0.921	0.917	0.923	0.763	0.783	0.756	0.73	0.752	0.747
14	0.895	0.895	0.913	0.649	0.634	0.63	0.757	0.756	0.757
15	0.811	0.808	0.82	0.919	0.918	0.921	0.868	0.878	0.868
16	0.789	0.792	0.792	0.676	0.674	0.674	0.784	0.795	0.791
17	0.868	0.869	0.868	0.892	0.9	0.905	0.892	0.92	0.875
18	0.868	0.875	0.872	0.703	0.703	0.703	0.842	0.829	0.862
19	0.737	0.759	0.751	0.757	0.753	0.756	0.811	0.812	0.81
20	0.921	0.919	0.923	0.921	0.919	0.923	0.921	0.919	0.923
22	0.895	0.884	0.902	0.895	0.889	0.917	0.895	0.895	0.895
23	0.919	0.921	0.918	0.811	0.807	0.837	0.811	0.82	0.808
24	0.895	0.9	0.909	0.711	0.724	0.721	0.676	0.677	0.674
25	0.892	0.893	0.896	0.811	0.816	0.816	0.895	0.892	0.892
26	0.784	0.798	0.781	0.789	0.787	0.787	0.73	0.732	0.731
27	0.838	0.853	0.841	0.811	0.821	0.83	0.811	0.811	0.807
28	0.838	0.839	0.841	0.649	0.649	0.648	0.757	0.778	0.79
29	0.789	0.793	0.786	0.73	0.72	0.72	0.895	0.895	0.899
30	0.789	0.787	0.787	0.789	0.798	0.798	0.763	0.761	0.763
Mean	0.823	0.830	0.827	0.802	0.802	0.804	0.81	0.806	0.795

- System type - 64-bit operating system, x64-based processor

No specific hardware such as graphic cards were used in the training and evaluation. The timing required for the training and then testing on one experimental run was as follows:

- Time of feature extraction for one 1 second segment [seconds]:

  - Absolute power: 0.045
  - Sample entropy: 0.038
  - Approximate entropy: 0.281
  - Hjorth's parameters: 0.019
  - Relative power: 0.136
  - Assymetry: 0.042
  - Petrosian fractal dimension: 0.006
  - Katz's fractal dimension: 0.01
  - Higuchi fractal dimension: 0.002
  - Microstate features: 0.273

- Training time: ~30.70 seconds
- Test time for one 1 second segment: 0.013 seconds

Chapter 7

Conclusion

The objective of the thesis was to understand the BCI, its current applications and limitations, choose the appropriate recording modality for the task of the motor imagery and propose a solution for the motor imagery task that would incorporate one of the newest EEG fields emerging in the last years - microstates.

Proposed solution gave an overview on the techniques and methods used to preprocess the EEG data, extract the representative microstate maps for different conditions and finally build a classifier that could distinguish between the left hand motor imagery and right hand motor imagery. To study the effects of the microstates on the classification, two different classifiers were proposed - one for the classification of the rest versus activity condition and one for the left versus right motor imagery conditions. The proposed solution was tested on 30 participants across 3 different experimental runs on both actual movement experiment as well as motor imagery experiment to compare the two, with the expectations that the actual movement will have a higher classification accuracy then the imagined movement. Additionally, different number of maps as well as different regions of map extractions were proposed.

The microstates themselves, unfortunately, did not bear enough informative power to distinguish between the different conditions on their own and therefore the features from other domains were also added to the classification. The initial hypothesis, that maybe extracting different maps from different areas can have a different impact on the experimental condition classification (such as maps from the motor cortex area could distinguish between left and right motor imagery while maps from frontocentral areas could distinguish well between the rest and activity) did not prove entirely true. For all subjects, extracting as many maps as possible have proven to be more successful then focusing on a smaller subset of the maps. This is a little to the contrary of the analysis of the resting state maps, where a smaller subset is usually sufficient. However, in the resting state analysis of the microstates, the objective is to usually distinguish between one group of healthy participants and a group of participants with some pathology. Slight modifications in the map patterns or small variations in their duration or transitions might have proven to be enough for the resting state analysis, but it might not be enough for more complex tasks.

The results of the classification and the comparison with the simpler model which was based only on the frequency features do suggest that the microstates can be used for the motor imagery task, as the classification accuracy while using them improved significantly and in both conditions (rest versus activity and left versus right motor imagery), the classification reached the accuracies above the chance point.

In the future, the microstates from multiple participants could be explored to find some definitive maps that could distinguish not only between the left and right motor imagery but between the actual movement as well. Resting state maps are very well defined and it is important to try finding a well defined maps for other conditions as well.

With regards to the microstate analysis itself, there are still some improvements that could potentially make an impact, most notable being the clustering algorithm used for map extraction. The golden standard as is now is either a K-Means or TAAHC, both of which require a priori definition of the number of maps to use and define GEV as a metric to use to assume the sufficient number of maps. While this might work in a resting state analysis, for cognitive or motor tasks this might not be enough and more then conventional number of maps is needed. It is then important to also define a metric that could conclude the sufficient number of maps other then relying on „at least 60% of GEV".

Bibliography

[1] *Paralysed man moves in mind-reading exoskeleton.* 2019. [Online; accessed October 23, 2022]. Available at: https://www-bbc-com.cdn.ampproject.org/c/s/www.bbc.com/news/amp/health-49907356.

[2] *Stroke facts.* Centers for Disease Control and Prevention, Oct 2022. [Online; accessed October 23, 2022]. Available at: https://www.cdc.gov/stroke/facts.htm.

[3] *What is autism spectrum disorder?* Centers for Disease Control and Prevention, Mar 2022. [Online; accessed October 24, 2022]. Available at: https://www.cdc.gov/ncbddd/autism/facts.html.

[4] ACCARDO, A., AFFINITO, M., CARROZZI, M. and BOUQUET, F. Use of the fractal dimension for the analysis of electroencephalographic time series. *Biological cybernetics.* Springer. 1997, vol. 77, no. 5, p. 339–350.

[5] AHN, M., LEE, M., CHOI, J. and JUN, S. C. A review of brain-computer interface games and an opinion survey from researchers, developers and users. *Sensors.* MDPI. 2014, vol. 14, no. 8, p. 14601–14633.

[6] ALLISON, B., GRAIMANN, B. and GRÄSER, A. Why use a BCI if you are healthy. In: *ACE Workshop-Brain-Computer Interfaces and Games.* 2007, p. 7–11.

[7] ALSAGGAF, E. A. and BAAISHARAH, S. S. Directions of autism diagnosis by electroencephalogram based brain computer interface: a review. *Life Science Journal.* 2014, vol. 11, no. 6, p. 298–304.

[8] AMARAL, C., MOUGA, S., SIMÕES, M., PEREIRA, H. C., BERNARDINO, I. et al. A feasibility clinical trial to improve social attention in autistic spectrum disorder (ASD) using a brain computer interface. *Frontiers in neuroscience.* Frontiers Media SA. 2018, vol. 12, p. 477.

[9] APPELHOFF, S., HURST, A. J., LAWRENCE, A., LI, A., MANTILLA RAMOS, Y. J. et al. PyPREP: A Python implementation of the preprocessing pipeline (PREP) for EEG data. Zenodo. march 2022. DOI: 10.5281/zenodo.6363576. Available at: https://doi.org/10.5281/zenodo.6363576.

[10] ARICÒ, P., BORGHINI, G., DI FLUMERI, G., SCIARAFFA, N., COLOSIMO, A. et al. Passive BCI in Operational Environments: Insights, Recent Advances, and Future Trends. *IEEE Transactions on Biomedical Engineering.* 2017, vol. 64, no. 7, p. 1431–1436. DOI: 10.1109/TBME.2017.2694856.

[11] ARPAIA, P., BRAVACCIO, C., CORRADO, G., DURACCIO, L., MOCCALDI, N. et al. Robotic Autism Rehabilitation by Wearable Brain-Computer Interface and Augmented Reality. In: *2020 IEEE International Symposium on Medical Measurements and Applications (MeMeA)*. 2020, p. 1–6. DOI: 10.1109/MeMeA49120.2020.9137144.

[12] BANIQUED, P. D. E., STANYER, E. C., AWAIS, M., ALAZMANI, A., JACKSON, A. E. et al. Brain–computer interface robotics for hand rehabilitation after stroke: A systematic review. *Journal of NeuroEngineering and Rehabilitation*. BioMed Central. 2021, vol. 18, no. 1, p. 1–25.

[13] BASTOS, A. M. and SCHOFFELEN, J.-M. A tutorial review of functional connectivity analysis methods and their interpretational pitfalls. *Frontiers in systems neuroscience*. Frontiers Media SA. 2016, vol. 9, p. 175.

[14] BELKACEM, A. N. and LAKAS, A. A Cooperative EEG-based BCI Control System for Robot–Drone Interaction. In: *2021 International Wireless Communications and Mobile Computing (IWCMC)*. 2021, p. 297–302. DOI: 10.1109/IWCMC51323.2021.9498781.

[15] BIASIUCCI, A., CHAVARRIAGA, R., HAMNER, B., LEEB, R., PICHIORRI, F. et al. Combining discriminant and topographic information in BCI: preliminary results on stroke patients. In: IEEE. *2011 5th international ieee/embs conference on neural engineering*. 2011, p. 290–293.

[16] BIDGOLY, A. J., BIDGOLY, H. J. and AREZOUMAND, Z. A survey on methods and challenges in EEG based authentication. *Computers & Security*. Elsevier. 2020, vol. 93, p. 101788.

[17] BIGDELY SHAMLO, N., MULLEN, T., KOTHE, C., SU, K.-M. and ROBBINS, K. A. The PREP pipeline: standardized preprocessing for large-scale EEG analysis. *Frontiers in neuroinformatics*. Frontiers Media SA. 2015, vol. 9, p. 16.

[18] BILLECI, L., SICCA, F., MAHARATNA, K., APICELLA, F., NARZISI, A. et al. On the application of quantitative EEG for characterizing autistic brain: a systematic review. *Frontiers in human neuroscience*. Frontiers Media SA. 2013, vol. 7, p. 442.

[19] BOWYER, S. M. Coherence a measure of the brain networks: past and present. *Neuropsychiatric Electrophysiology*. BioMed Central. 2016, vol. 2, no. 1, p. 1–12.

[20] BRITZ, J., VAN DE VILLE, D. and MICHEL, C. M. BOLD correlates of EEG topography reveal rapid resting-state network dynamics. *Neuroimage*. Elsevier. 2010, vol. 52, no. 4, p. 1162–1170.

[21] BRODBECK, V., KUHN, A., WEGNER, F. von, MORZELEWSKI, A., TAGLIAZUCCHI, E. et al. EEG microstates of wakefulness and NREM sleep. *Neuroimage*. Elsevier. 2012, vol. 62, no. 3, p. 2129–2139.

[22] BRODMANN, K. *Vergleichende Lokalisationslehre der Grosshirnrinde in ihren Prinzipien dargestellt auf Grund des Zellenbaues*. Barth, 1909.

[23] Bullock, M., Jackson, G. D. and Abbott, D. F. Artifact reduction in simultaneous EEG-fMRI: a systematic review of methods and contemporary usage. *Frontiers in neurology.* Frontiers Media SA. 2021, vol. 12, p. 622719.

[24] Burns, A., Adeli, H. and Buford, J. A. Brain–computer interface after nervous system injury. *The Neuroscientist.* Sage Publications Sage CA: Los Angeles, CA. 2014, vol. 20, no. 6, p. 639–651.

[25] Cajigas, I., Davis, K. C., Meschede Krasa, B., Prins, N. W., Gallo, S. et al. Implantable brain–computer interface for neuroprosthetic-enabled volitional hand grasp restoration in spinal cord injury. *Brain communications.* Oxford University Press. 2021, vol. 3, no. 4, p. fcab248.

[26] Castellanos, N. P. and Makarov, V. A. Recovering EEG brain signals: Artifact suppression with wavelet enhanced independent component analysis. *Journal of neuroscience methods.* Elsevier. 2006, vol. 158, no. 2, p. 300–312.

[27] Cattan, G. The use of brain–computer interfaces in games is not ready for the general public. *Frontiers in computer science.* Frontiers Media SA. 2021, vol. 3, p. 628773.

[28] Cecotti, H. and Ries, A. J. Best practice for single-trial detection of event-related potentials: Application to brain-computer interfaces. *International Journal of Psychophysiology.* Elsevier. 2017, vol. 111, p. 156–169.

[29] Chan, H.-L., Tsai, Y.-T., Meng, L.-F. and Wu, T. The removal of ocular artifacts from EEG signals using adaptive filters based on ocular source components. *Annals of biomedical engineering.* Springer. 2010, vol. 38, no. 11, p. 3489–3499.

[30] Chen, X., Wang, Y., Nakanishi, M., Gao, X., Jung, T.-P. et al. High-speed spelling with a noninvasive brain–computer interface. *Proceedings of the national academy of sciences.* National Acad Sciences. 2015, vol. 112, no. 44, p. E6058–E6067.

[31] Cheng, N., Phua, K. S., Lai, H. S., Tam, P. K., Tang, K. Y. et al. Brain-computer interface-based soft robotic glove rehabilitation for stroke. *IEEE Transactions on Biomedical Engineering.* IEEE. 2020, vol. 67, no. 12, p. 3339–3351.

[32] Cortez, S. A., Flores, C. and Andreu Perez, J. A smart home control prototype using a P300-based brain–computer interface for post-stroke patients. In: Springer. *Proceedings of the 5th Brazilian Technology Symposium.* 2021, p. 131–139.

[33] Cruz, A., Pires, G. and Nunes, U. J. Double ErrP detection for automatic error correction in an ERP-based BCI speller. *IEEE transactions on neural systems and rehabilitation engineering.* IEEE. 2017, vol. 26, no. 1, p. 26–36.

[34] Dandan, Z., Haiyan, D., Xinlin, H., Yunfeng, L., Congle, Z. et al. The combination of amplitude and sample entropy in EEG and its application to assessment of cerebral injuries in piglets. In: IEEE. *2008 International Conference on BioMedical Engineering and Informatics.* 2008, vol. 2, p. 525–529.

[35] DECETY, J. and JEANNEROD, M. Mentally simulated movements in virtual reality: does Fitt's law hold in motor imagery? *Behavioural brain research*. Elsevier. 1995, vol. 72, 1-2, p. 127–134.

[36] DEHAIS, F., DUPRES, A., DI FLUMERI, G., VERDIERE, K., BORGHINI, G. et al. Monitoring pilot's cognitive fatigue with engagement features in simulated and actual flight conditions using an hybrid fNIRS-EEG passive BCI. In: IEEE. *2018 IEEE international conference on systems, man, and cybernetics (SMC)*. 2018, p. 544–549.

[37] DELORME, A. and MAKEIG, S. EEGLAB: an open source toolbox for analysis of single-trial EEG dynamics including independent component analysis. *Journal of neuroscience methods*. Elsevier. 2004, vol. 134, no. 1, p. 9–21.

[38] DETRE, J. A. FMRI: Applications in Epilepsy. *Epilepsia*. vol. 45, s4, p. 26–31. DOI: https://doi.org/10.1111/j.0013-9580.2004.04006.x. Available at: https://onlinelibrary.wiley.com/doi/abs/10.1111/j.0013-9580.2004.04006.x.

[39] DHINDSA, J. *Generalized Methods for User-Centered Brain-Computer Interfacing*. Dissertation.

[40] DI FLUMERI, G., ARICÒ, P., BORGHINI, G., SCIARAFFA, N., DI FLORIO, A. et al. The dry revolution: Evaluation of three different EEG dry electrode types in terms of signal spectral features, mental states classification and usability. *Sensors*. MDPI. 2019, vol. 19, no. 6, p. 1365.

[41] DIEN, J. Issues in the application of the average reference: Review, critiques, and recommendations. *Behavior Research Methods, Instruments, & Computers*. Springer. 1998, vol. 30, no. 1, p. 34–43.

[42] DINOV, M. and LEECH, R. Modeling uncertainties in EEG microstates: Analysis of real and imagined motor movements using probabilistic clustering-driven training of probabilistic neural networks. *Frontiers in human neuroscience*. Frontiers Media SA. 2017, vol. 11, p. 534.

[43] DIPIETRO, L., PLANK, M., POIZNER, H. and KREBS, H. EEG microstate analysis in human motor corrections. In: IEEE. *2012 4th IEEE RAS & EMBS International Conference on Biomedical Robotics and Biomechatronics (BioRob)*. 2012, p. 1727–1732.

[44] DONG, L., LI, F., LIU, Q., WEN, X., LAI, Y. et al. MATLAB toolboxes for reference electrode standardization technique (REST) of scalp EEG. *Frontiers in neuroscience*. Frontiers Media SA. 2017, vol. 11, p. 601.

[45] DOROSTI, S. and KHOSROWABADI, R. Fractal dimension of EEG signal senses complexity of fractal animations. *BioRxiv*. Cold Spring Harbor Laboratory. 2021, p. 2021–02.

[46] DOUIBI, K., LE BARS, S., LEMONTEY, A., NAG, L., BALP, R. et al. Toward EEG-based BCI applications for industry 4.0: challenges and possible applications. *Frontiers in Human Neuroscience*. Frontiers. 2021, p. 456.

[47] DUNNING, J. P., PARVAZ, M. A., HAJCAK, G., MALONEY, T., ALIA KLEIN, N. et al. Motivated attention to cocaine and emotional cues in abstinent and current cocaine users–an ERP study. *European Journal of Neuroscience.* Wiley Online Library. 2011, vol. 33, no. 9, p. 1716–1723.

[48] EIMER, M. and HOLMES, A. Event-related brain potential correlates of emotional face processing. *Neuropsychologia.* Elsevier. 2007, vol. 45, no. 1, p. 15–31.

[49] ESTELLER, R., VACHTSEVANOS, G., ECHAUZ, J. and LITT, B. A comparison of waveform fractal dimension algorithms. *IEEE Transactions on Circuits and Systems I: Fundamental Theory and Applications.* IEEE. 2001, vol. 48, no. 2, p. 177–183.

[50] FAN, J., WADE, J. W., BIAN, D., KEY, A. P., WARREN, Z. E. et al. A Step towards EEG-based brain computer interface for autism intervention. In: *2015 37th Annual International Conference of the IEEE Engineering in Medicine and Biology Society (EMBC).* 2015, p. 3767–3770. DOI: 10.1109/EMBC.2015.7319213.

[51] FAUST, O., ACHARYA, U. R., ADELI, H. and ADELI, A. Wavelet-based EEG processing for computer-aided seizure detection and epilepsy diagnosis. *Seizure.* Elsevier. 2015, vol. 26, p. 56–64.

[52] FÉRAT, V., SCHELTIENNE, M., BRUNET, D., ROS, T. and MICHEL, C. Pycrostates: a Python library to study EEG microstates. *Journal of Open Source Software.* 2022, vol. 7, no. 78, p. 4564.

[53] FISCHLER, M. A. and BOLLES, R. C. Random sample consensus: a paradigm for model fitting with applications to image analysis and automated cartography. *Communications of the ACM.* ACM New York, NY, USA. 1981, vol. 24, no. 6, p. 381–395.

[54] FOX, M. D., SNYDER, A. Z., VINCENT, J. L., CORBETTA, M., VAN ESSEN, D. C. et al. The human brain is intrinsically organized into dynamic, anticorrelated functional networks. *Proceedings of the National Academy of Sciences.* National Acad Sciences. 2005, vol. 102, no. 27, p. 9673–9678.

[55] FRØLICH, L. and DOWDING, I. Removal of muscular artifacts in EEG signals: a comparison of linear decomposition methods. *Brain informatics.* Springer. 2018, vol. 5, no. 1, p. 13–22.

[56] GEMBLER, F., STAWICKI, P. and VOLOSYAK, I. Exploring the possibilities and limitations of multitarget SSVEP-based BCI applications. In: IEEE. *2016 38th Annual International Conference of the IEEE Engineering in Medicine and Biology Society (EMBC).* 2016, p. 1488–1491.

[57] GLOOR, P., BALL, G. and SCHAUL, N. Brain lesions that produce delta waves in the EEG. *Neurology.* AAN Enterprises. 1977, vol. 27, no. 4, p. 326–326.

[58] GLOVER, G. H. Overview of functional magnetic resonance imaging. *Neurosurgery Clinics.* Elsevier. 2011, vol. 22, no. 2, p. 133–139.

[59] GOLDMAN, D. The clinical use of the "average" reference electrode in monopolar recording. *Electroencephalography and clinical neurophysiology.* Elsevier. 1950, vol. 2, 1-4, p. 209–212.

[60] GOLDSTEIN, R. Z., COTTONE, L. A., JIA, Z., MALONEY, T., VOLKOW, N. D. et al. The effect of graded monetary reward on cognitive event-related potentials and behavior in young healthy adults. *International Journal of Psychophysiology.* Elsevier. 2006, vol. 62, no. 2, p. 272–279.

[61] GRAMFORT, A., LUESSI, M., LARSON, E., ENGEMANN, D. A., STROHMEIER, D. et al. MEG and EEG Data Analysis with MNE-Python. *Frontiers in Neuroscience.* 2013, vol. 7, no. 267, p. 1–13. DOI: 10.3389/fnins.2013.00267.

[62] GUGER, C., ALLISON, B. Z., GROSSWINDHAGER, B., PRÜCKL, R., HINTERMÜLLER, C. et al. How many people could use an SSVEP BCI? *Frontiers in neuroscience.* Frontiers Media SA. 2012, vol. 6, p. 169.

[63] HADIYOSO, S., MENGKO, T. L. E. and ZAKARIA, H. Complexity analysis of EEG signal in patients with cognitive impairment using the Hjorth descriptor. In: IEEE. *2019 2nd International Conference on Bioinformatics, Biotechnology and Biomedical Engineering (BioMIC)-Bioinformatics and Biomedical Engineering.* 2019, vol. 1, p. 1–5.

[64] HÄMÄLÄINEN, M. S. and ILMONIEMI, R. J. Interpreting magnetic fields of the brain: minimum norm estimates. *Medical & biological engineering & computing.* Springer. 1994, vol. 32, no. 1, p. 35–42.

[65] HAN, C.-H., KIM, Y.-W., KIM, D. Y., KIM, S. H., NENADIC, Z. et al. Electroencephalography-based endogenous brain–computer interface for online communication with a completely locked-in patient. *Journal of neuroengineering and rehabilitation.* Springer. 2019, vol. 16, no. 1, p. 1–13.

[66] HASELAGER, P., VLEK, R., HILL, J. and NIJBOER, F. A note on ethical aspects of BCI. *Neural Networks.* Elsevier. 2009, vol. 22, no. 9, p. 1352–1357.

[67] HERMES, D. and MILLER, K. J. Chapter 19 - iEEG: Dura-lining electrodes. In: RAMSEY, N. F. and R. MILLÁN, J. del, ed. *Brain-Computer Interfaces.* Elsevier, 2020, vol. 168, p. 263–277. Handbook of Clinical Neurology. DOI: https://doi.org/10.1016/B978-0-444-63934-9.00019-6. ISSN 0072-9752. Available at: https://www.sciencedirect.com/science/article/pii/B9780444639349000196.

[68] HIGUCHI, T. Approach to an irregular time series on the basis of the fractal theory. *Physica D: Nonlinear Phenomena.* Elsevier. 1988, vol. 31, no. 2, p. 277–283.

[69] HINRICHS, H., SCHOLZ, M., BAUM, A. K., KAM, J. W., KNIGHT, R. T. et al. Comparison between a wireless dry electrode EEG system with a conventional wired wet electrode EEG system for clinical applications. *Scientific reports.* Nature Publishing Group. 2020, vol. 10, no. 1, p. 1–14.

[70] HOFFMANN, S. and FALKENSTEIN, M. The correction of eye blink artefacts in the EEG: a comparison of two prominent methods. *PloS one.* Public Library of Science San Francisco, USA. 2008, vol. 3, no. 8, p. e3004.

[71] HU, S., KARAHAN, E. and VALDES SOSA, P. A. Restate the reference for EEG microstate analysis. *ArXiv preprint arXiv:1802.02701.* 2018.

[72] Huettel, S. A., Song, A. W., McCarthy, G. et al. *Functional magnetic resonance imaging.* Sinauer Associates Sunderland, 2004.

[73] Jafarifarmand, A. and Badamchizadeh, M. A. Real-time cardiac artifact removal from EEG using a hybrid approach. In: IEEE. *2018 International Conference BIOMDLORE.* 2018, p. 1–5.

[74] Jas, M., Engemann, D., Raimondo, F., Bekhti, Y. and Gramfort, A. Automated rejection and repair of bad trials in MEG/EEG. In: IEEE. *2016 international workshop on pattern recognition in neuroimaging (PRNI).* 2016, p. 1–4.

[75] Jas, M., Engemann, D. A., Bekhti, Y., Raimondo, F. and Gramfort, A. Autoreject: Automated artifact rejection for MEG and EEG data. *NeuroImage.* Elsevier. 2017, vol. 159, p. 417–429.

[76] Jiang, X., Bian, G.-B. and Tian, Z. Removal of artifacts from EEG signals: a review. *Sensors.* MDPI. 2019, vol. 19, no. 5, p. 987.

[77] Jiayi, G., Peng, Z., Xin, Z. and Mingshi, W. Sample entropy analysis of sleep EEG under different stages. In: *2007 IEEE/ICME International Conference on Complex Medical Engineering.* 2007.

[78] Kan, D. P. X. and Lee, P. F. Decrease alpha waves in depression: An electroencephalogram (EEG) study. In: IEEE. *2015 International Conference on BioSignal Analysis, Processing and Systems (ICBAPS).* 2015, p. 156–161.

[79] Karch, S., Paolini, M., Gschwendtner, S., Jeanty, H., Reckenfelderbäumer, A. et al. Real-Time fMRI Neurofeedback in Patients With Tobacco Use Disorder During Smoking Cessation: Functional Differences and Implications of the First Training Session in Regard to Future Abstinence or Relapse. *Frontiers in Human Neuroscience.* 2019, vol. 13. DOI: 10.3389/fnhum.2019.00065. ISSN 1662-5161. Available at: https://www.frontiersin.org/articles/10.3389/fnhum.2019.00065.

[80] Kawala Sterniuk, A., Browarska, N., Al Bakri, A., Pelc, M., Zygarlicki, J. et al. Summary of over fifty years with brain-computer interfaces—a review. *Brain Sciences.* MDPI. 2021, vol. 11, no. 1, p. 43.

[81] Khan, M. J. and Hong, K.-S. Passive BCI based on drowsiness detection: an fNIRS study. *Biomedical optics express.* Optica Publishing Group. 2015, vol. 6, no. 10, p. 4063–4078.

[82] Kirsch, M., Gruber, I., Ruf, M., Kiefer, F. and Kirsch, P. Real-time fMRI neurofeedback can reduce striatal cue reactivity to alcohol stimuli. *Addiction Biology.* june 2015, vol. 21. DOI: 10.1111/adb.12278.

[83] Ko, L.-W., Chang, Y., Wu, P.-L., Tzou, H.-A., Chen, S.-F. et al. Development of a smart helmet for strategical BCI applications. *Sensors.* MDPI. 2019, vol. 19, no. 8, p. 1867.

[84] KOENIG, T., LEHMANN, D., MERLO, M. C., KOCHI, K., HELL, D. et al. A deviant EEG brain microstate in acute, neuroleptic-naive schizophrenics at rest. *European archives of psychiatry and clinical neuroscience.* Springer. 1999, vol. 249, no. 4, p. 205–211.

[85] KURUVILLA, A. and FLINK, R. Intraoperative electrocorticography in epilepsy surgery: useful or not? *Seizure.* Elsevier. 2003, vol. 12, no. 8, p. 577–584.

[86] LADOUCE, S., DARMET, L., TORRE TRESOLS, J. J., VELUT, S., FERRARO, G. et al. Improving user experience of SSVEP BCI through low amplitude depth and high frequency stimuli design. *Scientific reports.* Nature Publishing Group. 2022, vol. 12, no. 1, p. 1–12.

[87] LANGE, K. W., REICHL, S., LANGE, K. M., TUCHA, L. and TUCHA, O. The history of attention deficit hyperactivity disorder. *ADHD Attention Deficit and Hyperactivity Disorders.* Springer. 2010, vol. 2, no. 4, p. 241–255.

[88] LATKA, M., WAS, Z., KOZIK, A. and WEST, B. J. Wavelet analysis of epileptic spikes. *Physical Review E.* APS. 2003, vol. 67, no. 5, p. 052902.

[89] LAZAROU, I., NIKOLOPOULOS, S., PETRANTONAKIS, P. C., KOMPATSIARIS, I. and TSOLAKI, M. EEG-based brain–computer interfaces for communication and rehabilitation of people with motor impairment: a novel approach of the 21 st Century. *Frontiers in human neuroscience.* Frontiers Media SA. 2018, vol. 12, p. 14.

[90] LEE, D.-H., JEONG, J.-H., AHN, H.-J. and LEE, S.-W. Design of an EEG-based Drone Swarm Control System using Endogenous BCI Paradigms. In: *2021 9th International Winter Conference on Brain-Computer Interface (BCI).* 2021, p. 1–5. DOI: 10.1109/BCI51272.2021.9385356.

[91] LEEUWIS, N., YOON, S. and ALIMARDANI, M. Functional Connectivity Analysis in Motor Imagery Brain Computer Interfaces. *Frontiers in Human Neuroscience.* Frontiers. 2021, p. 564.

[92] LEHMANN, D., FABER, P. L., GALDERISI, S., HERRMANN, W. M., KINOSHITA, T. et al. EEG microstate duration and syntax in acute, medication-naive, first-episode schizophrenia: a multi-center study. *Psychiatry Research: Neuroimaging.* Elsevier. 2005, vol. 138, no. 2, p. 141–156.

[93] LEI, X. and LIAO, K. Understanding the influences of EEG reference: a large-scale brain network perspective. *Frontiers in neuroscience.* Frontiers. 2017, p. 205.

[94] LI, Y., CHEN, M., SUN, S. and HUANG, Z. Exploring differences for motor imagery using Teager energy operator-based EEG microstate analyses. *Journal of Integrative Neuroscience.* IMR Press. 2021, vol. 20, no. 2, p. 411–417.

[95] LIANG, Z., WANG, Y., SUN, X., LI, D., VOSS, L. J. et al. EEG entropy measures in anesthesia. *Frontiers in computational neuroscience.* Frontiers Media SA. 2015, vol. 9, p. 16.

[96] LIM, C. G., POH, X. W. W., FUNG, S. S. D., GUAN, C., BAUTISTA, D. et al. A randomized controlled trial of a brain-computer interface based attention training

program for ADHD. *PloS one*. Public Library of Science San Francisco, CA USA. 2019, vol. 14, no. 5, p. e0216225.

[97] LINHARTOVÁ, P., LÁTALOVÁ, A., KÓŠA, B., KAŠPÁREK, T., SCHMAHL, C. et al. FMRI neurofeedback in emotion regulation: A literature review. *NeuroImage*. Elsevier. 2019, vol. 193, p. 75–92.

[98] LITTLE, S., POGOSYAN, A., NEAL, S., ZAVALA, B., ZRINZO, L. et al. Adaptive deep brain stimulation in advanced Parkinson disease. *Annals of neurology*. Wiley Online Library. 2013, vol. 74, no. 3, p. 449–457.

[99] LIU, M. and USHIBA, J. Brain–machine Interface (BMI)-based Neurorehabilitation for Post-stroke Upper Limb Paralysis. *The Keio Journal of Medicine*. The Keio Journal of Medicine. 2022.

[100] LIU, W., LIU, X., DAI, R. and TANG, X. Exploring differences between left and right hand motor imagery via spatio-temporal EEG microstate. *Computer Assisted Surgery*. Taylor & Francis. 2017, vol. 22, sup1, p. 258–266.

[101] LUCK, S. J. *An introduction to the event-related potential technique*. MIT press, 2014.

[102] LUO, T.-j., FAN, Y.-c., LV, J.-t. et al. Deep reinforcement learning from error-related potentials via an EEG-based brain-computer interface. In: IEEE. *2018 IEEE international conference on bioinformatics and biomedicine (BIBM)*. 2018, p. 697–701.

[103] MADDIRALA, A. K. and VELUVOLU, K. C. Eye-blink artifact removal from single channel EEG with k-means and SSA. *Scientific Reports*. Nature Publishing Group. 2021, vol. 11, no. 1, p. 1–14.

[104] MÄKELÄ, N., STENROOS, M., SARVAS, J. and ILMONIEMI, R. J. Truncated rap-music (trap-music) for MEG and EEG source localization. *NeuroImage*. Elsevier. 2018, vol. 167, p. 73–83.

[105] MALIK, A. S. and AMIN, H. U. *Designing EEG experiments for studying the brain: Design code and example datasets*. Academic Press, 2017.

[106] MANDELBROT, B. B. and MANDELBROT, B. B. *The fractal geometry of nature*. WH freeman New York, 1982.

[107] MCDERMOTT, B., PORTER, E., HUGHES, D., MCGINLEY, B., LANG, M. et al. Gamma band neural stimulation in humans and the promise of a new modality to prevent and treat Alzheimer's disease. *Journal of Alzheimer's Disease*. IOS Press. 2018, vol. 65, no. 2, p. 363–392.

[108] MELE, G., CAVALIERE, C., ALFANO, V., ORSINI, M., SALVATORE, M. et al. Simultaneous EEG-fMRI for functional neurological assessment. *Frontiers in Neurology*. Frontiers Media SA. 2019, vol. 10, p. 848.

[109] MELLINGER, J., SCHALK, G., BRAUN, C., PREISSL, H., ROSENSTIEL, W. et al. An MEG-based brain–computer interface (BCI). *Neuroimage*. Elsevier. 2007, vol. 36, no. 3, p. 581–593.

[110] MERANTE, A., ZHANG, Y., KUMAR, S. and NAM, C. S. Brain–Computer interfaces for spinal cord injury rehabilitation. In: *Neuroergonomics*. Springer, 2020, p. 315–328.

[111] MICHEL, C. M. and BRUNET, D. EEG source imaging: a practical review of the analysis steps. *Frontiers in neurology*. Frontiers Media SA. 2019, vol. 10, p. 325.

[112] MICHEL, C. M. and KOENIG, T. EEG microstates as a tool for studying the temporal dynamics of whole-brain neuronal networks: a review. *Neuroimage*. Elsevier. 2018, vol. 180, p. 577–593.

[113] MILJEVIC, A., BAILEY, N. W., VILA RODRIGUEZ, F., HERRING, S. E. and FITZGERALD, P. B. EEG-connectivity: A fundamental guide and checklist for optimal study design and evaluation. *Biological Psychiatry: Cognitive Neuroscience and Neuroimaging*. Elsevier. 2021.

[114] MONTOYA MARTÍNEZ, J., VANTHORNHOUT, J., BERTRAND, A. and FRANCART, T. Effect of number and placement of EEG electrodes on measurement of neural tracking of speech. *Plos one*. Public Library of Science San Francisco, CA USA. 2021, vol. 16, no. 2, p. e0246769.

[115] MORRIS ROSENDAHL, D. J. and CROCQ, M.-A. Neurodevelopmental disorders—the history and future of a diagnostic concept. *Dialogues in clinical neuroscience*. Taylor & Francis. 2022.

[116] MOSHER, J. C., BAILLET, S. and LEAHY, R. M. EEG source localization and imaging using multiple signal classification approaches. *Journal of Clinical Neurophysiology*. LWW. 1999, vol. 16, no. 3, p. 225–238.

[117] MOSHER, J. C. and LEAHY, R. M. Source localization using recursively applied and projected (RAP) MUSIC. *IEEE Transactions on signal processing*. IEEE. 1999, vol. 47, no. 2, p. 332–340.

[118] MUSK, E. An Integrated Brain-Machine Interface Platform With Thousands of Channels. *J Med Internet Res*. Oct 2019, vol. 21, no. 10, p. e16194. DOI: 10.2196/16194. ISSN 1438-8871. Available at: http://www.jmir.org/2019/10/e16194/.

[119] MUSSO, F., BRINKMEYER, J., MOBASCHER, A., WARBRICK, T. and WINTERER, G. Spontaneous brain activity and EEG microstates. A novel EEG/fMRI analysis approach to explore resting-state networks. *Neuroimage*. Elsevier. 2010, vol. 52, no. 4, p. 1149–1161.

[120] MUTHUKRISHNAN, S.-P., AHUJA, N., MEHTA, N. and SHARMA, R. Functional brain microstate predicts the outcome in a visuospatial working memory task. *Behavioural brain research*. Elsevier. 2016, vol. 314, p. 134–142.

[121] MYRDEN, A. and CHAU, T. Effects of user mental state on EEG-BCI performance. *Frontiers in human neuroscience*. Frontiers Media SA. 2015, vol. 9, p. 308.

[122] NASEER, N. and HONG, K.-S. FNIRS-based brain-computer interfaces: a review. *Frontiers in Human Neuroscience*. 2015, vol. 9. DOI: 10.3389/fnhum.2015.00003.

ISSN 1662-5161. Available at:
https://www.frontiersin.org/articles/10.3389/fnhum.2015.00003.

[123] NICOLAS ALONSO, L. F. and GOMEZ GIL, J. Brain Computer Interfaces, a Review. *Sensors.* 2012, vol. 12, no. 2, p. 1211–1279. DOI: 10.3390/s120201211. ISSN 1424-8220. Available at: https://www.mdpi.com/1424-8220/12/2/1211.

[124] NIDAL, K. and MALIK, A. S. *EEG/ERP analysis: methods and applications.* Crc Press, 2014.

[125] NOLTE, G., BAI, O., WHEATON, L., MARI, Z., VORBACH, S. et al. Identifying true brain interaction from EEG data using the imaginary part of coherency. *Clinical neurophysiology.* Elsevier. 2004, vol. 115, no. 10, p. 2292–2307.

[126] NORDEN, J. J. Understanding the Brain. In:. 2007.

[127] NUNEZ, P. L. REST: a good idea but not the gold standard. *Clinical neurophysiology: official journal of the International Federation of Clinical Neurophysiology.* NIH Public Access. 2010, vol. 121, no. 12, p. 2177.

[128] OCKLENBURG, S., FRIEDRICH, P., SCHMITZ, J., SCHLÜTER, C., GENC, E. et al. Beyond frontal alpha: investigating hemispheric asymmetries over the EEG frequency spectrum as a function of sex and handedness. *Laterality: Asymmetries of Body, Brain and Cognition.* Taylor & Francis. 2019, vol. 24, no. 5, p. 505–524.

[129] PAEK, A. Y., KILICARSLAN, A., KORENKO, B., GERGINOV, V., KNAPPE, S. et al. Towards a Portable Magnetoencephalography Based Brain Computer Interface with Optically-Pumped Magnetometers. In: *2020 42nd Annual International Conference of the IEEE Engineering in Medicine I& Biology Society (EMBC).* 2020, p. 3420–3423. DOI: 10.1109/EMBC44109.2020.9176159.

[130] PAN, J., XIAO, J., WANG, J., WANG, F., LI, J. et al. Disorders of Consciousness: Brain–Computer Interfaces for Awareness Detection, Auxiliary Diagnosis, Prognosis, and Rehabilitation in Patients with Disorders of Consciousness. In: Thieme Medical Publishers. *Seminars in Neurology.* 2022, vol. 42, no. 3, p. 363.

[131] PASCUAL MARQUI, R. D., MICHEL, C. M. and LEHMANN, D. Segmentation of brain electrical activity into microstates: model estimation and validation. *IEEE Transactions on Biomedical Engineering.* IEEE. 1995, vol. 42, no. 7, p. 658–665.

[132] PERRIN, F., PERNIER, J., BERTRAND, O. and ECHALLIER, J. F. Spherical splines for scalp potential and current density mapping. *Electroencephalography and clinical neurophysiology.* Elsevier. 1989, vol. 72, no. 2, p. 184–187.

[133] PH. D., M., DAS, S., KABIR, M., LIMA, A. and WATANOBE, Y. Brain-Computer Interface: Advancement and Challenges. *Sensors (Basel, Switzerland).* august 2021, vol. 21. DOI: 10.3390/s21175746.

[134] PICTON, T. W. The P300 wave of the human event-related potential. *Journal of clinical neurophysiology.* LWW. 1992, vol. 9, no. 4, p. 456–479.

[135] Pierpaolo, C., Franca, T., Gabriella, T., Patrique, F., Silvia, C. et al. Brain electrical microstate features as biomarkers of a stable motor output. *Journal of Neural Engineering*. IOP Publishing. 2022, vol. 19, no. 5, p. 056042.

[136] Pincus, S. M. Approximate entropy as a measure of system complexity. *Proceedings of the National Academy of Sciences*. National Acad Sciences. 1991, vol. 88, no. 6, p. 2297–2301.

[137] Pirondini, E., Coscia, M., Minguillon, J., Millán, J. d. R., Van De Ville, D. et al. EEG topographies provide subject-specific correlates of motor control. *Scientific reports*. Nature Publishing Group. 2017, vol. 7, no. 1, p. 1–16.

[138] Poewe, W., Seppi, K., Tanner, C. M., Halliday, G. M., Brundin, P. et al. Parkinson disease. *Nature reviews Disease primers*. Nature Publishing Group. 2017, vol. 3, no. 1, p. 1–21.

[139] Pontifex, M. B., Gwizdala, K. L., Parks, A. C., Billinger, M. and Brunner, C. Variability of ICA decomposition may impact EEG signals when used to remove eyeblink artifacts. *Psychophysiology*. Wiley Online Library. 2017, vol. 54, no. 3, p. 386–398.

[140] Proudfit, G. H., Bress, J. N., Foti, D., Kujawa, A. and Klein, D. N. Depression and event-related potentials: Emotional disengagement and reward insensitivity. *Current opinion in psychology*. Elsevier. 2015, vol. 4, p. 110–113.

[141] Quaresima, V. and Ferrari, M. Functional Near-Infrared Spectroscopy (fNIRS) for Assessing Cerebral Cortex Function During Human Behavior in Natural/Social Situations: A Concise Review. *Organizational Research Methods*. 2019, vol. 22, no. 1, p. 46–68. DOI: 10.1177/1094428116658959. Available at: https://doi.org/10.1177/1094428116658959.

[142] Rahmani, B., Wong, C. K., Norouzzadeh, P., Bodurka, J. and McKinney, B. Dynamical Hurst analysis identifies EEG channel differences between PTSD and healthy controls. *PloS one*. Public Library of Science San Francisco, CA USA. 2018, vol. 13, no. 7, p. e0199144.

[143] Rashid, M., Sulaiman, N., P P Abdul Majeed, A., Musa, R., Bari, B. et al. Current Status, Challenges, and Possible Solutions of EEG-Based Brain-Computer Interface: A Comprehensive Review. *Frontiers in Neurorobotics*. june 2020, vol. 14. DOI: 10.3389/fnbot.2020.00025.

[144] Ríos Herrera, W. A., Olguín Rodríguez, P. V., Arzate Mena, J. D., Corsi Cabrera, M., Escalona, J. et al. The influence of EEG references on the analysis of spatio-temporal interrelation patterns. *Frontiers in neuroscience*. Frontiers Media SA. 2019, vol. 13, p. 941.

[145] Rohani, D. A., Sorensen, H. B. and Puthusserypady, S. Brain-computer interface using P300 and virtual reality: a gaming approach for treating ADHD. In: IEEE. *2014 36th Annual International Conference of the IEEE Engineering in Medicine and Biology Society*. 2014, p. 3606–3609.

[146] Sabra, N. I. and Abdel Wahed, M. The use of MEG-based brain computer interface for classification of wrist movements in four different directions. In: *2011 28th National Radio Science Conference (NRSC)*. 2011, p. 1–7. DOI: 10.1109/NRSC.2011.5873644.

[147] Saha, S., Mamun, K. A., Ahmed, K., Mostafa, R., Naik, G. R. et al. Progress in brain computer interface: Challenges and opportunities. *Frontiers in Systems Neuroscience*. Frontiers Media SA. 2021, vol. 15, p. 578875.

[148] Samson Dollfus, D., Delapierre, G., Do Marcolino, C. and Blondeau, C. Normal and pathological changes in alpha rhythms. *International journal of psychophysiology*. Elsevier. 1997, vol. 26, 1-3, p. 395–409.

[149] Scally, B., Burke, M. R., Bunce, D. and Delvenne, J.-F. Resting-state EEG power and connectivity are associated with alpha peak frequency slowing in healthy aging. *Neurobiology of aging*. Elsevier. 2018, vol. 71, p. 149–155.

[150] Schalk, G., McFarland, D. J., Hinterberger, T., Birbaumer, N. and Wolpaw, J. R. BCI2000: a general-purpose brain-computer interface (BCI) system. *IEEE Transactions on biomedical engineering*. IEEE. 2004, vol. 51, no. 6, p. 1034–1043.

[151] Schwender, D., Daunderer, M., Mulzer, S., Klasing, S., Finsterer, U. et al. Spectral edge frequency of the electroencephalogram to monitor "depth" of anaesthesia with isoflurane or propofol. *British journal of anaesthesia*. Elsevier. 1996, vol. 77, no. 2, p. 179–184.

[152] Sebek, J., Bortel, R. and Sovka, P. Suppression of overlearning in independent component analysis used for removal of muscular artifacts from electroencephalographic records. *Plos one*. Public Library of Science San Francisco, CA USA. 2018, vol. 13, no. 8, p. e0201900.

[153] Seitzman, B. A., Abell, M., Bartley, S. C., Erickson, M. A., Bolbecker, A. R. et al. Cognitive manipulation of brain electric microstates. *Neuroimage*. Elsevier. 2017, vol. 146, p. 533–543.

[154] Seok, D., Lee, S., Kim, M., Cho, J. and Kim, C. Motion artifact removal techniques for wearable EEG and PPG sensor systems. *Frontiers in Electronics*. Frontiers Media SA. 2021, vol. 2, p. 685513.

[155] Seth, A. K., Barrett, A. B. and Barnett, L. Granger causality analysis in neuroscience and neuroimaging. *Journal of Neuroscience*. Soc Neuroscience. 2015, vol. 35, no. 8, p. 3293–3297.

[156] Shoker, L., Sanei, S. and Chambers, J. Artifact removal from electroencephalograms using a hybrid BSS-SVM algorithm. *IEEE Signal Processing Letters*. IEEE. 2005, vol. 12, no. 10, p. 721–724.

[157] Simon, C., Bolton, D. A., Kennedy, N. C., Soekadar, S. R. and Ruddy, K. L. Challenges and opportunities for the future of Brain-Computer Interface in neurorehabilitation. *Frontiers in Neuroscience*. Frontiers. 2021, p. 814.

[158] SINGH, S. P. Magnetoencephalography: basic principles. *Annals of Indian Academy of Neurology*. Wolters Kluwer–Medknow Publications. 2014, vol. 17, Suppl 1, p. S107.

[159] SINGLA, R. Ssvep-based bcis. *Evolving BCI Therapy: Engaging Brain State Dynamics*. BoD–Books on Demand. 2018, p. 91.

[160] SMITH, E. and DELARGY, M. Locked-in syndrome. *Bmj*. British Medical Journal Publishing Group. 2005, vol. 330, no. 7488, p. 406–409.

[161] STOKES, P. A. and PURDON, P. L. A study of problems encountered in Granger causality analysis from a neuroscience perspective. *Proceedings of the national academy of sciences*. National Acad Sciences. 2017, vol. 114, no. 34, p. E7063–E7072.

[162] SUMNERS, C. *Synapses: Crucial connections*. Sep 2018. Available at: https://vitalrecord.tamhsc.edu/synapses-crucial-connections/.

[163] SUR, S. and SINHA, V. K. Event-related potential: An overview. *Industrial psychiatry journal*. Wolters Kluwer–Medknow Publications. 2009, vol. 18, no. 1, p. 70.

[164] TAMANO, R., OGAWA, T., KATAGIRI, A., CAI, C., ASAI, T. et al. Event-related microstate dynamics represents working memory performance. *NeuroImage*. Elsevier. 2022, vol. 263, p. 119669.

[165] THOMPSON, M. C. Critiquing the concept of BCI illiteracy. *Science and engineering ethics*. Springer. 2019, vol. 25, no. 4, p. 1217–1233.

[166] VANSTEENSEL, M. J. and JAROSIEWICZ, B. Brain-computer interfaces for communication. *Handbook of clinical neurology*. Elsevier. 2020, vol. 168, p. 67–85.

[167] VANSTEENSEL, M. J., PELS, E. G., BLEICHNER, M. G., BRANCO, M. P., DENISON, T. et al. Fully implanted brain–computer interface in a locked-in patient with ALS. *New England Journal of Medicine*. Mass Medical Soc. 2016, vol. 375, no. 21, p. 2060–2066.

[168] VIDAL, J. J. Toward direct brain-computer communication. *Annual review of Biophysics and Bioengineering*. Annual Reviews 4139 El Camino Way, PO Box 10139, Palo Alto, CA 94303-0139, USA. 1973, vol. 2, no. 1, p. 157–180.

[169] VON WEGNER, F., KNAUT, P. and LAUFS, H. EEG microstate sequences from different clustering algorithms are information-theoretically invariant. *Frontiers in computational neuroscience*. Frontiers Media SA. 2018, vol. 12, p. 70.

[170] VOSS, P., THOMAS, M. E., CISNEROS FRANCO, J. M. and VILLERS SIDANI, E. de. Dynamic Brains and the Changing Rules of Neuroplasticity: Implications for Learning and Recovery. *Frontiers in Psychology*. 2017, vol. 8. DOI: 10.3389/fpsyg.2017.01657. ISSN 1664-1078. Available at: https://www.frontiersin.org/articles/10.3389/fpsyg.2017.01657.

[171] WACKERMANN, J., LEHMANN, D., MICHEL, C. and STRIK, W. Adaptive segmentation of spontaneous EEG map series into spatially defined microstates. *International Journal of Psychophysiology*. Elsevier. 1993, vol. 14, no. 3, p. 269–283.

[172] WALDERT, S. Invasive vs. non-invasive neuronal signals for brain-machine interfaces: will one prevail? *Frontiers in neuroscience*. Frontiers Media SA. 2016, vol. 10, p. 295.

[173] YANG, B., DUAN, K., FAN, C., HU, C. and WANG, J. Automatic ocular artifacts removal in EEG using deep learning. *Biomedical Signal Processing and Control*. Elsevier. 2018, vol. 43, p. 148–158.

[174] YANG, P., FAN, C., WANG, M. and LI, L. A comparative study of average, linked mastoid, and REST references for ERP components acquired during fMRI. *Frontiers in neuroscience*. Frontiers Media SA. 2017, vol. 11, p. 247.

[175] YANG, Y., ZHOU, M., NIU, Y., LI, C., CAO, R. et al. Epileptic seizure prediction based on permutation entropy. *Frontiers in computational neuroscience*. Frontiers Media SA. 2018, vol. 12, p. 55.

[176] YAO, D. A method to standardize a reference of scalp EEG recordings to a point at infinity. *Physiological measurement*. IOP Publishing. 2001, vol. 22, no. 4, p. 693.

[177] YAO, D., QIN, Y., HU, S., DONG, L., BRINGAS VEGA, M. L. et al. Which reference should we use for EEG and ERP practice? *Brain topography*. Springer. 2019, vol. 32, no. 4, p. 530–549.

[178] YIP, D. W. and LUI, F. Physiology, motor cortical. In: *StatPearls [Internet]*. StatPearls Publishing, 2021.

[179] YUMANG, A. N., VILLAVERDE, J. F., PADILLA, D. A. and GATDULA, M. M. V. Environmental Control System for Locked-in Syndrome Patients Using Eye Tracker. In: *Proceedings of the 2020 10th International Conference on Biomedical Engineering and Technology*. 2020, p. 234–239.

[180] ZAFAR, M. B., SHAH, K. A. and MALIK, H. A. Prospects of sustainable ADHD treatment through Brain-Computer Interface systems. In: IEEE. *2017 International Conference on Innovations in Electrical Engineering and Computational Technologies (ICIEECT)*. 2017, p. 1–6.

[181] ZAITCEV, A., COOK, G., LIU, W., PALEY, M. and MILNE, E. Source localization for brain-computer interfaces. In: *Brain-Computer Interfaces*. Springer, 2015, p. 125–153.

[182] ZEROUALI, Y., LINA, J.-M., SEKEROVIC, Z., GODBOUT, J., DUBE, J. et al. A time-frequency analysis of the dynamics of cortical networks of sleep spindles from MEG-EEG recordings. *Frontiers in neuroscience*. Frontiers Media SA. 2014, vol. 8, p. 310.

[183] ZHANG, D., SONG, H., XU, R., ZHOU, W., LING, Z. et al. Toward a minimally invasive brain–computer interface using a single subdural channel: A visual speller study. *NeuroImage*. 2013, vol. 71, p. 30–41. DOI:
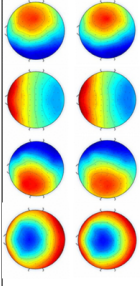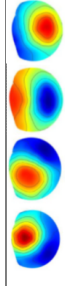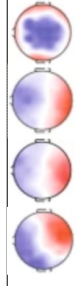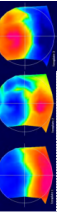
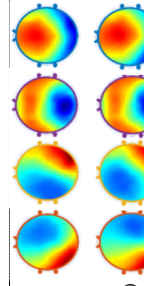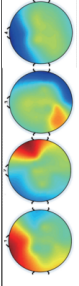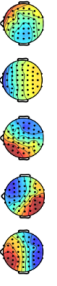https://doi.org/10.1016/j.neuroimage.2012.12.069. ISSN 1053-8119. Available at: https://www.sciencedirect.com/science/article/pii/S1053811913000086.

[184] Zhang, L., Shen, T., Zhang, R. and Hu, Y. Altered Electroencephalography Microstates During the Motor Preparation Process for Voluntary and Instructed Action. *Eng. Sci.* 2022, vol. 18, p. 159–167.

Appendix A

Review of the Microstate Analysis of Motor Imagery or Motor Execution

Table A.1: Review of the microstate analysis used in the motor execution or motor imagery tasks.

Authors	Task	Clustering Method	Identified Maps	
Dinov, Martin, and Robert Leech (2017) [42]	109 subject performing real and imagined movement of left and right hand - identification of maps for real and imagined movement	K-means and Fuzzy C-means		Real movement / Imagined movement
Liu, Weifeng, et al. (2017) [100]	Left and right hand motor imagery - identifying features from the microstate analysis that distinguish the movements	TAAHC		Imagined movement
Pierpaolo, Croce, et al. (2022) [135]	18 subjects pressing a bulb with right hand	K-means with Krzanowski–Lai criterion		Real movement
Pirondini, Elvira, et al. (2017) [137]	8 subjects - identification of maps for rest and various movements (reaching, grasping, holding)	Modified K-means		Real movement (reaching)
Dipietro, L., et al. (2012) [43]	2 subjects moving the handle of the wrist robotic device with the right hand - identification of the maps for the submovements	Modified K-means with Krzanowski–Lai criterion		Real movement
Zhang, Lipeng, et al. (2022) [184]	29 subjects performing real movement of left and right hand - identification of maps for left and right movements	Modified K-means		Real movement (left) / Real movement (right)
Li, Yabing, et al. (2021) [94]	Left and right hand motor imagery - identifying features from the microstate analysis that distinguish the movements	TAAHC		Imagined movement
Biasiucci, Andrea, et al. (2011) [15]	6 subjects - motor imagery of stroke patients - identification of features for distinguishing rest and motor imagery task	Custom		Imagined movement

93